Vaasan yliopisto
UNIVERSITY OF VAASA

RUIFENG DUAN

On Performance Analysis of Cognitive Radios

ACTA WASAENSIA 293

COMPUTER SCIENCE 10
TELECOMMUNICATION ENGINEERING

Reviewers

Professor Tapani Ristaniemi
University of Jyväskylä
Department of Mathematical Information Technology
P.O. Box 35
FI–40014 University of Jyväskylä

Professor Mohamed El-Tarhuni
Department of Electrical Engineering
American University of Sharjah
P.O. Box 26666, Sharjah
United Arab Emirates

Julkaisija
Vaasan yliopisto

Julkaisupäivämäärä
Tammikuu 2014

Tekijä(t)
Ruifeng Duan

Julkaisun tyyppi
Monografia

Julkaisusarjan nimi, osan numero
Acta Wasaensia, 293

Yhteystiedot
Vaasan yliopisto
Teknillinen tiedekunta
Tietotekniikan yksikkö
PL 700
65101 Vaasa

ISBN
978–952–476–510–7 (nid.)
978–952–476–511–4 (pdf)

ISSN
0355–2667 (Acta Wasaensia 292, painettu)
2323–9123 (Acta Wasaensia 292, verkkojulkaisu)
1455–7339 (Acta Wasaensia. Tietotekniikka 10, painettu)
2342–0693 (Acta Wasaensia. Tietotekniikka 10, verkkojulkaisu)

Sivumäärä
151

Kieli
Englanti

Julkaisun nimike
Kognitiivisen radion suorituskykyanalyysiä

Tiivistelmä
Sähkömagneettinen radiospektri on arvokas luonnonvara, jonka käytöstä päättävät valtiolliset toimielimet. Langattoman tietoliikenteen sovellusten ja palvelujen määrän kasvusta johtuen yksittäistä yhteyttä tai sovellusta varten voidaan tarjota yhä niukempi osa radiospektristä. Toisaalta Yhdysvaltain telehallintoviraston (Federal Communications Comission) hiljattain tekemät tutkimukset osoittavat, että merkittäviä osia lisensoiduista taajuuksista on käyttämättömänä aika–tila-avaruudessa jopa 85 % ajasta. Kognitiiviseen radioon perustuvan teknologian uskotaan laajalti mahdollistavan nykyistä tehokkaamman radiospektrin käytön. Tällöin kuluttajille voidaan tarjota myös nykyistä kehittyneempiä tietoliikennetekniikkaan perustuvia palveluita.

Eräs eroista perinteisten langattoman tietoliikenteen järjestelmien ja kognitiivisten radioitten muodostaman verkon välillä on se, että jälkimmäisessä interferenssiä eivät aiheuta ainoastaan sekundääriset vaan myös primääriset käyttäjät. Sekundääriset käyttäjät eivät saa aiheuttaa kynnysarvot ylittävää interferenssiä primääristen käyttäjien tietoliikenteeseen. Tutkimuskirjallisuudessa on osoitettu, että sekundaaristen verkkojen keskeiset suorituskykytekijät, kuten ergodinen kapasiteetti ja optimaaliset tehon allokointistrategiat, voivat poiketa huomattavasti vastaavista perinteisissä langattoman tietoliikenteen järjestelmissä. Tässä väitöskirjatyössä tutkitaan kognitiiviseen radioon liittyviä perustavanlaatuisia asioita ja kehitetään kognitiiviselle radiolle soveltuvia uusia radioresurssien hallintamenetelmiä. Tällaisia ovat muun muassa moniantennitekniikat, optimaaliset tehon allokointistrategiat, sekä systeemin suorituskyky. Nämä asiat ovat tärkeitä kognitiiviseen radioon perustuvan tietoliikennejärjestelmän käytännön suunnittelussa. Ne myös lisäävät ymmärrystä uudesta lupaavasta teknologiasta.

Asiasanat
Kognitiivinen radio, spektrin jakaminen, tehon allokointi, tehon säätö, ergodinen kapasiteetti, tehollinen kapasiteetti, vaihtelevuus

Publisher	**Date of publication**	
Vaasan yliopisto	January 2014	
Author(s) Ruifeng Duan	**Type of publication** Monograph	
	Name and number of series Acta Wasaensia, 293	
Contact information University of Vaasa Faculty of Technology Department of Computer Science P.O. Box 700 FI–65101 Vaasa Finland	**ISBN** 978–952–476–510–7 (print) 978–952–476–511–4 (online)	
	ISSN 0355–2667 (Acta Wasaensia 292, print) 2323–9123 (Acta Wasaensia 292, online) 1455–7339 (Acta Wasaensia. Computer Science 10, print) 2342–0693 (Acta Wasaensia. Computer Science 10, online)	
	Number of pages 151	**Language** English

Title of publication
On Performance Analysis of Cognitive Radios

Abstract
Along with increasing applications and services of wireless communications, the electromagnetic radio spectrum, a precious natural resource regulated by the government agencies, is becoming more and more scarce. However, the recent studies by the Federal Communications Commission showed that large portions of the licensed bands remain unused for as much as 85\% of the time and space. In order to utilize these spectrum more efficiently, cognitive radio (CR) has been recognized widely as a potential technology to increase access to spectrum and also make new and improved communication services available to the public.

Different from the traditional wireless communication systems, in CR networks the interference is caused not only by the secondary users (SUs), but also by the primary users (PUs). Additionally, the SUs should not cause unacceptable interference to the PUs. The literature has shown that the fundamental performance of the secondary networks, for instance, ergodic capacity and optimal power allocation strategies, can be much different from the ones of the traditional systems. In this thesis we investigate the fundamental problems and develop new radio resource management methods for CRs, for instance, multiple-antenna techniques, optimal power allocation strategies, and system capacity. These fundamental research tasks are important for practical use, such as system design, and understanding of this new promising technology.

Keywords
Cognitive radio, spectrum-sharing, power allocation, power control, ergodic capacity, effective capacity, diversity

ACKNOWLEDGEMENT

I would like to acknowledge my doctoral adviser, Professor Mohammed Salem Elmusrati, for all what he has done during my study in Finland. He has been providing me an environment for doing independent research. During my doctoral studies, I have had a totally high degree of freedom to choose my research topics and taking courses.

I would also like to thank Professor Riku Jäntti for his advices and valuable discussions. I would also like to thank Professor Dhadesugoor R. Vamman and Professor Siew Koay at Prairie View A&M University (Texas A&M University System) for their instructive advices and enjoyable cooperation during my visit. The everyday discussions with Professor Vamman and Professor Koay have been inspiring me and beneficial my future work.

I also want to thank Mr. Reino Virrankoski for his support. During 2009 my work in part was financially supported by his projects. I would like to thank the Department of Computer Science and the Faculty of Technology for the support. I have special thanks to all the staff, for instance, Professor Erkki Antila, Professor Kimmo Kauhaniemi , Petri Ingström, Dr. Jari Töyli, Professor Timo Mantere, Ulla Laakkonen, Dr. Virpi Juppo, and Tarja Salo. And I would like to thank Veli-Matti Eskonen and Juha Miettinen for making a friendly research environment. Moreover, I would like to thank all my friends in the ComSys Group, for instance, Omar Abu-Ella, Tobias Glocker, Matti Tuomala, Caner Cuhuc, Mike Mekkanen, Peilin Zhang.

I am thankful for the support I received from the “The Ella and Georg Ehrnrooth Foundation” in 2010, the “Vaasa University Foundation” during 2010-2011 and 2011-2012, and the SMACIW (Statistical Modeling and Control of Aggregate Interference in Wireless Systems, Decesion no. 265077) project funded by the Academy of Finland.

Finally, I would like to dedicate this dissertation to my family.

Special Acknowledgments to Pre-examiners:

I am grateful to the pre-examiners, Prof. Tapani Ristaniemi, University of Jyväskylä, Finland, and Prof. Mohamed El-Tarhuni, American University of Sharjah, United Arab Emirates, conducting a peer review for the dissertation for the permission to publish.

Ruifeng Duan
January 10, 2014
Vaasa, Finland

Contents

Figures

Tables

Abbreviations and Notations

ε_p	Predefined outage probability of the instantaneous rate of the PU
ε_s	Predefined outage probability of the instantaneous rate of the SU
log	Natural logarithm
$\log_a$	Logarithm with base a
$\mathbb{E}[\cdot]$	Expectation operator
$\mathcal{R}_{++}$	Positive real set
Pr	Probability
g_{pp}	The channel power gain of link PT-PR
g_{ps}	The channel power gain of link ST-PR
g_{sp}	The channel power gain of link PT-SR
g_{ss}	The channel power gain of link ST-SR
N_0	Additive white Gaussian noise density at the PU
N_1	Additive white Gaussian noise density at the SU
p_s	Transmit power of the SU
R_p	Required rate of the primary user
R_s	Required rate of the secondary user
AIP	Average interference power
ATP	Average transmit power
AWGN	Additive white Gaussian noise
B	Bandwidth
c.d.f.	Cumulative distribution function
CR	Cognitive radio

CSI	Channel State Information
EC	Effective capacity
GSC	Generalized Selection Combining
MRC	Maximal ratio combing
OPA	Optimal power allocation
p.d.f.	Probability density function
PIP	Peak interference power
PR	Primary receiver
PT	Primary transmitter
PTP	Peak transmit power
PU	Primary user or licensed user
QoS	Quality of service
SINR	Signal to interference and noise ratio
SR	Secondary receiver
ST	Secondary transmitter
SU	Secondary user or unlicensed user

1 INTRODUCTION

1.1 Background

Wireless communications have experienced a rapid growth in the past decades. The demands for providing high-rate and high-quality services have been increasing. In order for coping with these demands, various new wireless communication technologies have been emerging, for instance, fourth generation (4G) cellular networks and beyond, wireless Ad Hoc networks, software-defined radio, wireless regional area networks (WRANs). All the wireless communications need radio spectrum as the medium for transmission. The electromagnetic radio spectrum is a precious natural resource, which currently is regulated by the government agencies, such as the Federal Communications Commission (FCC) in the United States and the Electronic Communications Committee (ECC) in Europe. The frequency use of the wireless systems, e.g. cellular systems, are characterized by statistic spectrum allocations. As a consequence, one serious problem is arising that there is a spectrum scarcity at usable bands. The FCC's frequency allocation chart indicates that most of the available spectrum are allocated (NTIA 2003). However, the recent studies by the FCC's Spectrum Policy Task Force showed that large portions of the licensed bands remain unused temporally and geographically for as much as 85% (FCC 2002). In order to utilize these spectrum "white spaces" and "sparse use spaces", the FCC in (2003b) has issued a Notice of Proposed Rule Making and Order (ET Docket No. 03-322) advancing *cognitive radio* (CR) technology as a candidate to implement opportunistic spectrum sharing. The CR technology also makes new and improved communication services available to the public. In addition, CR is a promising green technology for human being (Grace *et al.* 2009). We use Figure 1 to illustrate the current command-and-control spectrum allocation strategy. Although, there are some free parking slots, they are reserved. The

concept of CR coined by Mitola emerged from the application of software-defined radio (Mitola 2000). Since then cognitive radio has received much research interest, such as dynamic spectrum access, spectrum sensing, information-theoretic analysis. There are a few slightly different versions of the definition of cognitive radio in several classic and highly-cited publications on CR, for instance, (Akyildiz *et al.* 2006; Goldsmith *et al.* 2009; Haykin 2005; Mitola 2000; Mitola & Maguire 1999), as following:

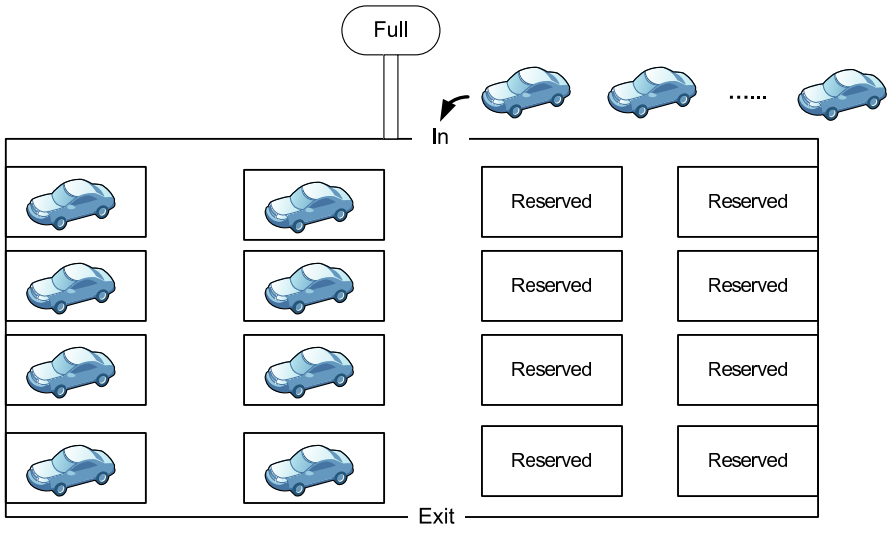

Figure 1. An illustration of current spectrum allocation using a parking lot.

"The term cognitive radio identifies the point at which wireless personal digital assistants (PDAs) and the related networks are sufficiently computationally intelligent about radio resources and related computer-to-computer communications to: a) detect user communications needs as a function of use context, and b) to provide radio resources and wireless services most appropriate to those needs." (Mitola 2000).

"Cognitive radio is an intelligent wireless communication system that is aware of its surrounding environment (i.e., outside world), and uses the methodology of understanding-by-building to learn from the environment and adapt its internal states to statistical variations in the incoming RF stimuli by making corresponding changes in certain operating parameters (for instance, transmit-power, carrier-frequency, and modulation strategy) in real-time, with two primary objectives in mind: a) highly reliable communications whenever and wherever needed, b) efficient utilization of the radio spectrum." (Haykin 2005).

"A cognitive radio is a wireless communication system that intelligently utilizes any available side information about the a) activity, b) channel conditions, c) codebooks, or d) messages of other nodes with which it shares the spectrum." (Goldsmith *et al.* 2009).

Although the above definitions are slightly different, the common key points are that the CR systems/devices should be smart, adaptive, able to utilize the diversities as many as possible without causing harmful interference to the primary users. In (Mitola 2000; Mitola & Maguire 1999), the concept and the architecture are developed in details. (Haykin 2005) provides and develops the details of cognitive radio based on the signal-processing and adaptive procedures, where a modified basic cognitive cycle is proposed focusing on three fundamental cognitive tasks: 1) radio environment estimation including interference estimation and spectrum sensing, 2) channel estimation and capacity prediction, 3) transmit power control/allocation and dynamic spectrum management. In (Akyildiz *et al.* 2006), the authors survey the dynamic spectrum access protocols and present a definition, functions and some research challenges of the DARPAs approach on Dynamic Spectrum Access network, the so-called NeXtGeneration (xG) program (Ramanathan & Partridge 2005). In (Goldsmith *et al.* 2009), the survey is mainly from the information-theoretic point of view that the cognitive radios may improve their achievable transmission rate. This thesis provides guidelines for analyzing and designing the promising technology for mitigating the spectrum scarcity.

Therefore, some new methods need to be defined for cognitive radios on managing and qualifying the interference to the primary users caused by the secondary users. The reason is that the traditional method for controlling interference is based on the transmitter operations. However, for spectrum sharing networks between the licensed users, or primary users, and the unlicensed users, or secondary users, the approach for assessing the interference should take into consideration both the transmitters and receivers. From the information-theoretic point view, Gastpar pointed out in (Gastpar 2007) that interference constraints at the transmitter side and the receiver side can be much different. The FCC established an interference temperature metric in 'Notice of Inquiry and Notice of Proposed Rulemaking (ET Docket No. 03-237)' to quantify and manage interference and to expand available unlicensed operation in certain fixed, mobile and satellite frequency bands (FCC 2003a). The interference temperature introduced by the FCC is depicted in Figure 2 for measuring interference. This interference temperature could be beneficial to the licensed users through providing some transmission opportunities to the unlicensed users if the aggregated interference plus noise is well controlled.

From Figure 2, it is shown that the interference temperature limit provides a maximum cap, or worst case, on the cumulative interference plus noise. Stemmed from

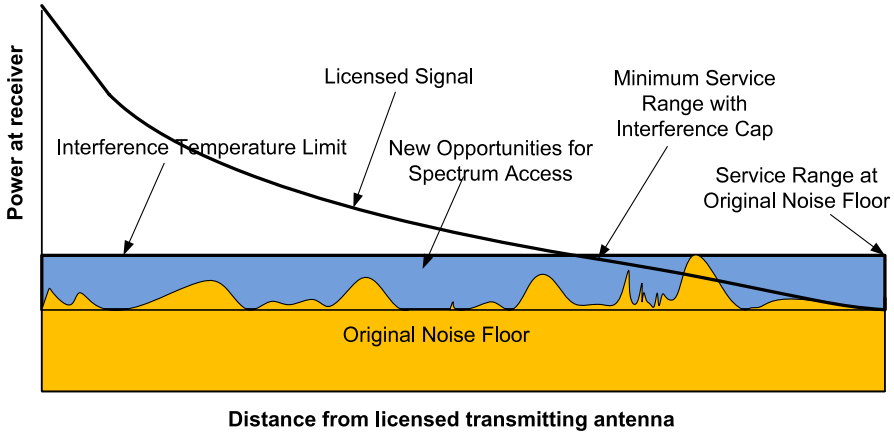

Figure 2. Interference Temperature (FCC 2003a).

the concept of interference temperature, other interference constraints for the secondary users have been proposed in literature, for instance, average interference power, primary outage probability constraint, and primary user capacity loss. We will study the influence of these constraints on the performance of the secondary users in the following chapters of this thesis.

1.2 Cognitive Radios Network Paradigms

There are three cognitive radio paradigms in literature: underlay, overlay, and Interweave (Goldsmith *et al.* 2009). This classification is based on the available network side information and the regulations.

In *underlay paradigm* (Goldsmith *et al.* 2009), the secondary and primary users could transmit simultaneously, if the interference caused by the secondary users to the licensed users is below a predefined threshold. This paradigm assumes that the secondary user has the channel state information (CSI) of the interference channel from the secondary transmitter to the primary receiver, which can be gathered by the spectrum manager, primary receiver or a third-party device and then fed back to the secondary transmitter (Peha 2009). Of course, this CSI can be assumed to be perfect for simplicity. However, in practice it is always imperfect due to, such as, fading, Doppler, limited feedback channel, and measurement error. The interference can be regulated by the interference temperature.

In *overlay paradigm* (Goldsmith *et al.* 2009), the secondary users need to assist the primary users in maintaining or improving performance through using sophisticated signal processing and coding techniques in order to obtain some resources from the primary users for their own transmission. Therefore this paradigm requires that the cognitive users have the codebook side information and the message of the primary users, e.g. the secondary users may use some of the transmit power to relay the primary users' message.

Interweave paradigm (Goldsmith *et al.* 2009), on the other hand, is different from the previous two paradigms that the secondary users require accurate information of the spectrum use. In other words, the secondary users opportunistically transmit exploiting spectrum holes in time, space, or frequency.

Figure 3 graphically illustrates the three paradigms.

1.3 Challenges in Cognitive Radio Networks

The improvement of spectrum underutilization problem by cognitive radio technology comes at the price of causing additional interference to licensed users. In the underlay scenario, under some constraints what is the performance that the secondary network can achieve. In addition, for interweave paradigm cognitive radio network, how accurate a secondary user monitors and detects spectrum holes. For overlay cognitive radio networks, how the secondary users assist the primary communication, and the proper resource allocation schemes. In this dissertation, we focus on the fundamental performance analysis of underlay CRs.

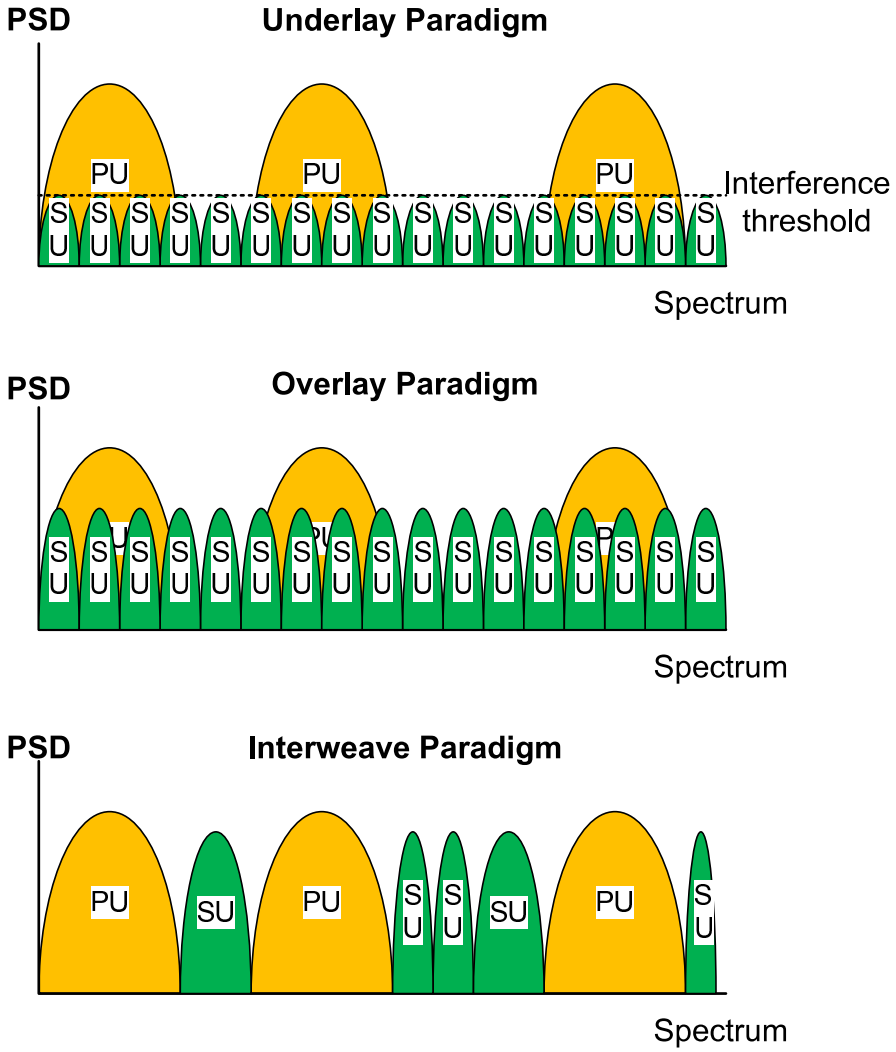

Figure 3. Cognitive radio network paradigms

1.4 Contributions of the Thesis

This thesis focuses on the fundamental analysis of cognitive-shared networks in terms of ergodic capacity, effective capacity, and optimal power allocation. These fundamental research tasks are essentially important for practical use, e.g. system design, and understanding of this new promising technology. The research tasks of this dissertation are associated to the chapters from 3 to 7, which are illustrated as the following contributions.

In the first instance, we in Chapter 3 (Duan *et al.* 2010a) studied the capacity of the spectrum sharing cognitive radio (CR) with maximal ratio combining (MRC) diversity at the secondary receiver (SR) under asymmetric fading, where the chan-

nel from secondary transmitter (ST) to primary receiver (PR) suffers Nakagami-*m* fading while the one from secondary transmitter to its receiver follows Rayleigh multipath fading. The closed-form expression of the ergodic capacity was derived along with the optimal power allocation scheme. Our mathematical analysis and numerical results show that higher capacity can be achieved with MRC combining diversity at the SR. In addition, when the ST-PR channel has less severe fading which strongly affects the capacity of the CR channel, utilizing MRC combining technique for CR systems could reduce the capacity loss of the SU because of the strong interference to the PR.

Second, in Chapter 4 (Duan *et al.* 2010b), we studied the capacity of the spectrum sharing CR with MRC at the SR under Rayleigh fading. Particularly, the secondary user does not have perfect instantaneous channel information of the ST-PR link, where the estimation error is considered. The closed-form expression of the ergodic capacity was derived along with the optimal power allocation scheme. Our mathematical analysis and numerical results depict not only that with MRC combining diversity at the secondary receiver higher capacity is achieved, but also that the estimation error could be compensated. For instance, we show that even when the estimation error variance is large, for example $\sigma^2 = 0.8$, to increase the degrees of MRC combining diversity, for instance L = 8, is able to achieve more capacity than in estimation error free case $\sigma^2 = 0$.

Third, in Chapter 5 we investigated the performance of a cognitive-shared system that employs generalized selection combining under primary outage probability in Rayleigh fading. The closed-form expressions of the ergodic capacity and the symbol error probability of a cognitive-shared channel have been proposed. The results show that the channel from the secondary transmitter to the primary receiver is of prominence on the performance of the secondary user.

In the fourth contribution presented in Chapter 6, we investigated the effective capacity of a cognitive-shared channel with implementing transmit antenna selection at the secondary transmitter and maximal ratio combining at the secondary receiver under different transmit antenna selection schemes: minimum interference selection, maximum secondary composite channel gain selection, and the maximum channel ratio selection. Closed-form expressions for the effective capacity have been presented and validated through simulations.

Finally, we proposed an multiobjective distributed power control algorithm for spectrum sharing cognitive radios (MODPCCR). As we know from literature that

for spectrum sharing cognitive radios the most important factor is the strict limited interference caused to the primary users. Our proposed MODPCCR algorithm is able to achieve certain SINR under the strict interference power constraint to primary users. On this problem, we assumed that there was no perfect channel state information (CSI) of the ST-PR links to be provided to the secondary transmitters. Implementing MODPCCR algorithm on the secondary users could protect the primary users and achieve certain signal to noise and interference ratio (SINR) for the secondary users.

In the aforementioned contributions, the author of this dissertation, Ruifeng Duan, was the first and corresponding author, and the work have been done under the supervision of the co-authors.

1.5 Structure and Organization of the Thesis

The rest of the thesis is organized as follows. We start in Chapter 2 to review some important concepts related to cognitive radio, for instance, ergodic capacity, and optimal power allocation. In Chapter 3, we study the optimal power allocation of the secondary user in order to maximize the ergodic capacity with maximal ratio combing technique at the secondary receiver over fading channels. In Chapter 4, the ergodic capacity and the optimal power allocation of the SU are investigated with the consideration of imperfect channel estimation and the MRC technique at the secondary receiver. Chapter 5 investigates the performance of the SU in terms of the ergodic capacity and the average symbol error rate under the primary outage probability when the generalized selection combining is implemented at the secondary receiver. The effective capacity of the SU is studied with transmit antenna selection and maximal ratio combing techniques implemented at the secondary transmitter and the receiver, respectively. In Chapter 7, we propose a novel and practical multiobjective power control algorithm for cognitive radios. The last chapter concludes this dissertation along with a discussion of further research.

1.6 General Assumptions and Terminology

1.6.1 General assumptions

- *Channel fading*: we adopted *block fading* or *quasi-static fading*, where the channel state does not change during each block, and the channel states

are uncorrelated between blocks. The block fading environment has been adopted widely in the literature (Caire *et al.* 1999; Ozarow *et al.* 1994; Tse & Viswanath 2005). In addition, we omit the channel state variables in the representations of the channel gains. For instance, we use g_{ss} in stead of $g_{ss}(\nu)$ to denote the instantaneous channel power gain of ST-SR at state ν.

- We assumed that the primary user(s) are located far away from the secondary receiver so that there is no significant interference to the secondary user (Ding *et al.* 2011; Ghasemi & Sousa 2007; Lee *et al.* 2011; Musavian & Aissa 2009b; Zhong *et al.* 2011). In addition, the interference from the primary user to the secondary user could be considered being absorbed into the noise if the random Gaussian codebooks are applied at the primary transmitters (Duong *et al.* 2012; Etkin *et al.* 2007; Kim *et al.* 2012).

1.6.2 Terminology:

In this dissertation, we use primary user, noncognitive user for the licensed user, interchangeably; secondary user, cognitive user, for the unlicensed user.

2 POWER ALLOCATION FOR COGNITIVE RADIOS: A SURVEY

As we know from the introduction chapter that power allocation is of great importance in managing the interference in spectrum sharing networks, maximizing the spectrum reuse, increasing communication capacity, and making our living environment greener (Goldsmith & Varaiya 1997; Knopp & Humblet 1995; Yates 1995). In this chapter we review the most important and up-to-date results of the power allocation approaches proposed in literature from an information-theoretic perspective. Therefore, we will take a look at the optimal power allocation of the secondary users in order to maximize their ergodic capacity and effective capacity over fading channels. This survey improves the understanding of ultimate performance limits of the cognitive radios and the cognitive radio systems design.

2.1 Introduction

Spatial considerations for frequency reuse have been extensively studied in cellular systems. However, these systems differ from the cognitive radio (CR) case in a number of significant ways (Hoven & Sahai 2005). As the command-and-control structure of frequency allocation for traditional wireless communications, most of the interference in these systems is caused by the terminals operating with the same operator, this is so-called within-system interference. This kind of interference can be well controlled through planning. For these systems, power control has been studied in SIR-based, e.g. (Chiang *et al.* 2008), and information-theoretic contexts for fading and non-fading channels, for instance (Goldsmith & Varaiya 1997; Kaya & Ulukus 2004; Knopp & Humblet 1995; Yates 1995). However, in cognitive radio networks, the interference is caused not only by the secondary users (SUs), or cognitive users, sharing the same spectrum, but also by the primary users (PUs), or licensed users, who share the spectrum. Additionally, the secondary users should not cause unacceptable interference to the primary users. In this thesis we focus on the information-theoretic approaches, i.e., reviewing the optimal power allocation approaches for the SUs to maximize the achievable rate under certain constraints. The framework employed to evaluate the power allocation schemes and the other performance matrices is mainly based on information theory (Cover & Thomas 2006).

There is a growing body of literature on power control/allocation in CR systems. In (Chen *et al.* 2008) and (Srinivasa & Jafar 2010), power control for one pair of secondary users coexisting with one pair of primary users is considered. In (Chen *et al.* 2008), the secondary transmitter adjusts its transmission power to maximize its data rate without increasing the outage probability at the primary receiver. The authors in (Srinivasa & Jafar 2010) proposed the optimal power control schemes based on the soft sensing information, and the capacity of the secondary user was maximized under a peak power constraint at the primary receiver. Power control for opportunistic spectrum access (OSA) in TV bands is investigated in (Islam *et al.* 2008) and (Qian *et al.* 2007), where the primary users transmit all the time and spatial (rather than temporal) spectrum opportunities are exploited by secondary users. For the interference control of the secondary users over television white spaces, the author proposed the power density and deployment based transmit power control of the secondary users such that the quality of the TV services is not violated by the aggregated interference (Koufos *et al.* 2011).

Gastpar (2004; 2007) investigated the ergodic capacity of different non-fading addit-ive-white-Gaussian noise (AWGN) channels. The transmit power of the SU is regulated by the average interference power received at a third-party receiver. The author illustrated that the received-signal constraints can lead to substantially different results as compared to transmitted-signal constraints. There are some important discovers which are different from a conventional point-to-point communication. Without fading the author showed that in the point-to-point case, the transmit and received-power constraints are largely equivalent. While in network cases, they can lead to quite different conclusions, for example, multiple access channels with dependent sources and feedback, and collaborative communication scenarios. Ghasemi and Sousa (2007) showed that in many cases significant capacity gains may be achieved if the channels are varying due to fading and shadowing under either the average or the peak interference power constraint. In (Suraweera *et al.* 2010), the authors extended the work in (Ghasemi & Sousa 2007) by investigating the achievable capacity gains in asymmetric fading environments. Musavian and Aïssa in (2009b) studied the capacity gains offered by the spectrum-sharing approach in a Rayleigh fading environment subject to both average and peak received-power constraints at the primary receiver. Kang et al. (2009) studied the optimal power allocation strategies to achieve the ergodic, delay-limited, and outage capacities of a secondary fading channel subject to a diverse combinations of peak/average transmit and/or peak/average interference power constraints. The

authors observed that fading of the channel from secondary transmitter to primary receiver can be a good phenomenon for maximizing the capacity of SU fading channel. Zhang (2009) concluded that the average-interference-power (AIP) constraint can be more advantageous over the peak-interference-power for minimizing the resultant capacity loss of the primary fading channel, and AIP should be used for the purposes of both protecting the PR communications as well as maximizing the CR capacity. Therefore, we review the channel model and the concepts of capacity in the following, and then survey the main results of optimal power allocation approaches for cognitive radios.

2.2 Channel Model and Concepts of Capacity

In this section we introduce the channel model, and review two important concepts, i.e., ergodic capacity and effective capacity. We consider independent and identically distributed additive white Gaussian noise (AWGN) block-fading channels. The block-fading, or quasi-static, channel model was introduced in (Ozarow *et al.* 1994) and has been commonly used in the literature for studying wireless communications systems over slowly-varying fading channels (Biglieri *et al.* 1998; Ozarow *et al.* 1994), through which a codeword spans only a certain number of fading blocks. During each fading block, the channel gain remains constant while varying from block to block. The interference from the primary user to the secondary is neglected according to the assumptions presented in Section 1.6.

For imperfect channel information scenarios, we adopt the following channel estimation methods for measuring the channel gain of ST-PR link, which has been widely used in literature, e.g. (Musavian & Aissa 2009b). For Rayleigh fading channels, the complex channel gain from the secondary transmitter to the primary receiver, c_{ps}, is zero mean circularly symmetric complex Gaussian distributed variable with the imaginary and real parts having variances of 0.5. However, the CR transmitter is only provided with partial channel information of c_{ps}, namely $\tilde{c}_{ps}$, where c_{ps} and $\tilde{c}_{ps}$ are jointly ergodic and stationary Gaussian processes. The secondary user performs minimum mean square error estimation (MMSE) of c_{ps} given $\tilde{c}_{ps}$, such that $\hat{c}_{ps}[n] = \mathcal{E}\left\{c_{ps}[n] \mid \tilde{c}_{ps}[n], \tilde{c}_{ps}[n-1], \ldots\right\}$, where $[n]$ denotes the time index. The MMSE estimation error can be presented as $\check{c}_{ps}[n] = c_{ps}[n] - \hat{c}_{ps}[n]$, and $\check{c}_{ps}[n]$ and $\hat{c}_{ps}[n]$ are zero mean circularly symmetric complex Gaussian distributed variables with variances $\frac{1-\sigma^2}{2}$ and $\frac{\sigma^2}{2}$ respectively. So the associated channel power gain can be presented as $g = \left|c_{ps}\right|^2$, $\hat{g} = \left|\hat{c}_{ps}\right|^2$,

and the channel power gain estimation error by $\breve{g} = \left|\breve{c}_{ps}\right|^2$. The probability density function of estimated channel power gain, $\hat{g}$, is characterized by (Musavian & Aissa 2009a):

$$f_{\hat{g}}(\hat{g}) = \frac{1}{1-\sigma^2} e^{-\frac{\hat{g}}{1-\sigma^2}}, \quad \hat{g} \geq 0 \tag{2.1}$$

2.2.1 Ergodic Capacity

This subsection reviews the ergodic capacity formulation of the secondary user. With perfect channel state information (CSI) of the secondary link (ST-SR) and the secondary transmitter to the primary receiver (ST-PR), the ergodic capacity of the secondary user is given in (Ghasemi & Sousa 2007) by

$$\textbf{Ergodic capacity:} \quad \mathbb{E}_{g_{ss},g_{ps}}\left[\log\left(1+\frac{p_s(g_{ss},g_{ps})g_{ss}}{N_1 B}\right)\right] \tag{2.2}$$

where $p_s(g_{ss},g_{ps})$ is the transmit power of the secondary transmitter, g_{ss} and g_{ps} denote the channel power gains of ST-SR and ST-PR, respectively. N_1 represents the additive white noise density at the secondary receiver. $\log(\cdot)$ denotes the natural logarithm operator, and $\mathbb{E}_{\mathbf{x}}$ denotes the expectation operator over $\mathbf{x}$ in this thesis. The secondary user chooses the optimal transmit power to maximize the achievable rate according to the instantaneous CSI of the two channels instead of only its own CSI as in the traditional wireless communications systems. The maximization is over power allocation functions that are being discussed later in certain problems.

2.2.2 Effective Capacity

From literature, we know that the ergodic capacity has no transmission delay limitation, while the outage capacity does not allow any delay (Tse & Hanly 1998). In order to study the delay performance, the concept of effective capacity (EC) was developed in (Wu & Negi 2003; 2004) to define the maximum arrival data rate that can be supported by the channel subject to the required communication delay. It is a link-layer channel model and can be interpreted as the dual of effective bandwidth (Chang & Thomas 1995). The quality of service (QoS) is represented by a term, named QoS exponent $\theta \in \mathcal{R}_{++}$. The EC bridges the ergodic capacity and the outage capacity. When the QoS exponent $\theta \to 0$, it means that there is no

delay limitation, and the EC equals the ergodic capacity. On the other hand, the link cannot tolerate any delay as $\theta \to \infty$. This concept has received much attention in the point-to-point communication scenarios, e.g., (Tang & Zhang 2007a;b), as well as in cognitive radios, e.g., (Akin & Gursoy 2010; Musavian & Aissa 2010) and references therein. The effective capacity along with energy efficiency was also investigated in (Gursoy *et al.* 2009).

Let $q(x)$ be the queue length of a stationary ergodic arrival and service process. The probability that $q(x)$ exceeds a certain threshold T_q decays exponentially as a function of T_q, and the delay QoS exponent is defined in (Wu & Negi 2003) as

$$\theta = -\lim_{T_q \to \infty} \frac{\log(\Pr\{q(\infty) > T_q\})}{T_q}. \tag{2.3}$$

It is worth noting that $\theta \to 0$ indicates that the system has no delay constraint, while $\theta \to \infty$ implies a stringent delay constraint. The effective capacity is defined in (Wu & Negi 2003: eqn. (12)) by

$$EC(\theta) = -\lim_{t \to \infty} \frac{1}{\theta t} \log\left[\mathbb{E}\left(e^{-\theta \Sigma_{i=0}^{t} R[i]}\right)\right], \; t \geq 0 \tag{2.4}$$

where $\{R[i], i = 1, 2, ...\}$ denotes a discrete-time service process of the maximum achievable instantaneous service rate of time $[i]$, which is assumed to be ergodic and stationary. For a block fading channel, the EC can be reduced to (Tang & Zhang 2007b),

$$EC(\theta) = -\frac{1}{\theta} \log\left[\mathbb{E}\left(e^{-\theta R[i]}\right)\right]. \tag{2.5}$$

The maximum achievable instantaneous service rate $R[i]$ of block i can be expressed as $R[i] = TB\log(1+\gamma[i])$, where T denotes the block length duration, B is the channel bandwidth, and $\gamma[i]$ is the instantaneous SINR of block i.

2.3 Ergodic Capacity

This section reviews the optimal power allocation policies of the secondary user in order to maximize its ergodic capacity (maximum achievable rate) under various constraints categorized as short-term and long-term constraints. In the literature, many results have been proposed for cognitive radios. Ghasemi and Sousa (2007) studied the optimal power allocation strategies for the secondary user through

showing that with the same limit on the received power level, the channel ergodic capacity for a range of fading models (e.g., Rayleigh, Nakagami-*m* and log-normal fading) exceeds that of the non-fading AWGN channel.

The remainder of this section review some main results in terms of the ergodic capacity of the SU under the short-term constraints, long-term constraints, or the combination of short-term and long-term constraints. The constraints are categorized as follows. 1) short-term constraints: peak transmit power, peak interference power, and outage probability at certain channel state; 2) long-term constraints: average transmit power, and average interference power. Intuitively, the short-term constraints are more stringent than the long-term ones. The following results hold in (Ghasemi & Sousa 2007; Musavian & Aissa 2009a;b; Suraweera *et al.* 2010; Wang *et al.* 2009; Zhang 2009). We omit the proofs which can be found in the associated papers.

2.3.1 Short Term Constraints

In this subsection, we review the optimal power allocation strategies for cognitive radio in order to maximize its ergodic capacity constrained on various combinations of short-term constraints, i.e., peak transmit power (PTP) denoted as $P_{\max}$, peak interference power (PIP) denoted as Q_{pk}. One formulation of the optimization problem is given by

$$\mathbf{O_1}: \quad \underset{p_s(g_{ss},g_{ps})\geq 0}{\text{maximize}} \quad \mathbb{E}\left[\log\left(1+\frac{p_s(g_{ss},g_{ps})g_{ss}}{N_1 B}\right)\right] \tag{2.6}$$

$$\mathbf{C_1^1}: \quad p_s(g_{ss},g_{ps})g_{ps} \leq Q_{pk} \tag{2.7}$$

$$\mathbf{C_1^2}: \quad p_s(g_{ss},g_{ps}) \leq P_{\max} \tag{2.8}$$

where $\mathbf{C_1^1}$ and $\mathbf{C_2^1}$ denote the PIP constraint and PTP constraint, respectively, associated to the objective function $\mathbf{O_1}$. Intuitively, the SU transmits using the power of $\min(P_{\max}, \frac{Q_{pk}}{g_{ps}})$, which is also given in (Kang *et al.* 2009). In this scenario, the SU transmitter exploits only the interference channel state information (CSI).

The fading of the ST-PR channel determines the ergodic capacity of the SU. In consequence, given $P_{\max}$ the SU achieves higher ergodic capacity when ST-PR channel experiences sever fading, e.g. Rayleigh, than the case that ST-PR is an

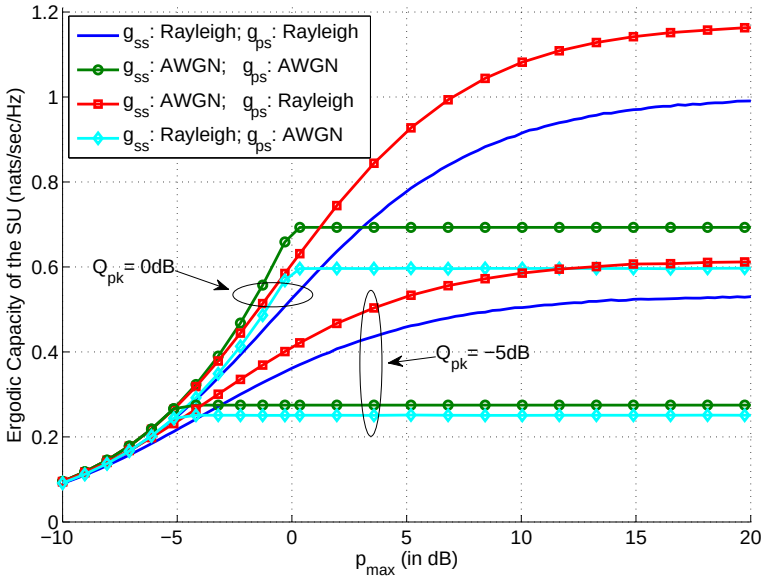

Figure 4. Ergodic capacity of the secondary user with different values of peak interference constraints over AWGN and/or Rayleigh fading channels.

AWGN without fading or Rician channel. Such that the fade state of ST-PR is a good phenomenon for maximizing the capacity of the SU. The challenging issue for this scheme is to provide the accurate CSI of ST-PR at the secondary transmitter. The instantaneous CSI can be fed back to the secondary transmitter (Kang *et al.* 2009; Peha 2009).

Figure 4 illustrates the achieved ergodic capacity of the secondary user versus various peak transmit powers along with different values of the peak interference power, where we assumed that all the mean values of the channel power gains are 1. We can observe that when the PIP constraint is dominant, i.e. $P_{\max} \ll Q_{pk}$, the secondary user may simply transmit at the maximum power to achieve its ergodic capacity. Additionally, under $P_{\max} \ll Q_{pk}$, the fades of g_{ps} are not beneficial to the ergodic capacity of the SU. This is because over Rayleigh fading the SU is not able to exploit some transmission opportunities due to its peak transmit power constraint.

2.3.1.1 Mean Value-based Power Allocation

The optimal power strategy discussed in previous subsection requires the instantaneous CSI of the ST-PR link. In this subsection, we review the mean-value based power allocation (MVPA) and the ergodic capacity of a cognitive-share radio under the outage probability constraint of the interference power to the primary user (Lim *et al.* 2012). This means that the secondary user has only the statistical information of the channel ST-PR. The ergodic capacity optimization problem based on MVPA can be formulated as (Lim *et al.* 2012)

$$C = \underset{\overline{g}_{ps}, g_{ss}}{\text{maximize}} \quad \int_0^{\infty} \log\left(1 + \frac{g_{ss} p_s(\overline{g}_{ps}, g_{ss})}{N_1 B}\right) f_{g_{ss}}(g_{ss})\, dg_{ss}. \tag{2.9}$$

$$\text{s.t.} \quad \Pr\left\{g_{ps} p_s(\overline{g}_{ps}, g_{ss}) \geq Q_{pk}\right\} \leq P_O^{th} \tag{2.10}$$

where B denotes the bandwidth, $\overline{g}_{ps}$ represents the mean value of g_{ps} that is assumed to be known at the secondary transmitter, $p_s(\overline{g}_{ps}, g_{ss})$ denotes the transmit power of the ST, $f_{g_{ss}}(g_{ss})$ is the probability density function of g_{ss} which is the channel power gain of the ST-SR link, and P_O^{th} denotes the predefined outage probability threshold that the instantaneous interference is allowed to exceed the predefined peak interference power constraint Q_{pk}. For Rayleigh fading, which is assumed in this subsection, $f_{g_{ss}}(g_{ss}) = \frac{1}{\overline{g}_{ss}} \exp\left\{-\frac{g_{ss}}{\overline{g}_{ss}}\right\}$, and N_1 is the additive white Gaussian noise density at the SR. log denotes natural logarithm operation.

The ergodic capacity of the SU with MVPA can be achieved through employing a frame work presented by Zouheir Rezki and Mohamed-Slim Alouini in (Rezki & Alouini 2012). According to (Rezki & Alouini 2012), the interference outage probability constraint in the above optimization problem is equivalent to

$$p_s(g_{ss}, \overline{g}_{ps}) \leq \frac{Q_{pk}}{F_{g_{ps}}^{-1}(1 - P_O^{th})} \tag{2.11}$$

where $F_{g_{ps}}^{-1}(1 - P_O^{th})$ denotes the inverse c.d.f. of g_{ps}. For Rayleigh fading scenarios, the probability density function of the channel power gain is continuous and not null so that $F_{g_{ps}}^{-1}(\cdot)$ exists. This new transformed constraint is called a variable peak transmit power constraint in (Rezki & Alouini 2012). In MVPA the secondary transmitter has the statistical information in stead of the instantaneous ST-PR channel state information. In addition, $F_{g_{ps}}^{-1}(1 - P_O^{th})$ takes a fixed value (Rezki & Alouini 2012). This means that the secondary user uses fixed transmit power which is not variant with respect to g_{ss}. Based on the setting that g_{ps} is

exponentially distributed with a mean of $\overline{g}_{ps}$, i.e., $F_{g_{ps}}^{-1}(1-P_O^{th}) = \overline{g}_{ps}\log\left(\frac{1}{P_O^{th}}\right)$. Consequently, the fixed transmit power for the secondary transmitter is

$$p_s(g_{ss},\overline{g}_{ps}) \leq \frac{Q_{pk}}{\overline{g}_{ps}\log\left(\frac{1}{P_O^{th}}\right)} \tag{2.12}$$

where we may use the notation $p_s(\overline{g}_{ps})$ rather than $p_s(g_{ss},\overline{g}_{ps})$. We can obtain the ergodic capacity of the SU exploiting MVPA as following

$$\begin{aligned} C &= \int_0^\infty \log\left(1+\frac{g_{ss}p_s(\overline{g}_{ps})}{N_1B}\right) f_{g_{ss}}(g_{ss})\,dg_{ss}. \\ &= \int_0^\infty \log\left(1+\frac{g_{ss}p_s(\overline{g}_{ps})}{N_1B}\right) \frac{1}{\overline{g}_{ss}} e^{-\frac{g_{ss}}{\overline{g}_{ss}}}\,dg_{ss}. \\ &= -e^{\frac{N_1B}{\overline{g}_{ss}p_s(\overline{g}_{ps})}} \mathsf{E}_{\mathsf{i}}\left(-\frac{N_1B}{\overline{g}_{ss}p_s(\overline{g}_{ps})}\right) \end{aligned} \tag{2.13}$$

where in the last two steps we have the help of (Gradshteyn & Ryzhik 2007: 4.337-2), and $\mathsf{E}_{\mathsf{i}}(x) = \int_{-\infty}^{x} \frac{e^t}{t}dt, x<0$ denotes the exponential integral function (Gradshteyn & Ryzhik 2007: 8.211-1). This result also was shown in (Lim *et al.* 2012) using a different method of proof. The ergodic capacity versus Q_{pk} and P_O^{th} are plotted in Figure 5 and in Figure 6, respectively. We have to point out that in the discussed environment if $P_O^{th} \to 0$, the secondary user needs to stop transmission.

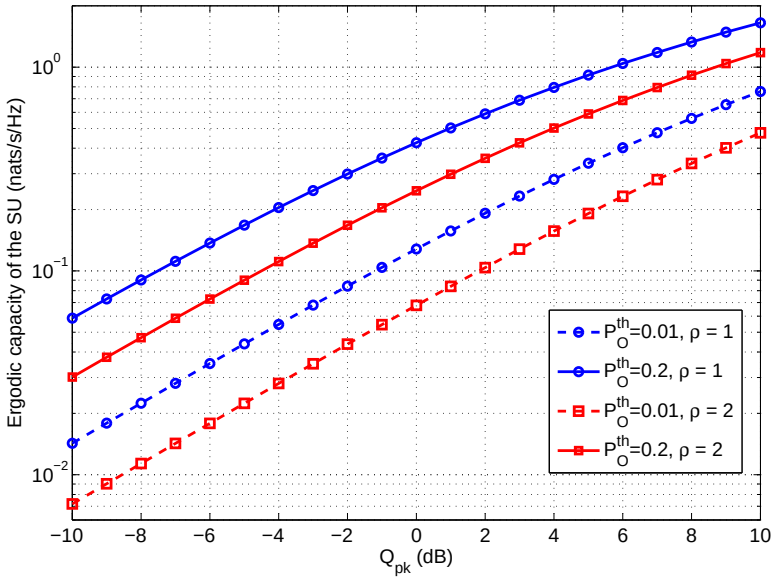

Figure 5. Ergodic capacity of the SU versus Q_{pk} for different values of P_O^{th} and $\rho = \overline{g}_{ps}/\overline{g}_{ss}$.

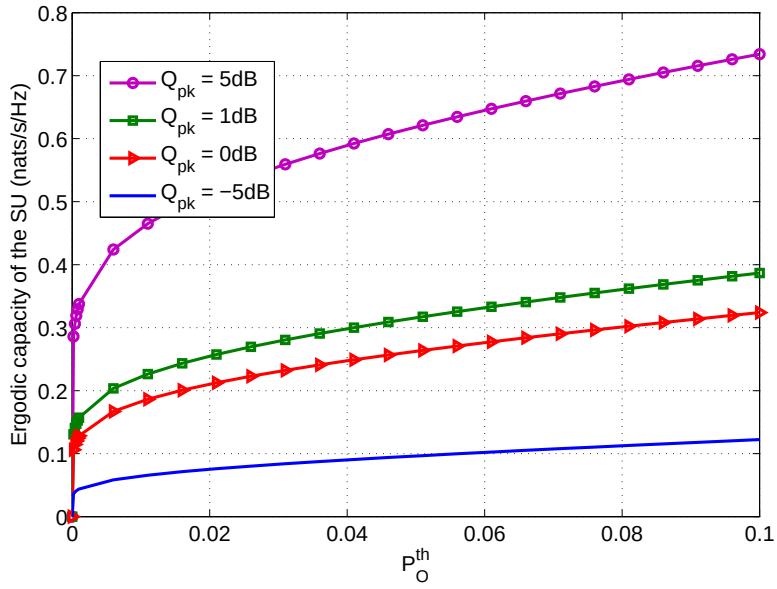

Figure 6. Ergodic capacity of the SU versus P_O^{th} for different values of Q_{pk} and $\rho = \overline{g}_{ps}/\overline{g}_{ss} = 1$.

2.3.2 Long Term Constraints

We consider the long-term constraints are as follows: average transmit power constraint (ATP) and average interference power constraint (AIP) at the primary user. One formulation of the optimization problem is given by

$$\mathbf{O_2}: \quad \underset{p_s(g_{ss},g_{ps})\geq 0}{\text{maximize}} \quad \mathbb{E}\left[\log\left(1+\frac{p_s(g_{ss},g_{ps})g_{ss}}{N_1 B}\right)\right] \tag{2.14}$$

$$\mathbf{C_2^1}: \quad \mathbb{E}\left\{p_s(g_{ss},g_{ps})g_{ps}\right\} \leq Q_{av} \tag{2.15}$$

$$\mathbf{C_2^2}: \quad \mathbb{E}\left\{p_s(g_{ss},g_{ps})\right\} \leq P_{av} \tag{2.16}$$

where $\mathbf{C_2^1}$ and $\mathbf{C_2^2}$ denote the AIP constraint and ATP constraint, respectively, associated to objective function $\mathbf{O_2}$. Q_{av} represents the predefined average interference power caused by the SU at the primary receiver, and P_{av} denotes the average transmit power.

Here we have to point out that besides the mentioned long-term constraints above there is another constraint called primary capacity loss constraint (PCLC) proposed in (Zhang 2008). This method was shown to be better than the common ones, e.g. the average and/or peak interference power constraints, in terms of achievable ergodic capacities of both the primary and the secondary links. It protects the primary transmission by ensuring that the maximum ergodic capacity loss of the primary link, due to the secondary transmission, is no greater than some predefined value. However, to enable the scheme, not only the CSI of the secondary fading channel and the fading channel from the secondary transmitter to the primary receiver, but also the CSI of the primary direct link. For details please refer to (Zhang 2008).

2.3.2.1 AIP constraint only with perfect CSI

In this scenario, the secondary user aims to maximize its ergodic capacity under the average interference power (AIP) constraint predefined by the primary user. This problem is denoted as $(\mathbf{O_2}, \mathbf{C_2^1})$. The optimal power allocation scheme is waterfilling, which is given in (Ghasemi & Sousa 2007) by

$$p_s^*(g_{ss},g_{ps}) = \left[\frac{1}{\lambda g_{ps}} - \frac{N_1 B}{g_{ss}}\right]^+, \tag{2.17}$$

Table 1. Ergodic Capacity of the SU with perfect SCI under AIP constraint.

g_{ss}	g_{ps}	Ergodic Capacity (nats/s/Hz)
AWGN	AWGN	$\log\left(1+\frac{Q_{av}}{N_1B}\right)$
Lognormal (σ^2)	Lognormal (σ^2)	$\frac{\log\gamma_0}{2}\left[1+\text{erf}\left(\frac{\log\gamma_0}{2\sigma}\right)\right]+\frac{\sigma}{\sqrt{\pi}}\exp\left(-\frac{\log^2\gamma_0}{4\sigma^2}\right)$
Exponential (1)	Exponential (1)	$\log(1+\gamma_0)$
Nakagami ($m=2$)	Nakagami ($m=2$)	$\log(1+\gamma_0)-\frac{\gamma_0}{(1+\gamma_0)^2}$

* $\gamma_0 = 1/\lambda N_1 B$

where $[x]^+ = \max(x,0)$, and g_{ss} and g_{ps} denote the channel power gains from the secondary transmitter to the secondary receiver (ST-SR) and primary receiver (ST-PR), respectively. N_1 is the noise density at the SR, B denotes the bandwidth, and $\lambda \geq 0$ is the Lagrangian multiplier satisfying the AIP constraint given by (2.15). From the power allocation strategy, it is obvious that when the secondary link is in a good condition, the secondary user may not transmit if the interference link is also in a good condition, which is dislike the conventional waterfilling strategy in (Cover & Thomas 2006). The authors in (Ghasemi & Sousa 2007) named this strategy as a 2-dimensional waterfilling. The ergodic capacity is given by

(2.18)
$$C = \mathbb{E}\left[\log\left(1+\left[\frac{g_{ss}}{\lambda N_1 B g_{ps}}-1\right]^+\right)\right] = \iint_{\frac{g_{ss}}{\lambda N_1 B g_{ps}}\geq 1} \log\left(\frac{g_{ss}}{\lambda N_1 B g_{ps}}\right) dg_{ss}dg_{ps}$$

Table 1, which holds in (Ghasemi & Sousa 2007), illustrates expressions of the ergodic capacity of the SU given the channel distributions. Figure 7 depicts the ergodic capacity. Fading is beneficial to the cognitive radios. In the low Q_{av} (normalized by N_1B) regime, with fading the CR achieves mush better ergodic capacity than the AWGN case. On the other hand, in high Q_{av} (normalized by N_1B) regime, all the ergodic capacity approaches to the AWGN ergodic capacity. For some ranges of Q_{av} (normalized by N_1B), the fading degrades the ergodic capacity. This can be explained as that the CR can not utilize all the transmission opportunities because of the average interference power constraint.

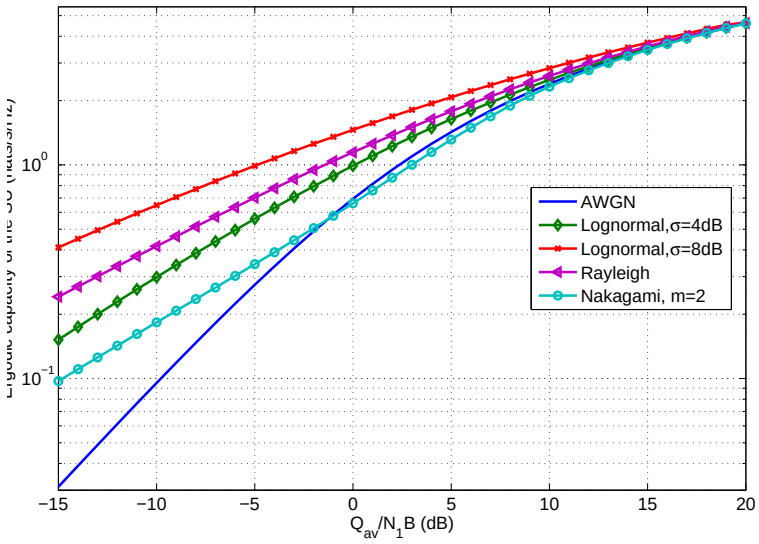

Figure 7. Ergodic capacity of the SU with perfect CSI under AIP constraint in different fading scenarios.

The above considers the perfect CSI. However, as we know that the channel gains may be obtained through measurements which suffers estimate errors. Therefore, the following illustrates the effects of imperfect CSI on the power allocation and ergodic capacity of the secondary user.

2.3.2.2 AIP constraint with imperfect CSI

The previous strategy considers the perfect channel state information. However, there may have estimate errors on the channel gains. According to the channel estimate mode reviewed in Section 2.2, the optimization problem and the OPA for the SU in fading environments with imperfect channel information of interference link has been presented in (Musavian & Aissa 2009b) as follows.

$$\mathbf{O_3}: \quad \underset{p_s(g_{ss},\hat{g}_{ps})\geq 0}{\text{maximize}} \quad \mathbb{E}\left[\log\left(1+\frac{g_{ss}p_s(g_{ss},\hat{g}_{ps})}{N_1B}\right)\right] \tag{2.19}$$

$$\mathbf{C_3^1}: \quad \mathbb{E}_{g_{ss},\hat{g}_{ps}}\left[p_s(g_{ss},\hat{g}_{ps})\hat{g}_{ps}\right]+\sigma_e^2\mathbb{E}_{g_{ss},\hat{g}_{ps}}\left[p_s(g_{ss},\hat{g}_{ps})\right]\leq Q_{av} \tag{2.20}$$

where $\hat{g}_{ps}$ denotes the estimated channel power gain of the ST-PR link, and σ_e^2 represents the variance of the channel power gain estimation error. In addition, $\mathbb{E}_{g_{ss},\hat{g}_{ps}}[\cdot]$ defines the expectation over joint probability density function of g_{ss} and $\hat{g}_{ps}$. We can see that there is a penalty on the transmission power of the secondary

user because of the imperfect channel estimation. Then Using the Lagrangian method, the optimal power allocation can be directly obtained as

$$p_s^*(g_{ss}, \hat{g}_{ps}) = \max\left\{0, \frac{1}{\lambda\,(\hat{g}_{ps} + \sigma_e^2)} - \frac{N_1 B}{g_{ss}}\right\} \tag{2.21}$$

where the Lagrangian multiplier $\lambda \geq 0$ satisfies the average interference power constraint, and $\max\{0, \cdot\}$ operator guarantees nonnegative transmit power.

The analytic results with/without perfect CSI are illustrated in Figure 8. The SU loses its capacity because of the channel estimate error that the SU has to lower its transmit power to satisfy the AIP constraint. In addition, it is worth noting that at higher values of AIP constraint, the ergodic capacity of the SU with estimate error under Rayleigh fading is less than the one under AWGN, since the SU has to use less transmit power in order to satisfy the AIP constraint so that loses some opportunities for transmission. Therefore, it is important to study the ergodic capacity with other techniques for mitigating the influence of the estimation error, e.g., diversity technique. The diversity technique is an efficient means to increase the channel capacity (Alouini & Goldsmith 1999; Brennan 2003; Telatar 1999). We will study the OPA strategy of the secondary user under the imperfect CSI and receiving MRC diversity, and the resultant ergodic capacity in the following chapters.

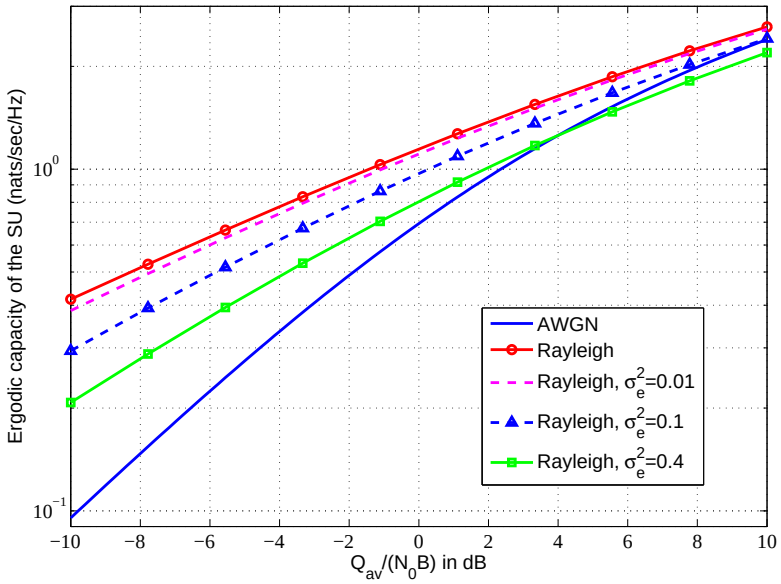

Figure 8. The ergodic capacity of the SU under AIP constraint for AWGN, and Rayleigh fading with/without estimation errors of ST-PR.

2.3.2.3 ATP and AIP Constraints

Under average transmit power constraint and average interference power constraint predefined by the primary user, the optimization problem is given by ($\mathbf{O_2}$, $\mathbf{C_2^1}$, $\mathbf{C_2^2}$) in (2.14), (2.15), and (2.16), respectively. The associated optimal power allocation scheme for the secondary user to maximize the ergodic capacity is given in (Kang *et al.* 2009) by

$$p_s^*(g_{ss}, g_{ps}) = \left(\frac{1}{\mu + \lambda g_{ps}} - \frac{N_1 B}{g_{ss}} \right)^+, \tag{2.22}$$

where μ and λ are the nonnegative Lagrangian variables associated with the average transmit power constraint in (2.16) and average interference power constraint in (2.15), respectively. We can see that this scheme is also waterfilling. However, the water lever is related to not only the interference channel condition, but also the average transmit power. Intuitively, even having enough power budget for transmission and the CR link has a very good condition, the secondary user may not able to transmit if the interference channel in a very good condition. To solve this problem ($\mathbf{O_2}$, $\mathbf{C_2^1}$, $\mathbf{C_2^2}$) we used ellipsoid method (Bland *et al.* 1981; Boyd & Vandenberghe 2004), shown in Table 2.

Table 2. Ellipsoid Method: Pseudocode.

1) Initialization: (subscript or superscript, k, denotes the kth loop)
   λ_1: Lagrangian multiplier associated to AIP.
   μ_1: Lagrangian multiplier associated to ATP.
   A_1: a 2×2 positive-definite matrix. An Ellipsoid, E_k, can be defined as
   $$\mathbf{E}_k(x_k, A_k) = \left\{ \begin{bmatrix} \lambda_k \\ \mu_k \end{bmatrix} : \left(\begin{bmatrix} \lambda_k \\ \mu_k \end{bmatrix} - x_k \right)^T A_k^{-1} \left(\begin{bmatrix} \lambda_k \\ \mu_k \end{bmatrix} - x_k \right) \leq 1 \right\}, \text{ where}$$
   x_k is the center of $\mathbf{E}_k$.
2) repeat{
   a) calculate $p_s^{(k)}$ using (2.22).
   b) calculate the subgradients at $\begin{bmatrix} \lambda_k \\ \mu_k \end{bmatrix}$ using
   $$sg = \begin{bmatrix} Q_{pk} - \mathbb{E}\left\{ p_s^{(k)}(g_{ss}, g_{ps}) g_{ps} \right\} \\ P_{av} - \mathbb{E}\left\{ p_s^{(k)}(g_{ss}, g_{ps}) \right\} \end{bmatrix}$$
   and normalized subgradients $\tilde{sg} = sg / \sqrt{sg^T A_k sg}$
   c) update the multipliers and the ellipsoid by
   $$\begin{bmatrix} \lambda_{k+1} \\ \mu_{k+1} \end{bmatrix} = \begin{bmatrix} \lambda_k \\ \mu_k \end{bmatrix} - \frac{A_k \tilde{sg}}{2+1}.$$
   $$A_{k+1} = \frac{2^2}{(2+1)^2 - 1} \left(A_k - \frac{2}{2+1} A_k \tilde{sg} \tilde{sg}^T A_k \right).$$
   } until $\mathbb{E}\left\{ p_s^{(k)}(g_{ss}, g_{ps}) g_{ps} \right\} - Q_{pk} \leq 0$, $\mathbb{E}\left\{ p_s^{(k)}(g_{ss}, g_{ps}) \right\} - P_{av} \leq 0$,
   and $\sqrt{sg^T A_k sg} < \varepsilon$, where ε is the desired accuracy.

We show the simulation results in the Figure 9 and in Figure 10, where we illustrate the ergodic capacity of the SU using bits/s/Hz instead of nats/s/Hz only for a purpose of comparison with the original results shown in (Kang *et al.* 2009). We can see from the figures that at low P_{av} case the ergodic capacity is mainly affected by the average transmit power constraint, in other words, ATP dominates AIP. On the other hand, at high P_{av} regime, AIP dominates ATP.

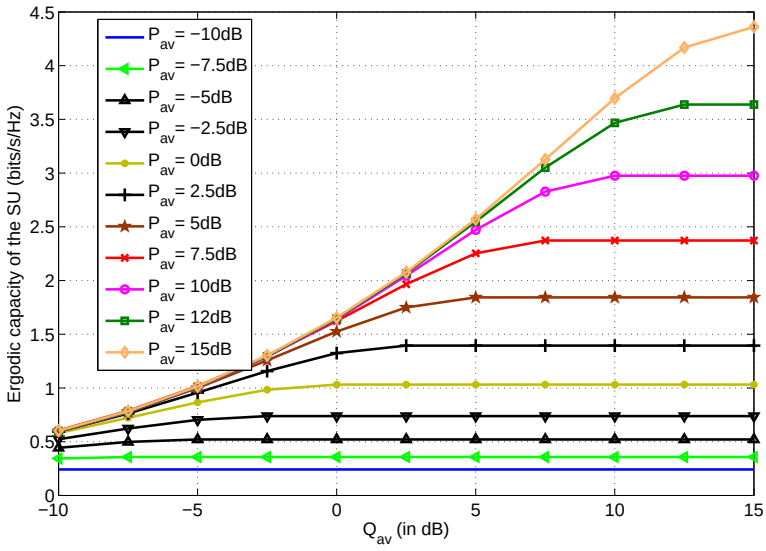

Figure 9. The ergodic capacity of the SU under AIP and ATP constraints.

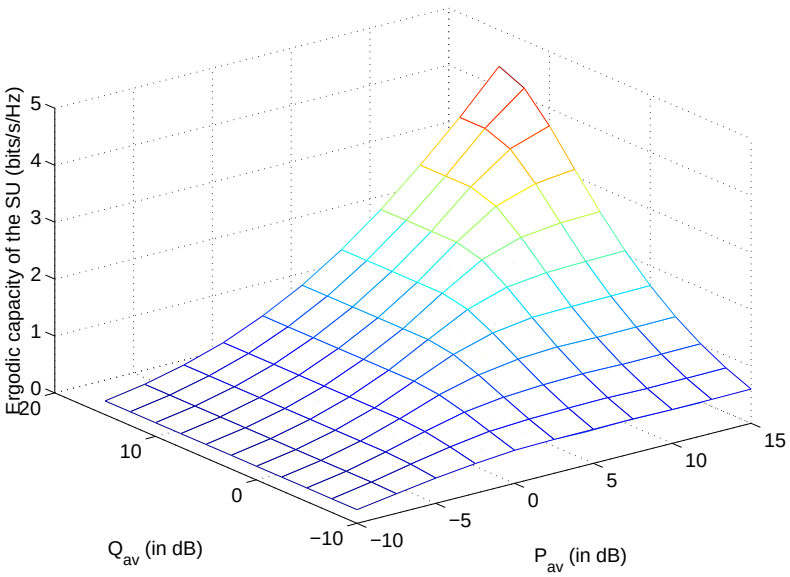

Figure 10. The ergodic capacity of the SU under AIP and ATP constraints.

2.3.2.4 AIP constraint with imperfect CSI and receive MRC

The optimal power allocation schemes and the associated ergodic capacity of the SU with receive MRC and imperfect ST-PR channel state information under the AIP constraint are presented in detail in Chapter 4.

From previous analysis, we can see that under the long-term constraints the optimal power allocation approaches are (modified) waterfilling, and the water-level is jointly decided by the long-term constraints. In the following, we will take a look at how the combined constraints, long-term and short-term, influence the power allocation and the ergodic capacity.

2.3.3 Combined Long-term and Short-term Constraints

This section reviews the optimal power allocation schemes and the ergodic capacity of the secondary user under the combined long-term and short-term constraints, which is pretty different from the long-term constraints cases (Khojastepour & Aazhang 2004). The optimization problem may be formulated as

$$\mathbf{O_4}: \quad \underset{p_s(g_{ss},g_{ps})\geq 0}{\text{maximize}} \quad \mathbb{E}\left\{\log\left(1+\frac{g_{ss}p_s(g_{ss},g_{ps})}{N_1B}\right)\right\} \tag{2.23}$$

$$\mathbf{C_4^1}: \quad p_s(g_{ss},g_{ps})g_{ps} \leq Q_{pk} \tag{2.24}$$

$$\mathbf{C_4^2}: \quad p_s(g_{ss},g_{ps}) \leq P_{pk} \tag{2.25}$$

$$\mathbf{C_4^3}: \quad \mathbb{E}\left\{p_s(g_{ss},g_{ps})g_{ps}\right\} \leq Q_{av} \tag{2.26}$$

$$\mathbf{C_4^4}: \quad \mathbb{E}\left\{p_s(g_{ss},g_{ps})\right\} \leq P_{av} \tag{2.27}$$

where (2.24) represents the peak interference power (PIP) constraint, (2.25) is the peak transmit power (PTP) constraint indicating the maximal transmit power of the SU, (2.26) and (2.27) are the average interference power (AIP) constraint and the average transmit power (ATP) constraint, respectively. The optimization problem can be solved by using Lagrangian method. The numerical results can be obtained through using bisection method.

2.3.3.1 PIP and AIP Constraints

Under the PIP and AIP constraints predefined by the primary user, the optimization problem is given by $(\mathbf{O_4}, \mathbf{C_4^1}, \mathbf{C_4^3})$ in (2.23), (2.24), and (2.26). The resultant optimal power allocation for the secondary user holds in (Musavian & Aissa 2009a) by

$$p^*(g_{ss},g_{ps}) = \begin{cases} \frac{Q_{pk}}{g_{ps}}, & \frac{g_{ps}}{g_{ss}} < \frac{\lambda_0}{N_1B} \\ \frac{1}{\lambda_1 g_{ps}} - \frac{N_1B}{g_{ss}}, & \frac{\lambda_0}{N_1B} \leq \frac{g_{ps}}{g_{ss}} \leq \frac{\lambda_1}{N_1B} \\ 0, & \text{otherwise} \end{cases} \tag{2.28}$$

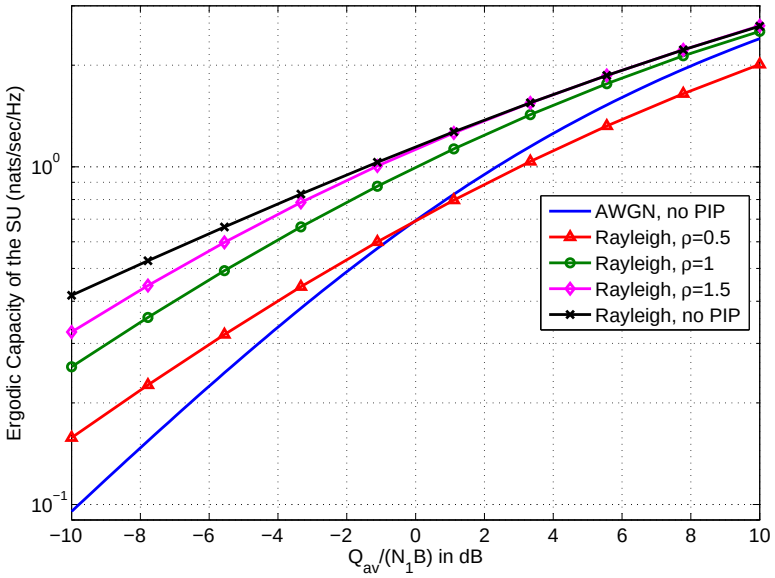

Figure 11. Ergodic capacity of the SU under average and peak interference constraints for AWGN and Rayleigh fading with different values of $\rho = \frac{Q_{pk}}{Q_{av}}$.

where the Lagrangian multipliers $\lambda_0 \geq 0$ and $\lambda_1 \geq 0$ are associated to the PIP constraint given by (2.24) and AIP constraint by (2.26), respectively. We can see that the optimal power control to achieve the secondary maximum ergodic capacity under joint peak and average interference power constraints at the primary receiver is a function of the channel state information of the secondary user and of the link ST-PR. Compared to the case that there is only AIP constraint, this strategy is a combination of channel inversion and water-filling. The ratio of the channel gains, $\frac{g_{ps}}{g_{ss}}$, plays a key role in this case. In Figure 11, the ergodic capacity of the SU is plotted for AWGN and Rayleigh fading with different ratios of $\rho = \frac{Q_{pk}}{Q_{av}}$. In addition, for $\rho > 1$ the figure states that at higher values of $Q_{av}/(N_1B)$, the PIP constraint can be ignored. Moreover, when $\rho < 1$ the secondary user loses some opportunities for transmission resulting in lower ergodic capacity than the AWGN case at higher regime of $Q_{av}/(N_1B)$.

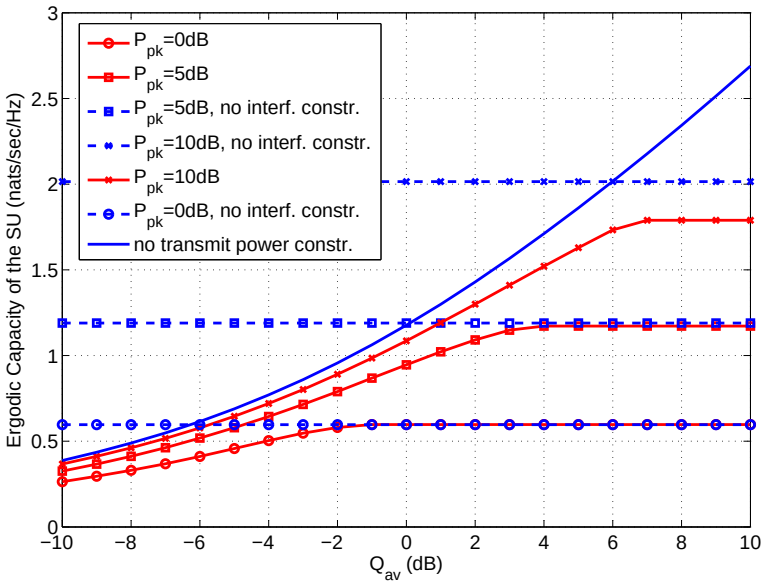

Figure 12. Ergodic capacity of the SU under different values of PTP and AIP constraints over Rayleigh fading.

2.3.3.2 PTP and AIP Constraints

The optimization problem under peak transmit power constraint (PTP) and average interference power constraint is given by $(\mathbf{O_4}, \mathbf{C_4^2}, \mathbf{C_4^3})$ in (2.23), (2.25), and (2.26). The optimal power allocation for the secondary user to maximize the ergodic capacity holds in (Kang *et al.* 2009) as

$$p_s^*(g_{ss}, g_{ps}) = \begin{cases} P_{pk}, & g_{ps} \leq \frac{1}{\lambda\left(P_{pk}+\frac{N_1 B}{g_{ss}}\right)} \\ \frac{1}{\lambda g_{ps}} - \frac{N_1 B}{g_{ss}}, & \frac{1}{\lambda\left(P_{pk}+\frac{N_1 B}{g_{ss}}\right)} < g_{ps} < \frac{g_{ss}}{\lambda N_1 B} \\ 0, & \frac{g_{ss}}{\lambda N_1 B} \leq g_{ps} \end{cases} \tag{2.29}$$

The Lagrangian multiplier λ satisfies the following KTT condition

$$\mathbb{E}_{g_{ss},g_{ps}}\left[g_{ps} p_s^*(g_{ss}, g_{ps})\right] = Q_{av} \tag{2.30}$$

The optimal power allocation scheme is a combination of the fixed power transmission and the water filling approach. Figure 12 depicts the simulation results.

If there is no interference power constraint, the secondary user transmits by using its maximal transmit power. With the combination of PTP and AIP constraints, if the value of the AIP constraint is smaller compared to the value of the PTP, the secondary user looses some opportunities to transmit. This corresponds to the AIP-dominant regime. On the other hand, if the PTP is dominant, the ergodic capacity is unbounded by the ergodic capacity with the ATP constraint. This is because that the SU has a lot of chances to transmit, but the PTP limits the ergodic capacity.

2.3.3.3 ATP and PIP Constraints

Under the average transmit power constraint and peak interference power constraint, the optimization problem is formulated by $(\mathbf{O_4}, \mathbf{C_4^1}, \mathbf{C_4^4})$ in (2.23), (2.24), and (2.27). The resultant optimal power allocation for the secondary user holds in (Kang *et al.* 2009) as

$$p_s^*(g_{ss}, g_{ps}) = \begin{cases} \frac{Q_{pk}}{g_{ps}}, & g_{ps} \geq \frac{Q_{pk}}{\frac{1}{\lambda} - \frac{N_1 B}{g_{ss}}}, g_{ss} > \lambda N_1 B \\ \frac{1}{\lambda} - \frac{N_1 B}{g_{ss}}, & g_{ps} < \frac{Q_{pk}}{\frac{1}{\lambda} - \frac{N_1 B}{g_{ss}}}, g_{ss} > \lambda N_1 B \\ 0, & g_{ss} \leq \lambda N_1 B \end{cases} \tag{2.31}$$

It is intuitive that the power allocation scheme is a combination of channel inverse and waterfilling. The waterfilling reflects the average transmit power constraint and the channel inverse reflects the peak interference power constraint. The simulation results are shown in Figure 13. The ergodic capacity of the SU is capped by $\log\left(1 + \frac{Q_{pk}}{g_{ps} N_1 B} g_{ss}\right)$. In the low-ATP regime, the ergodic capacity is dominated by the ATP constraint, while in the high-ATP regime the ergodic capacity is limited by the PIP. These can be explained as follows: In the low-ATP regime, the power allocation scheme is mainly the water-filling, and in in the high-ATP regime the power allocation scheme is performed as the channel inversion.

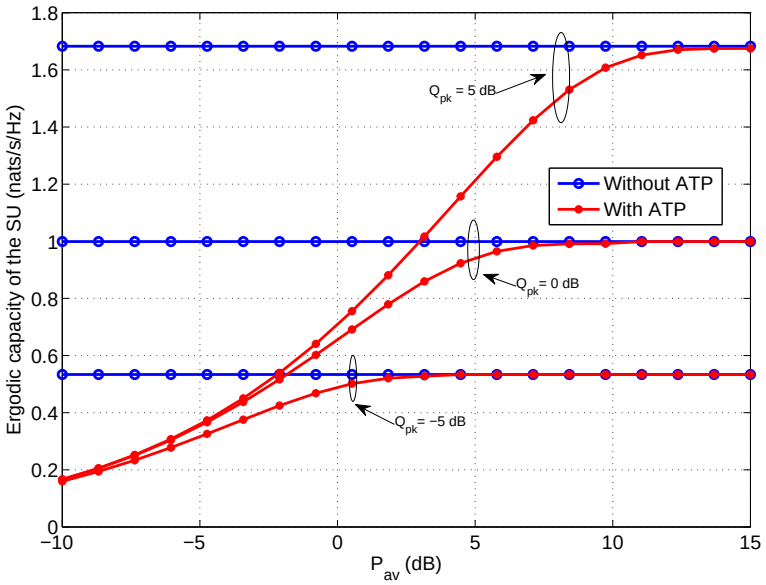

Figure 13. Ergodic capacity of the SU under different values of ATP and PIP Constraints over Rayleigh fading.

2.3.4 Summary

We can see that the strategies how the secondary user allocates the optimal transmit power to maximize the ergodic capacity are decided by the types of constraints. When the constraint is the peak interference constraint, the OPA is the channel inversion with respect to the interference channel from the secondary transmitter to the primary receiver (ST-PR). If the constraint is the average interference constraint, the OPA is the water-filling scheme, where the water level is decided by the interference channel, ST-PR, power gain. For the combined long-term and/or short-term constraints, the OPA schemes are combined channel inversion and water filling or two-dimensional water filling. As we know that in the analysis of ergodic capacity, the delay limit is not considered which means that it can be approaching to infinity. In the successive section, we review the effective capacity which takes the delay into consideration.

2.4 Effective Capacity

The concept of effective capacity (EC) has been reviewed in subsection 2.2.2. This section reviews some results of optimal power allocation strategies and effective

capacity of the secondary user over block fading channels. The objective function and possible constraints are listed in the following,

$$\mathbf{O_5}: \quad \underset{p_s(\theta,g_{ss},g_{ps})\geq 0}{\text{maximize}} \quad -\frac{1}{\theta}\log\left[\mathbb{E}\left(e^{-\theta TB\log\left(1+\frac{p_s(\theta,g_{ss},g_{ps})g_{ss}}{N_1B}\right)}\right)\right] \tag{2.32}$$

Constraints:

$$\mathbf{C_5^1}: \quad p_s(\theta,g_{ss},g_{ps})g_{ps} \leq Q_{pk} \tag{2.33}$$

$$\mathbf{C_5^2}: \quad p_s(\theta,g_{ss},g_{ps}) \leq P_{pk} \tag{2.34}$$

$$\mathbf{C_5^3}: \quad \mathbb{E}\left\{p_s(\theta,g_{ss},g_{ps})g_{ps}\right\} \leq Q_{av} \tag{2.35}$$

$$\mathbf{C_5^4}: \quad \mathbb{E}\left\{p_s(\theta,g_{ss},g_{ps})\right\} \leq P_{av} \tag{2.36}$$

where T denotes the block length duration, B is the channel bandwidth, θ is the delay exponent, P_{pk} denotes the maximum allowed peak transmit power, P_{av} denotes the average transmit power constraint, and Q_{pk} and Q_{av} represent the peak and average interference power threshold, respectively. We can use Lagrangian method to solve the optimization problems with different combinations of constraints. Without loss of generality we assume that $TB = 1$ and $N_1B = 1$ in following simulations.

2.4.1 Short-term Constraint

The same as in the previous sections that the short-term constraints include the peak transmit power constraint and the peak interference power constraint.

2.4.1.1 PTP and PIP Constraints

The optimization problem is given by $(\mathbf{O_5}, \mathbf{C_5^1}, \mathbf{C_5^3})$ in (2.32), (2.33), and (2.34). The power allocation strategy is straightforward obtained that the SU transmits using the power of $\min\left(P_{pk}, \frac{Q_{pk}}{g_{ps}}\right)$. Then the effective capacity can be obtained as

$$EC = -\frac{1}{\theta}\log\left\{\mathbb{E}\left[\left(1+\frac{\min\left(P_{pk},\frac{Q_{pk}}{g_{ps}}\right)g_{ss}}{N_1B}\right)^{-\theta TB}\right]\right\} \tag{2.37}$$

Given the distributions of the fading channels, the expression of the EC can be obtained numerically, since, to the best of our knowledge, there are no closed-form expressions for the common fading scenarios, e.g., Rayleigh and Nakagami-m. Thus we derive the upper bound expression, i.e. without considering the peak

transmit power constraint, under independent Rayleigh fading for the effective capacity of this case as a verification. Let h denote the ratio of two independent exponential variables $\frac{g_{ss}}{g_{ps}}$, and $\bar{h}$ be the mean ratio of $\overline{g}_{ss}/\overline{g}_{ps}$. Then we have the p.d.f. of h by using (Papoulis & Pillai 2002: 5-15) as

$$f(h) = \frac{\overline{h}}{\left(h+\overline{h}\right)^2} \tag{2.38}$$

$$\begin{aligned} EC^{ub} &= -\frac{1}{\theta}\log\left\{\mathbb{E}\left[\left(1+\frac{Q_{pk}g_{ss}}{g_{ps}N_1B}\right)^{-\theta TB}\right]\right\} \\ &= -\frac{1}{\theta}\log\left\{\underbrace{\mathbb{E}\left[\left(1+\frac{Q_{pk}h}{N_1B}\right)^{-\theta TB}\right]}_{\mathcal{C}_1}\right\} \end{aligned}$$

where

$$\begin{aligned} \mathcal{C}_1 &= \int_0^\infty \left(1+\frac{Q_{pk}h}{N_1B}\right)^{-\theta TB}\frac{\overline{h}}{\left(h+\overline{h}\right)^2}dh \\ &= \mathcal{B}(1,1+\theta TB)\,{}_2F_1\left(\theta TB,1;\theta TB+2,1-\frac{Q\overline{h}}{N_1B}\right) \end{aligned}$$

where, in the last step, we have used (Gradshteyn & Ryzhik 2007: 3.197-1), ${}_2F_1\left(a,b;c,d\right)$ is hypergeometric function (Gradshteyn & Ryzhik 2007: 9.14), and $\mathcal{B}(a,b)$ denotes the beta function (Gradshteyn & Ryzhik 2007: 8.38).

Then we have

$$EC^{ub} = -\frac{1}{\theta}\log\left\{\mathcal{B}(1,1+\theta TB)\,{}_2F_1\left(\theta TB,1;\theta TB+2,1-\frac{Q\overline{h}}{N_1B}\right)\right\} \tag{2.39}$$

Figures 14 and 15 illustrate the effective capacity of the SU versus different values of the delay component along with the different ratios of PIP and PTP over Rayleigh fading. In the simulation we assume that the mean value of the channel power gains are 1, and the AWGN power at the receiver is 1. First, it is intuitive that when the value of Q_{pk} decreases, i.e. ρ decreases, the effective capacity of the SU decreases. Second, when the value of ρ is bigger than 1 , for instance, $\rho = 1$ and $\rho = 100$, the effective capacity of the SU increases slowly and will converge.

This is because the peak transmit power constraint becomes to dominate. In the two figures, we also show the upper bounds given by Eq. (2.39), i.e. no peak transmit power constraint, for $Q_{pk} = -5$dB and $Q_{pk} = 5$dB.

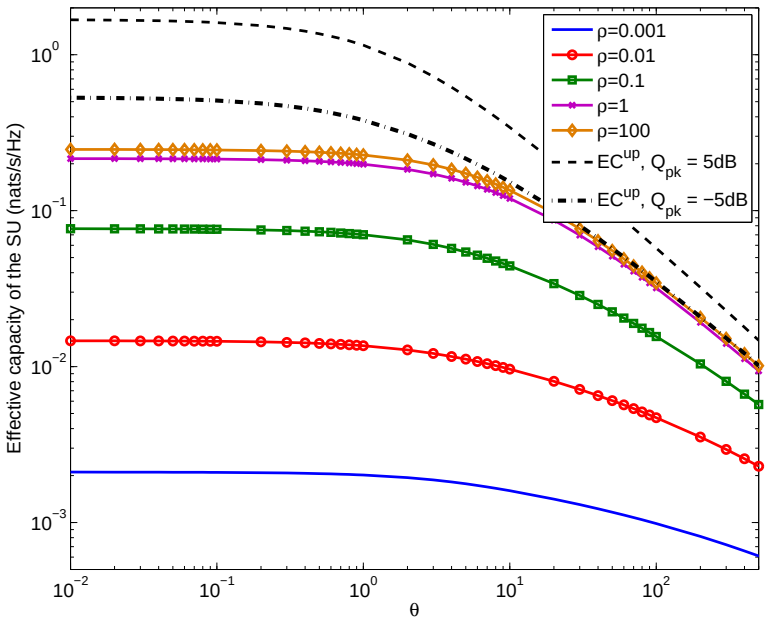

Figure 14. Effective capacity of the SU under different values of θ over Rayleigh fading with $P_{pk} = -5dB$, where $\rho = Q_{pk}/P_{pk}$.

2.4.2 Long-term Constraints

In the following, we review the optimal power allocation strategies and the simulation results of the effective capacity of the SU under long-term constraints.

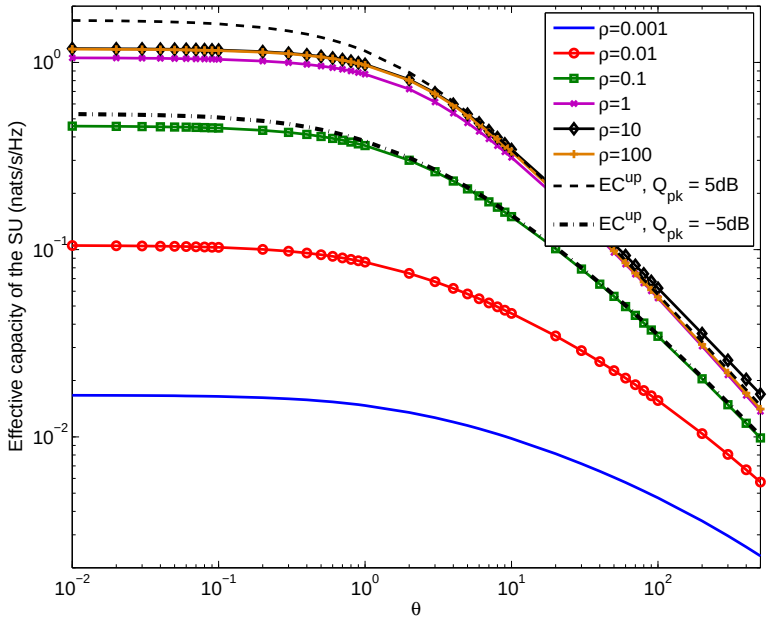

Figure 15. Effective capacity of the SU under different values of θ over Rayleigh fading with $P_{pk} = 5dB$, where $\rho = Q_{pk}/P_{pk}$.

2.4.2.1 AIP Constraint

Under average interference power constraint and secondary QoS constraint, the optimization problem is given by $(\mathbf{O_5}, \mathbf{C_5^3})$ in (2.32) and (2.34). The resultant optimal power allocation for the secondary user to maximize effective capacity holds in (Musavian & Aissa 2010) by

$$p_s^*(\theta, g_{ss}, g_{ps}) = \begin{cases} N_1 B \left[\frac{\beta^{\frac{1}{1+\alpha}}}{g_{ps}^{\frac{1}{1+\alpha}} g_{ss}^{\frac{\alpha}{1+\alpha}}} - \frac{1}{g_{ss}} \right]^+, & g_{ps} \leq \beta g_{ss} \\ 0, & \text{otherwise} \end{cases} \tag{2.40}$$

where $[x]^+ = \max(0,x)$, $\alpha = \theta TB$, $\beta = \frac{\alpha}{\lambda N_1 B}$, and λ is the non-negative Lagrangian variable associated with the average interference power constraint. Based on the above optimal power allocation scheme, the closed-form expression of the effective capacity of the SU over Nakagami-m fading channels was derived in (Musavian & Aissa 2010). Here we show the simulations over i.i.d. Rayleigh fading channels.

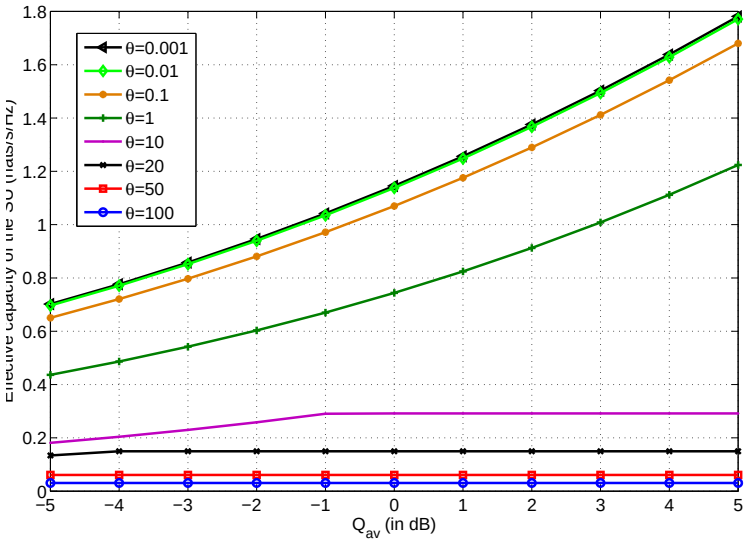

Figure 16. Effective capacity of the SU under different values of θ over Rayleigh fading.

From the simulation shown in Figure 16 we can see that when the delay is stringent (θ has large values), the average interference power constraint sightly influences the effective capacity of the SU. This is because the SU needs to transmit at very low rate in order to fulfill the delay requirement. This is, the delay component dominates the effective capacity of the SU. On the other hand, θ is small, the AIP has dramatic influence on the effective capacity. The reason is that in lower AIP regime the SU has very limited amount of opportunities to transmit; however, in higher AIP regime, the SU could utilize almost all the opportunities for its transmission. Now the AIP dominates the effective capacity of the SU.

2.4.2.2 ATP and AIP Constraints

The results of the effective capacity under the average interference power and average transmit power constraints along with the QoS constraint, to the best of our knowledge, have not been proposed in literature. In following we show our results.

The optimization problem is given by $(\mathbf{O_5}, \mathbf{C_5^3}, \mathbf{C_5^4})$ in (2.32), (2.35), and (2.36). The resultant optimal power allocation for the secondary user to maximize effec-

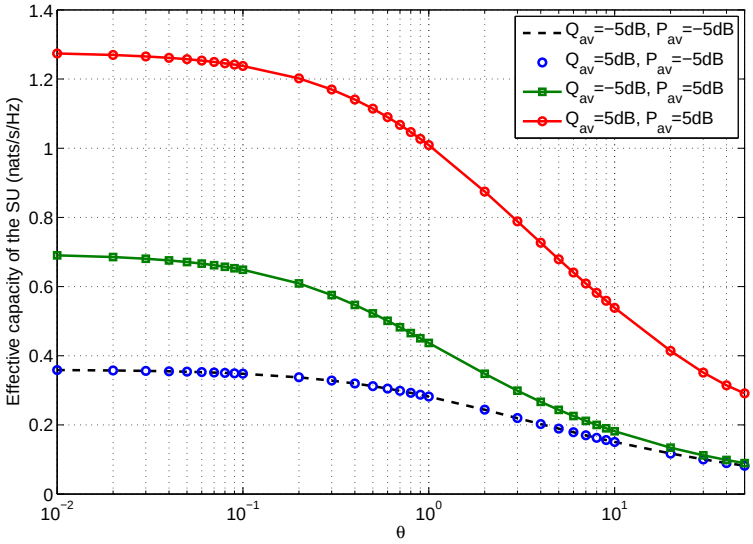

Figure 17. Effective capacity of the SU over Rayleigh fading.

tive capacity can be obtained by using Lagrangian method as

$$p_s^*(\theta, g_{ss}, g_{ps}) = N_1 B \left[\frac{\alpha^{\frac{1}{1+\alpha}}}{(N_1 B(\lambda g_{ps} + \mu))^{\frac{1}{1+\alpha}} g_{ss}^{\frac{\alpha}{1+\alpha}}} - \frac{1}{g_{ss}} \right]^+ \tag{2.41}$$

where $\alpha = \theta TB$, and λ and μ are the non-negative Lagrangian variables associated with the AIP constraint in (2.35) and ATP constraint in (2.36), respectively. To the best of our knowledge, with the above optimal power allocation scheme there is no closed-expression of the effective capacity. Here we show the simulations in Figure 17 for i.i.d. Rayleigh fading channels. The optimal power can be obtained applying the pseudocode in Table 2 by using proper transmit power and interference constraints. From the Figure, one thing we need to point out is that in the low ATP, $P_{av} = -5dB$, the ATP constraint dominates the effective capacity of the secondary user. This suggests us that when ATP$\ll$AIP, the secondary user can ignore the average interference constraint.

2.4.3 Combined Long- and Short-Term Constraints

To the best of our knowledge, the results of the effective capacity under the combined long-term and short-term constraints have not been proposed in literature. In following we show our results.

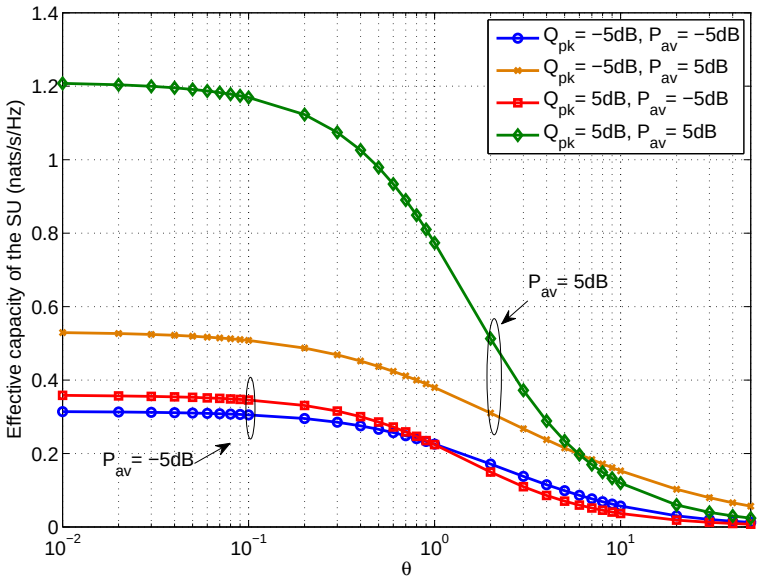

Figure 18. Effective capacity of the SU over Rayleigh fading under PIP and ATP constraints.

2.4.3.1 ATP and PIP Constraints

Under average transmit power and peak interference power constraints, and delay constraint, the optimization problem is given by $(\mathbf{O_5}, \mathbf{C_5^1}, \mathbf{C_6^4})$ in (2.32), (2.33) and (2.36). Using Lagrangian method, the resultant optimal power allocation for the secondary user to maximize effective capacity is obtained as

$$p_s^*(\theta, g_{ss}, g_{ps}) = \begin{cases} \min\left\{ \frac{Q_{pk}}{g_{ps}}, N_1 B \left[\frac{\beta^{\frac{1}{1+\alpha}}}{g_{ss}^{\frac{\alpha}{1+\alpha}}} - \frac{1}{g_{ss}} \right]^+ \right\}, & 1 \leq \beta g_{ss} \\ 0, & \text{otherwise} \end{cases} \tag{2.42}$$

where $\alpha = \theta TB$, $\beta = \frac{\alpha}{\lambda N_1 B}$, and λ is the non-negative Lagrangian variable associated with the average transmit power constraint. This power allocation is a water-filling scheme but capped by the peak interference power constraint. Therefore, the water level is defined by these two constraints. To the best of our knowledge, there is no closed-form expression for the effective capacity for this case. Here we show the simulations for i.i.d. Rayleigh fading channels in Figure 18.

In Figure 18, we can discover two differences from the previous case which is under AIP and ATP constraints. First, in low ATP, $P_{av} = -5dB$, cases, the values of the effective capacity for $Q_{pk} = -5$dB and $Q_{pk} = 5$dB are slightly different.

When the value of the delay component θ is small, i.e. the delay is not stringent, the higher Q_{pk} value, the larger effective capacity. However, when θ is big, the EC has lower values when $Q_{pk} = 5$dB than $Q_{pk} = -5$dB. Second, in the case that $P_{av} = 5$dB, the gap of the effective capacity of the two cases, $Q_{pk} = 5$dB and $Q_{pk} = -5$dB, increases. The effect of the Q_{pk} is similar in the lower and higher value regimes of θ. The phenomenon can be explained as follows: when θ is small, the secondary user is able to utilize higher power to transmit when the opportunities appear with the average transmit power budget; however, when delay requirement is stringent, the secondary user needs to maintain a constant rate as possible not to use a higher power to obtain a higher instantaneous transmission rate. In later case, the secondary user has more opportunities than the former case for transmission.

2.4.3.2 PTP and AIP Constraints

Under peak transmit power and average interference power constraints, and delay constraint, the optimization problem is given by $(\mathbf{O_5}, \mathbf{C_5^2}, \mathbf{C_5^3})$ in (2.32), (2.34) and (2.35). Using Lagrangian method, the resultant optimal power allocation for the secondary user to maximize effective capacity is obtained as

$$p_s^*(\theta, g_{ss}, g_{ps}) = \begin{cases} \min\left\{ P_{pk}, N_1 B \left[\frac{\beta^{\frac{1}{1+\alpha}}}{g_{ps}^{\frac{1}{1+\alpha}} g_{ss}^{\frac{\alpha}{1+\alpha}}} - \frac{1}{g_{ss}} \right]^+ \right\}, & g_{ps} \leq \beta g_{ss} \\ 0, & \text{otherwise} \end{cases} \tag{2.43}$$

where $\alpha = \theta TB$, $\beta = \frac{\alpha}{\lambda N_1 B}$, and λ is the non-negative Lagrangian variable associated with the average interference power constraint. This power allocation scheme is capped by the peak transmit power. Thus the water level of the water filling algorithm is different from the AIP-only case and the ATP-PIP scenario that the water level is changing from block to block. To the best of our knowledge, there is no closed-form expression for the effective capacity for this case. In Figure 19 we show the simulations for i.i.d. Rayleigh fading channels.

From Figure 19 we can see that when the average interference power constraint is low, $Q_{av} = -5$dB, higher peak transmit power threshold is not an advantage at the higher P_{pk} regime. In addition, the effective capacity of the case of $Q_{av} = 5$dB and $P_{av} = -5$dB is supreme over the case of $Q_{av} = -5$dB and $P_{av} = 5$dB at the stringent delay regime. This can be explained as that when θ is large, the secondary user

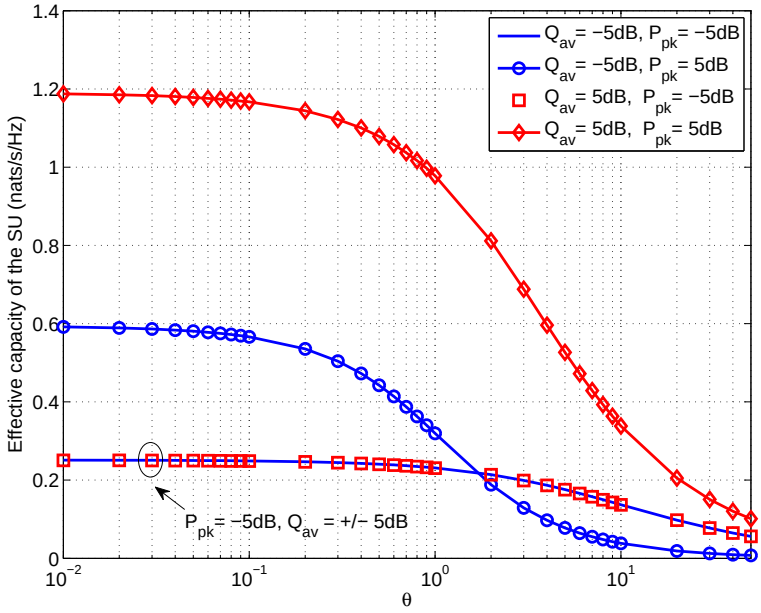

Figure 19. Effective capacity of the SU over Rayleigh fading under AIP and PTP constraints.

needs to maintain the rate as constant as possible, and in lower Q_{av} and higher P_{pk} case the SU has much less opportunities to transmit than the case of higher Q_{av} and lower P_{pk}. Moreover, when the PTP constraint is lower and not bigger than Q_{av}, $P_{pk} = -5$dB, the AIP constraint can be ignored.

2.5 Conclusion

In this chapter, we reviewed the main results of the optimal power allocation schemes for cognitive radios under different constraints and objectives.

The optimal power allocation schemes mainly can be categorized as following:

- *Channel inversion*: when only the peak interference power constraint is applied, i.e. short-term constraint.
- *Two-dimensional waterfilling*: when the average transmit and/or interference power constraints are applied, i.e. long-term constraints.
- *Capped two-dimensional waterfilling*: when the average/peak transmit power constraint and peak/average interference power constraint are considered, i.e. combined long- and short-constraints.

The ergodic capacity is mainly influenced by the interference channel from the secondary transmitter to the primary receiver. In addition, the effective capacity is affected by the delay component besides the interference channel. Especially, the short-term constraints, i.e. peak transmit power and peak interference power constraints, have different influences on the effective capacity over lower and higher delay component regimes.

In order to improve the performance of the secondary system, we present the results of applying multiple antenna techniques at the secondary transmitter or receiver. The optimal power allocation schemes, ergodic capacity, effective capacity are studied in the specific chapters.

3 ERGODIC CAPACITY OF A COGNITIVE-SHARED SYSTEM WITH MRC UNDER ASYMMETRIC FADING*

3.1 Introduction

In this chapter we study the ergodic capacity of a spectrum sharing cognitive radio (CR) with Maximal Ratio Combining (MRC) diversity at the secondary receiver under asymmetric fading. We consider that the channel from secondary transmitter to primary receiver, ST-PR, suffers Nakagami-*m* fading while the one from the secondary transmitter to its receiver, ST-SR, experiences Rayleigh fading. This asymmetric scenario is practical because the interference channel from the secondary transmitter to the primary receiver (ST-PR) can be different from the one from the secondary transmitter to the secondary receiver (ST-SR) in reality (Suraweera *et al.* 2009). In addition, the Nakagami-*m* gives great flexibilities to study different scenarios, i.e. $m = 1$ Nakagami-*m* becomes Rayleigh, $m \to \infty$, it approaches the Gaussian distribution, and Rician can be obtained by choosing proper values of $1 < m < \infty$. Moreover, the ST-PR channel plays a key role on the achievable rate of the secondary user (Kang *et al.* 2009; Peha 2009). In this chapter we demonstrate through mathematical analysis and numerical simulation that exploiting MRC at the secondary receiver the secondary user is able to achieve higher ergodic capacity than using single receive antenna, and reduces the effect of the ST-PR channel when it is in less severe fading, i.e. m has bigger values, which strongly affects the capacity of CR channel.

From the previous chapters, it is clear that the electromagnetic radio spectrum is a precious natural resource regulated by the government agencies. The cognitive radio technology enables utilizing the scarce spectrum in a more efficient manner (Haykin 2005; Mitola 2000). This technology has been promoted by the Federal of Communications Commission (FCC) in the United States and by the Electronic Communications Committee (ECC) in Europe. Research on the capacity of spectrum sharing cognitive radio have attracted many researchers due to that the traditional capacity study of fading channels is under transmitter-centred constraints,

*Reprinted with permission from "Capacity for Spectrum Sharing Cognitive Radios with MRC Diversity at the Secondary Receiver under Asymmetric Fading" by Ruifeng Duan, M. Elmusrati, R. Jäntti and R. Virrankoski, In *Proc. IEEE Global Telecommunications Conference*, pp. 1-5, Copyright [2010] by the IEEE.

while it is not suitable for cognitive radio since we have to protect the primary users. The received-signal constraints can lead to substantially different results as compared to transmitted-signal constraints (Gastpar 2004). For instance, Gastpar (2004) proved, for a point-to-point AWGN non-fading channel, that the ergodic capacity under the transmit and the received-power constraints are largely equivalent. In network cases, however, they can lead to quite different conclusions, for example, multiple access channels with dependent sources and feedback, and collaborative communication scenarios.

Ghasemi and Sousa (2007) rightly pointed out that in many cases significant capacity gains can be achieved if the channels are varying due to fading under either the average or the peak interference power constraint through studying the ergodic capacity of the secondary user under Rayleigh, Nakagami-m and Log-normal fading. In (Suraweera *et al.* 2008), the authors extended the work in (Ghasemi & Sousa 2007) by investigating the achievable capacity gains in asymmetric fading environments. Musavian and Aïssa (2009b) revealed the capacity gains offered by the spectrum-sharing approach in a Rayleigh fading environment subject to both average and peak received-power constraints at the primary receiver. In (Zhang 2009), Zhang has drawn attention to the fact that the average-interference-power (AIP) constraint can be more advantageous over the peak-interference-power in order for minimizing the resultant capacity loss of the primary fading channel.

The mentioned research work above paid attention to the single receive antenna scenarios. The benefits in term of ergodic capacity of exploiting multiple receive antennas have been investigated in (Alouini & Goldsmith 1999) for a Rayleigh fading channel under the average transmit power constraint. In this chapter, we aim to investigate the ergodic capacity of a cognitive-shared block fading channel with receive MRC at the secondary receiver under asymmetric fading. This is due to the fact that in some scenarios there may have different spectral activities in the vicinity of the primary user and in the vicinity of the secondary receiver, such that these two links, ST-PR and ST-SR, could experience different fading (Jafar & Srinivasa 2007). The ergodic capacity of the secondary user for different m values and different combining diversities are analyzed mathematically and validated numerically. The results indicated that the receive MRC contributes more ergodic capacity even for non-severe fading ST-PR channel (in our simulation $m = 10$) than using a single receive antenna. This states that when the ST-PR link condition is getting better, for instance, m is increasing, the capacity of CR will decrease. However, by using more diversity for CR, we obtain higher capacity.

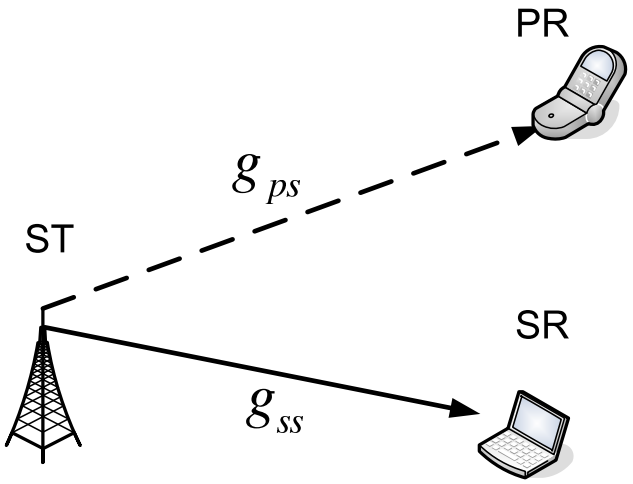

Figure 20. A cognitive-shared System model.

The remainder of this chapter is organized as follows. The channel and system model are proposed in Section 3.2. The ergodic capacity of a spectrum sharing cognitive radio with receives MRC is investigated in Section 3.3. Section 3.4 validates the analytical results through simulations. Finally, the last section concludes this chapter.

3.2 System and Channel Models

In this section we describe the channel and system models. A widely used system is consider in this chapter (Ghasemi & Sousa 2007), which is depicted in Figure 20. The CR transmission system block diagram of the MRC receiver is illustrated in Figure 21 (Alouini & Goldsmith 1999; Jakes 1994). We assume a block-fading environment (Caire *et al.* 1999; Ozarow *et al.* 1994). The ST-SR link experiences Rayleigh fading with unit mean, and the secondary receiver (refers to the receiver of the secondary user) is equipped with a L-branch MRC combiner, which are independent to each other. So that the composite channel power gain, g_{ss}, is characterized by the Chi-square (χ^2) distribution with $2L$ degrees of freedom, and the related probability density function of g_{ss} is given as follows (Jakes 1994; Proakis & Salehi 2008):

$$f_{g_{ss}}(g_{ss}) = \frac{g_{ss}^{L-1} e^{-g_{ss}}}{(L-1)!}, \quad g_{ss} \geq 0 \tag{3.1}$$

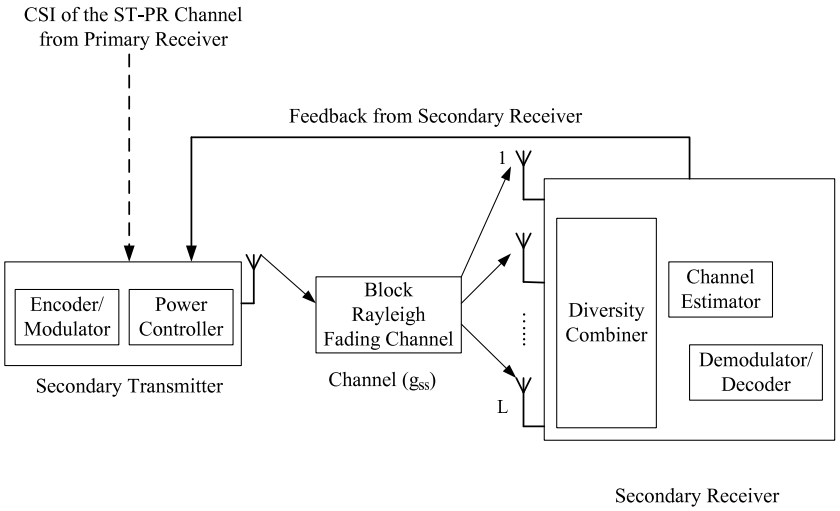

Figure 21. Transmission System Block Diagram of MRC.

where the noise at each branch is assumed to be uncorrelated additive white Gaussian noise (AWGN). The ST-PR link experiences Nakagami-*m* fading with unit mean value, such that the channel power gain, g_{ps}, is characterized by Gamma distribution given by (Nakagami 1960):

$$f_{g_{ps}}(g_{ps}) = \frac{m^m g_{ps}^{m-1}}{\Gamma(m)} e^{-m g_{ps}}, \quad g_{ps} \geq 0 \tag{3.2}$$

where without loosing generality we assume that the average channel power gain is one.

From the literature, performing MRC requires the perfect knowledge of the branch amplitudes and phases which is so-called perfect combining. In addition, with perfect combining the MRC technique achieves the optimal diversity that offers the maximal capacity improvement compared to other combining techniques, for example scanning diversity, selective diversity, equal-gain diversity (Alouini & Goldsmith 1999; Brennan 2003; Jakes 1994). In this chapter we assume that perfect channel state information (CSI) of the two links is known at both the transmitter and the receiver of the secondary user.

3.3 Ergodic Capacity of MRC Under AIP

The channel ergodic capacity of a point-to-point Rayleigh fading channel with receive MRC has been studied in (Alouini & Goldsmith 1999), where the authors revealed the capacity gains obtained by using MRC diversity combining. In this section, we study a cognitive-shared channel that the average interference power constraint caused to the primary user is considered for an asymmetric fading scenario. The expression of the ergodic capacity per Hz of a cognitive radio channel is given in (Ghasemi & Sousa 2007) by

$$\frac{C}{B} = \mathbb{E}_{g_{ss},g_{ps}}\left[\log\left(1+\frac{g_{ss}p(g_{ss},g_{ps})}{N_1 B}\right)\right] \tag{3.3}$$

where B [Hz] is the channel bandwidth, $p(g_{ss},g_{ps})$ is a mapping from the joint instantaneous fading state (g_{ss},g_{ps}) to a non-negative real set, and N_1 is the AWGN noise power spectral density at the secondary receiver. The two channels, g_{ss},g_{ps}, are assumed to be independent to each other. Then the ergodic capacity maximization problem can be expressed as

$$\underset{p(g_{ss},g_{ps})\geq 0}{\text{maximize}} \quad \mathbb{E}\left[\log\left(1+\frac{g_{ss}p(g_{ss},g_{ps})}{N_1 B}\right)\right] \tag{3.4}$$

$$\text{subject to} \quad \mathbb{E}_{g_{ss},g_{ps}}\left[p(g_{ss},g_{ps})g_{ps}\right] \leq Q_{av} \tag{3.5}$$

where Q_{av} is the average interference power constraint at the primary receiver. The solution of the above optimization problem can be obtained by using Lagrangian optimization approach (Boyd & Vandenberghe 2004) as following

$$p^*(g_{ss},g_{ps}) = \left[\frac{1}{\lambda g_{ps}} - \frac{N_1 B}{g_{ss}}\right]^+ \tag{3.6}$$

where $[\cdot]^+$ denotes $\max(.,0)$, and λ is the nonnegative dual variables corresponding to the constraint (3.5) satisfying the following complementary slackness conditions (Boyd & Vandenberghe 2004):

$$\mathbb{E}_{g_{ss},g_{ps}}\left[p(g_{ss},g_{ps})g_{ps}\right] - Q_{av} = 0 \tag{3.7}$$

Given an AIP constraint, after a few mathematical manipulation, see Appendix 1 for details, the ergodic capacity with MRC of the secondary user using optimal

power and rate adaptation is obtained by substituting (3.1) and (3.2) into (3.4) as

$$\begin{aligned}\frac{C}{B} &= \mathbb{E}_{g_{ss},g_{ps}}\left[\log\left(1+\left[\frac{1}{\lambda g_{ps}}-\frac{N_1B}{g_{ss}}\right]^{+}\frac{g_{ss}}{N_1B}\right)\right] \\ &= \int_0^{\infty}\int_{\frac{g_{ps}}{\gamma_0}}^{\infty}\log\left(\frac{\gamma_0 g_{ss}}{g_{ps}}\right)\frac{m^m g_{ps}^{m-1}e^{-mg_{ps}}}{\Gamma(m)}\frac{g_{ss}^{L-1}e^{-g_{ss}}}{(L-1)!}dg_{ss}dg_{ps} \\ &= \frac{m^{m-1}\gamma_0^m}{\Gamma(m)}\sum_{k=0}^{L-1}\frac{\Gamma(m+k)}{(1+m\gamma_0)^{m+k}k!}\times {}_2F_1\left(1,m+k;m+1;\frac{m\gamma_0}{1+m\gamma_0}\right) \qquad (3.8)\end{aligned}$$

where $\gamma_0 = 1/\lambda N_1 B$, $\Gamma(x)$ denotes the Gamma function defined as

$$\Gamma(x) = \int_0^{\infty} t^{x-1}e^{-t}dt \qquad (3.9)$$

and ${}_2F_1(a,b;c;z)$ is the Gauss's hypergeometric function (Abramowitz & Stegun 1964).

We now simplify the average received interference power constraint by inserting (3.1) and (3.2) into (3.5). After a few mathematical manipulation we obtain,

$$\begin{aligned}\frac{Q_{av}}{N_1B} &= \mathbb{E}_{g_{ss},g_{ps}}\left[\frac{p(g_{ss},g_{ps})g_{ps}}{N_1B}\right] \\ &= \int_0^{\infty}\int_0^{\gamma_0 g_{ss}}\left(\gamma_0-\frac{g_{ps}}{g_{ss}}\right)\frac{m^m g_{ps}^{m-1}e^{-mg_{ps}}}{\Gamma(m)}\times\frac{g_{ss}^{L-1}e^{-g_{ss}}}{(L-1)!}dg_{ps}dg_{ss} \\ &= \frac{m^{m-1}\gamma_0^{m+1}\Gamma(L+m)}{(1+m\gamma_0)^{L+m}\Gamma(m)(L-1)!} \\ &\times\left[{}_2F_1\left(1,L+m;m+1;\frac{m\gamma_0}{1+m\gamma_0}\right)\right. \\ &\left.-\frac{m}{1+m}{}_2F_1\left(1,L+m;m+2;\frac{m\gamma_0}{1+m\gamma_0}\right)\right] \qquad (3.10)\end{aligned}$$

where $\Gamma(x)$ denotes the Gamma function, and ${}_2F_1(a,b;c;z)$ is the Gauss's hypergeometric function (Abramowitz & Stegun 1964). The poof is shown in Appendix 1.

3.4 Numerical Results

In this section, we show the numerical results for the mathematical analysis. Figures 22, 23 and 24 compare the ergodic capacity of the secondary user per unit bandwidth versus $Q_{av}/(N_1B)$ (dB), called α in (Ghasemi & Sousa 2007), under the average received power constraint and different combining diversities (L

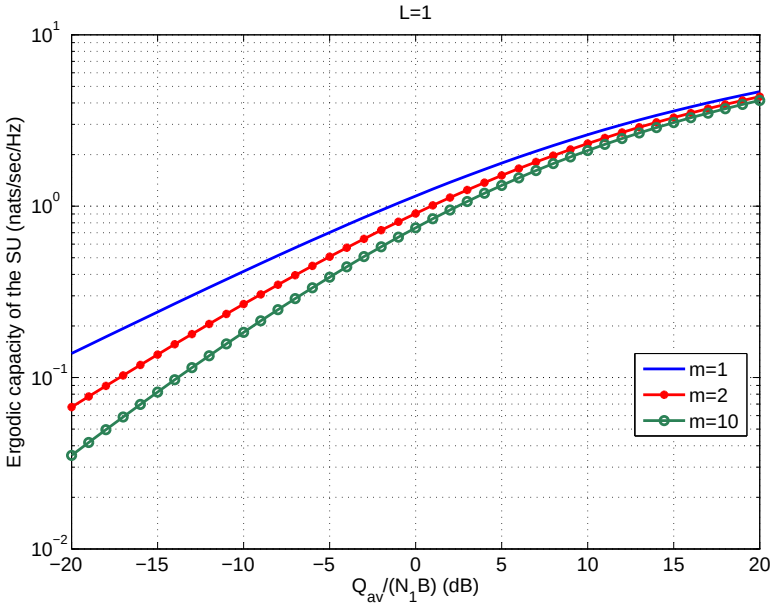

Figure 22. The ergodic capacity of the SU without receive MRC, i.e. $L = 1$, under AIP constraint and different Nakagami-m fading of ST-PR link.

branches) and different ST-PR Nakagami-m fading (different m values). We can observe that given L the ergodic capacity of the SU decreases when the m value increases. Intuitively, when the ST-PR link is getting less severe, the interference to the primary system is increasing. In addition, with the same Nakagami-m fading (same m value), the more degrees of diversity the SU has, the higher ergodic capacity is obtained. Let us compare Figures 22 and 24, we could see that given the $Q_{av}/N_1B = -20dB$, the case of $L = 8, m = 10$ has the similar ergodic capacity to that of $L = 1, m = 1$. This means we could mitigate the ergodic capacity loss caused by the strong interference on ST-PR channel through providing more degrees of diversity for the SU. As a validation, in this simulation $L = 1$ and $m = 1$ yields the result in (Ghasemi & Sousa 2007).

Figure 25 and Figure 26 compare the ergodic capacity of the SU for different degrees of diversity when m is given. The results are consistent with previous illustration that increasing the degrees of diversity provides higher capacity. In addition, for a less fading case, e.g. $m = 10$, the increase of degrees of diversity, for instance $L = 8$, provides more benefits than the case of $L = 1, m = 1$.

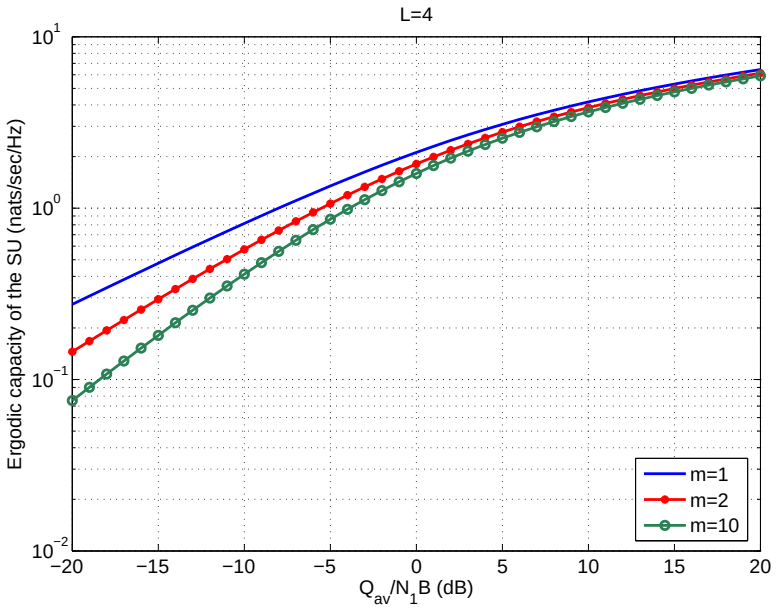

Figure 23. The ergodic capacity of the SU with receive MRC, $L = 4$, under AIP constraint and different Nakagami-*m* fading of ST-PR link.

3.5 Conclusion

This chapter studies the ergodic capacity of a cognitive-shared system with the maximal ratio combining technique at the secondary receiver in an asymmetric fading scenario, where the channel from the secondary transmitter to the primary receiver suffers Nakagami-*m* fading while the one from the secondary transmitter to its receiver experiences Rayleigh fading. Our mathematical analysis and numerical results indicate that with MRC at the secondary receiver, the secondary user achieves higher ergodic capacity than using the single antenna receiver. In addition, when the of the ST-PR channel has less severe fading which strongly affects the capacity of CR channel, exploiting the MRC technique for a cognitive system could compensate the capacity loss caused by the interference power constraint predefined by the primary user. In this chapter, the secondary transmitter is provided the perfect channel information of link from the secondary transmitter to the primary receiver through feedback. However, the channel measurement can have some errors, i.e., the secondary transmitter obtains the erratic channel information. This is also an important factor that causes the ergodic capacity loss to the secondary user. We will investigate this fundamental problem in the coming chapter.

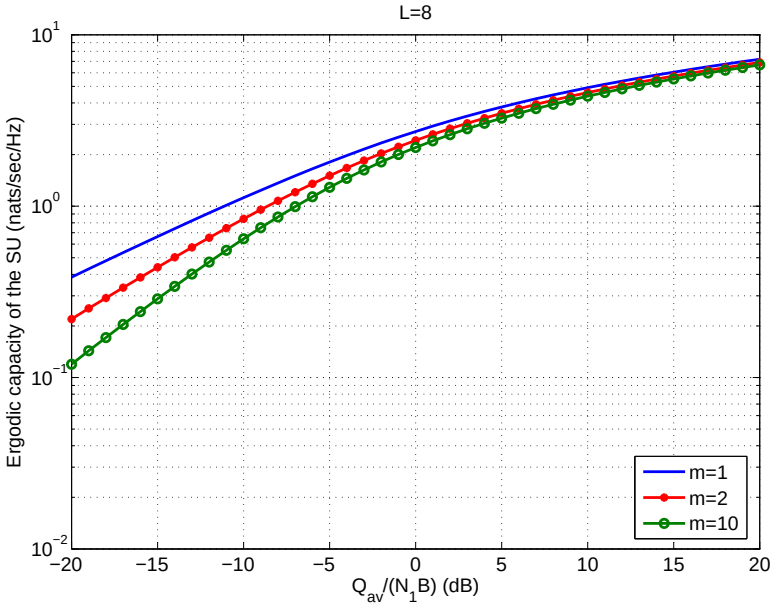

Figure 24. The ergodic capacity of the SU with receive MRC, $L = 8$, under AIP constraint and different Nakagami-m fading of ST-PR link.

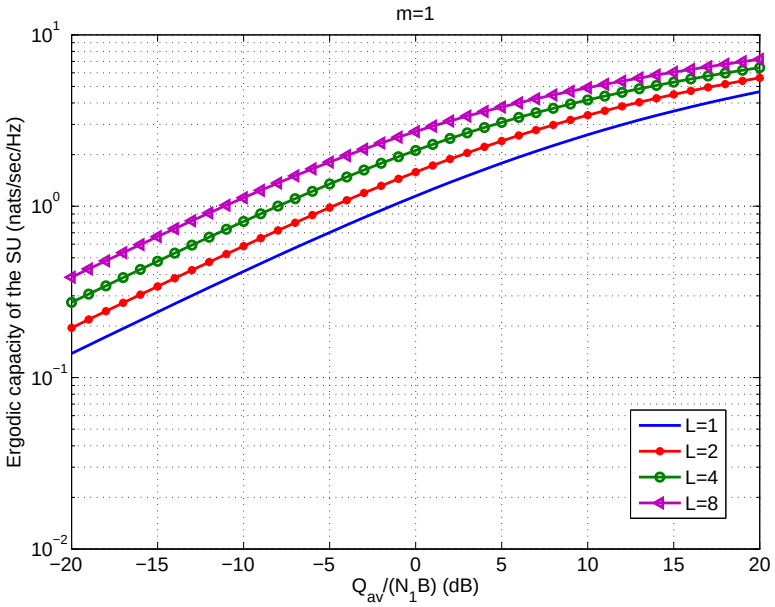

Figure 25. Comparison of the ergodic capacity of the SU versus the average interference power constraint, where the diversity order $L = 1, 2, 4, 8$, and $m = 1$ of the ST-PR link.

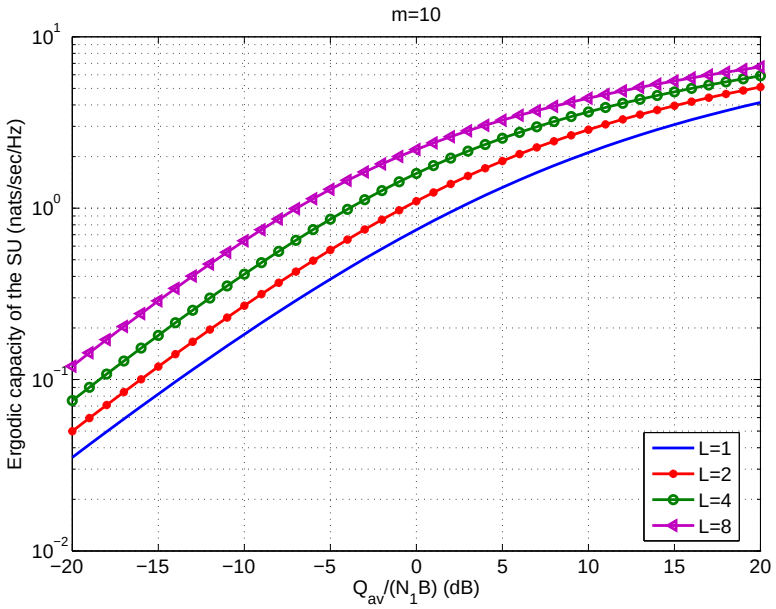

Figure 26. Comparison of the ergodic capacity of the SU versus the average interference power constraint, where the diversity order $L = 1, 2, 4, 8$, and $m = 10$ of the ST-PR link.

4 ERGODIC CAPACITY OF A COGNITIVE SYSTEM WITH RECEIVE MRC AND IMPERFECT CHANNEL INFORMATION*

In this chapter we study the ergodic capacity of a cognitive-shared system with maximal ratio combining (MRC) technique equipped at the secondary receiver in Rayleigh fading environment. The secondary user (SU) does not have perfect channel information of the link between the secondary transmitter and the primary receiver (ST-PR), where the estimation error is considered. We investigate the ergodic capacity of the SU through mathematical analysis and numerical simulation. The results show that beside the feature of employing the MRC technique at the secondary receiver to enhance the ergodic capacity, it can also compensates the capacity degradation caused by the imperfect channel estimation of the ST-PR link. For instance, we show that even the estimation error variance is large, for example $\sigma_e^2 = 0.8$, to increase the degrees of MRC combining diversity, for instance $L = 8$, is able to achieve higher capacity than in the estimation error free case without MRC.

4.1 Introduction

As we know from previous chapters that the study on ergodic capacity of a spectrum-sharing cognitive radio has attracted many researchers due to that the traditional capacity study of fading channels is not suitable for the cognitive radio. Suraweera *et al.* (2008) extended the work in (Ghasemi & Sousa 2007) by investigating the achievable capacity gains in asymmetric fading environments. In (Musavian & Aissa 2009a), the authors analysed the capacity gains of opportunistic spectrum-sharing channels in fading environments with imperfect channel state information (CSI) of the ST-PR link. The results show that the ergodic capacity of the SU decreases when the estimation errors exist so that the SU has to reduce the transmit power to fulfil the average interference power constraint predefined by the primary user. Then we investigated the ergodic capacity of the SU with receive MRC in asymmetric fading scenario in the previous chapter (published in part in

*Reprinted with permission from "Capacity for Spectrum Sharing Cognitive Radios with MRC Diversity and Imperfect Channel Information from Primary User" by Ruifeng Duan, R. Jäntti, M. Elmusrati, and R. Virrankoski, In *Proc. IEEE Global Telecommunications Conference*, pp. 1-5, Copyright [2010] by the IEEE.

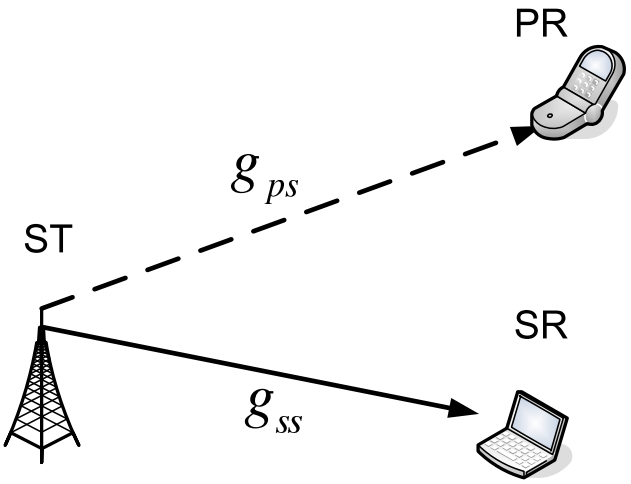

Figure 27. System model of a cognitive-shared network.

(Duan *et al.* 2010a)). The MRC technique does help the SU to improve its ergodic capacity.

In this chapter, we investigate the ergodic capacity of the SU with receive MRC, and the SU transmitter is provided the imperfect CSI of the ST-PR link. The analytical analysis is conducted and validated through simulations, for different estimation error variances, $\sigma_e^2 = 0, 0.1, 0.3, 0.8$, and different degrees of diversity. The results show that the receive MRC not only improves the ergodic capacity of the SU, but also compensates the effects of imperfect channel information caused by erratic channel estimation.

The remainder of this chapter is organized as follows. The channel and system models are proposed in Section 4.2. The ergodic capacity of a cognitive-shared channel with receive MRC and imperfect channel information is investigated in Section 4.3. Section 4.4 validates the analytical results through simulations. Finally, the last section concludes this chapter.

4.2 System and Channel Model

This section describes the channel and system models. A common spectrum sharing system model, which is also used in previous chapter, is adopted that is shown in Figure 27. The cognitive radio (CR) transmission system block diagram of

maximal ratio combining (MRC) is illustrated in Figure 28 (Alouini & Goldsmith 1999; Jakes 1994).

We assume that the wireless channels are slowly-varying block fading the same as in the previous chapter. The ST-SR link is a Rayleigh fading channel, and the secondary receiver is equipped with a L-branch MRC combiner. Each branch of the combiner is independent to each other. So that the channel power gain, g_{ss}, is characterized by Chi-square (χ^2) distribution with $2L$ degrees of freedom, and the related probability density function of g_{ss} with unit mean is given by (Jakes 1994; Proakis & Salehi 2008)

$$f_{g_{ss}}(g_{ss}) = \frac{g_{ss}^{L-1} e^{-g_{ss}}}{(L-1)!}, \quad g_{ss} \geq 0 \tag{4.1}$$

where without loosing generality we assume that the average channel power gain of the link from the secondary transmitter to each branch is one, and the noise at each branch is assumed to be uncorrelated additive white Gaussian noise (AWGN).

In this chapter we adopt the channel estimation model presented in (Musavian & Aissa 2009a) for the following channel formulation. The ST-PR link experiences Rayleigh fading, whose complex channel gain, denoted as c_{ps}, is zero mean circularly symmetric complex Gaussian distributed variable with the imaginary and real parts having variances of 0.5. However, the SU transmitter is only provided with the partial channel information of c_{ps}, i.e. $\tilde{c}_{ps}$, where c_{ps} and $\tilde{c}_{ps}$ are jointly ergodic and stationary Gaussian processes. The secondary user performs minimum mean square error estimation (MMSE) of c_{ps} given $\tilde{c}_{ps}$, such that $\hat{c}_{ps}[n] = \mathcal{E}\left\{c_{ps}[n] \,|\, \tilde{c}_{ps}[n], \tilde{c}_{ps}[n-1], ...\right\}$, where $[n]$ denotes the time index. The MMSE estimation error can be presented as $\check{c}_{ps}[n] = c_{ps}[n] - \hat{c}_{ps}[n]$, and $\check{c}_{ps}[n]$ and $\hat{c}_{ps}[n]$ are zero mean circularly symmetric complex Gaussian distributed variables with variances $\frac{1-\sigma_e^2}{2}$ and $\frac{\sigma_e^2}{2}$ respectively. So the associated channel power gain can be presented as $g_{ps} = \left|c_{ps}\right|^2$, $\hat{g}_{ps} = \left|\hat{c}_{ps}\right|^2$, and the channel power gain estimation error by $\check{g}_{ps} = \left|\check{c}_{ps}\right|^2$. The probability density function of estimated channel power gain, $\hat{g}_{ps}$, is characterized by (Musavian & Aissa 2009a):

$$f_{\hat{g}_{ps}}(\hat{g}_{ps}) = \frac{1}{1-\sigma_e^2} \exp\left\{-\frac{\hat{g}_{ps}}{1-\sigma_e^2}\right\}, \quad \hat{g}_{ps} \geq 0. \tag{4.2}$$

As we know from literature that MRC technique, performing perfect combining, requires perfect knowledge of the channel amplitudes and phases. Such that MRC

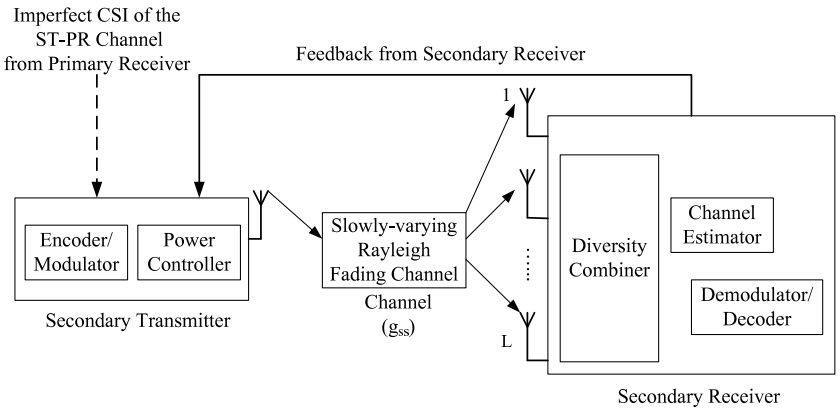

Figure 28. Transmission System Block Diagram of MRC.

provides the optimal diversity and offers the maximal capacity improvement compared to other combining techniques, for example scanning diversity, selective diversity, equal-gain diversity (Alouini & Goldsmith 1999; Brennan 2003; Jakes 1994). In this chapter we assume that perfect channel state information (CSI) of the ST-SR link is known at both the secondary transmitter and the secondary receiver.

4.3 Ergodic Capacity of MRC Under AIP and Imperfect CSI

The channel ergodic capacity of a Rayleigh fading with receive MRC at the receiver for single communication link has been studied in (Alouini & Goldsmith 1999), where the authors illustrated the ergodic capacity gains obtained by using MRC. We also, in the previous chapter, investigated the ergodic capacity of a cognitive-shared channel with receive MRC under asymmetric fading and average interference power (AIP) constraint at the primary receiver. In this section, we study the ergodic capacity and the optimal power allocation having a same system structure, however, with imperfect channel information, i.e., the secondary user only has partial information of the ST-PR link. The constraint is set to be the AIP constraint predefined at the primary receiver.

In (Musavian & Aissa 2009a), the authors showed that the average interference power constraint at the primary receiver with the estimated channel gain can be defined as

$$\mathbb{E}_{g_{ss},\hat{g}_{ps}}\left[p_s(g_{ss},\hat{g}_{ps})\hat{g}_{ps}\right]+\sigma_e^2\bar{P}\leq Q_{av} \tag{4.3}$$

where $p_s(g_{ss},\hat{g}_{ps})$ denotes the transmit power of the secondary transmitter, which is a mapping from the joint fading state $(g_{ss},\hat{g}_{ps})$ to a non-negative real set. $\bar{P}=\mathbb{E}_{g_{ss},\hat{g}_{ps}}\left[p_s(g_{ss},\hat{g}_{ps})\right]$ denotes the average transmit power of the secondary user. Intuitively the SU has to reduce its transmit power to satisfy the average interference power constraint due to the imperfect channel estimation. This motivated us to study the performance in terms of ergodic capacity of the secondary user through exploiting receive MRC to mitigate the capacity degradation.

The ergodic capacity of a cognitive radio channel has been defined in (Ghasemi & Sousa 2007) by

$$\frac{C}{B}=\mathbb{E}_{g_{ss},\hat{g}_{ps}}\left[\log\left(1+\frac{g_{ss}p_s(g_{ss},\hat{g}_{ps})}{N_1B}\right)\right] \tag{4.4}$$

where B [Hz] is the channel bandwidth , and N_1 is the AWGN noise power spectral density at the secondary receiver. The two channels, $\hat{g}_{ps}$, g_{ss}, are assumed to be independent to each other. Then the ergodic capacity maximization problem for the SU can be expressed as

$$\underset{p_s(g_{ss},\hat{g}_{ps})}{\text{maximize}} \quad \mathbb{E}\left[\log\left(1+\frac{g_{ss}p_s(g_{ss},\hat{g}_{ps})}{N_1B}\right)\right] \tag{4.5}$$

$$\text{subject to} \quad \mathbb{E}_{g_{ss},\hat{g}_{ps}}\left[p_s(g_{ss},\hat{g}_{ps})\hat{g}_{ps}\right]+\sigma_e^2\bar{P}\leq Q_{av} \tag{4.6}$$

where Q_{av} is the predefined average interference power constraint at the primary receiver. The solution of the above optimization problem can be obtained by using Lagrangian optimization approach (Boyd & Vandenberghe 2004).

$$p_s^*(g_{ss},\hat{g}_{ps})=\left[\frac{1}{\lambda(\hat{g}_{ps}+\sigma_e^2)}-\frac{N_1B}{g_{ss}}\right]^+ \tag{4.7}$$

where $[\cdot]^+$ denotes $\max(.,0)$ and λ is the nonnegative dual variables corresponding to the constraint (4.6), which satisfy the following complementary slackness

condition (Boyd & Vandenberghe 2004):

$$\mathbb{E}_{g_{ss},\hat{g}_{ps}}\left[p_s^*(g_{ss},\hat{g}_{ps})\hat{g}_{ps}\right]+\sigma_e^2\bar{P}-Q_{av}=0 \tag{4.8}$$

Since all the transmission power should be nonnegative, the power allocation strategy (4.7) can be represented as

$$p_s^*(g_{ss},\hat{g}_{ps})=\begin{cases}\frac{1}{\lambda(\hat{g}_{ps}+\sigma_e^2)}-\frac{N_1B}{g_{ss}}, & 0\le\hat{g}_{ps}\le\frac{g_{ss}}{\lambda N_1B}-\sigma_e^2\\ 0, & \text{otherwise}\end{cases} \tag{4.9}$$

We may simplify the average interference power constraint expression by inserting (4.1) and (4.2) into (4.6). And $0\le\hat{g}_{ps}\le\frac{g_{ss}}{\lambda N_1B}-\sigma_e^2$ in (4.9) is equivalent to $\hat{g}_{ps}\le\frac{g_{ss}}{\lambda N_1B}-\sigma_e^2$ and $g_{ss}\ge\lambda N_1B\sigma_e^2$. After a few mathematical manipulation (see Appendix 2 for details), we obtain

$$\begin{aligned}\frac{Q_{av}}{N_1B}&=\mathbb{E}_{g_{ss},\hat{g}_{ps}}\left[\frac{p_s(g_{ss},\hat{g}_{ps})\hat{g}_{ps}}{N_1B}\right]+\frac{\sigma_e^2\bar{P}}{N_1B}\\&=\int_{\frac{\sigma_e^2}{\gamma_0}}^{\infty}\int_0^{\gamma_0 g_{ss}-\sigma_e^2}\left(\gamma_0-\frac{\hat{g}_{ps}+\sigma_e^2}{g_{ss}}\right)\frac{1}{1-\sigma_e^2}e^{-\frac{\hat{g}_{ps}}{1-\sigma_e^2}}\frac{g_{ss}^{L-1}e^{-g_{ss}}}{(L-1)!}d\hat{g}_{ps}dg_{ss}\\&=\frac{1}{(L-1)!}\left[\gamma_0\Gamma\left(L,\frac{\sigma_e^2}{\gamma_0}\right)-\Gamma\left(L-1,\frac{\sigma_e^2}{\gamma_0}\right)\right.\\&\left.+\frac{(1-\sigma_e^2)^L e^{\frac{\sigma_e^2}{1-\sigma_e^2}}}{(1+\gamma_0-\sigma_e^2)^{L-1}}\Gamma\left(L-1,\frac{\sigma_e^2}{1-\sigma_e^2}+\frac{\sigma_e^2}{\gamma_0}\right)\right]\end{aligned} \tag{4.10}$$

where $\gamma_0=1/(\lambda N_1B)$, and $\Gamma(\alpha,x)$ denotes the incomplete gamma function defined as (Abramowitz & Stegun 1964)

$$\Gamma(\alpha,x)=\int_x^{\infty}t^{\alpha-1}e^{-t}dt \tag{4.11}$$

As a validation, with the help of $\Gamma(0,x)=-\mathsf{Ei}(-x),\forall x>0$ and $\Gamma(1,x)=e^{-x}$, when $L=1$, (4.10) yields the result in (Musavian & Aissa 2009a: Eqn. 11), i.e.,

$$\frac{Q_{av}}{N_1B}=\gamma_0 e^{\frac{\sigma_e^2}{\gamma_0}}+\mathsf{Ei}\left(-\frac{\sigma_e^2}{\gamma_0}\right)-(1-\sigma_e^2)e^{\frac{\sigma_e^2}{1-\sigma_e^2}}\mathsf{Ei}\left(-\frac{\sigma_e^2}{1-\sigma_e^2}-\frac{\sigma_e^2}{\gamma_0}\right) \tag{4.12}$$

where $\mathsf{Ei}(x)$ is the exponential integral function defined by $\mathsf{Ei}(x)=-\int_{-x}^{\infty}\frac{e^{-t}}{t}dt$ in (Abramowitz & Stegun 1964).

Given an average interference power constraint, after a few mathematical manipulation (see Appendix 2), the ergodic capacity of the SU with receive MRC over Rayleigh fading is obtained by substituting (4.1) and (4.2) into (4.5),

$$\begin{aligned}(4.13)\quad \frac{C}{B} &= \mathbb{E}_{g_{ss},\hat{g}_{ps}}\left[\log\left(\frac{\gamma_0 g_{ss}}{\hat{g}_{ps}+\sigma_e^2}\right)\right] \\ &= \int_0^{\infty}\int_{\frac{\hat{g}_{ps}+\sigma_e^2}{\gamma_0}}^{\infty}\log\left(\frac{\gamma_0 g_{ss}}{\hat{g}_{ps}+\sigma_e^2}\right)\frac{e^{-\frac{\hat{g}_{ps}}{1-\sigma_e^2}}}{1-\sigma_e^2}\frac{g_{ss}^{L-1}e^{-g_{ss}}}{(L-1)!}\,dg_{ss}d\hat{g}_{ps} \\ &= \sum_{k=0}^{L-1}\frac{1}{k!}\left[\Gamma\left(k,\frac{\sigma_e^2}{\gamma_0}\right)-e^{\frac{\sigma_e^2}{1-\sigma_e^2}}\left(\frac{1-\sigma_e^2}{1-\sigma_e^2+\gamma_0}\right)^k\Gamma\left(k,\frac{\sigma_e^2}{\gamma_0}+\frac{\sigma_e^2}{1-\sigma_e^2}\right)\right]\end{aligned}$$

When $L=1$, (4.13) yields the result in (Musavian & Aissa 2009a: Eqn. (13))

$$(4.14)\qquad \frac{C}{B} = e^{\frac{\sigma_e^2}{1-\sigma_e^2}}\,\mathrm{Ei}\left(-\frac{\sigma_e^2}{\gamma_0}-\frac{\sigma_e^2}{1-\sigma_e^2}\right)-\mathrm{Ei}\left(\frac{\sigma_e^2}{\gamma_0}\right)$$

4.4 Simulation Results

In this section, we validate analytical analysis through numerical simulations. Figure 29 illustrates the comparison of the ergodic capacity of the SU per unit bandwidth versus $Q_{av}/(N_1 B)$ (dB), for example in (Ghasemi & Sousa 2007) called α, under the average interference power constraint at the primary receiver and different degrees of combining diversities, i.e. different values of L, and different variances of channel estimation error of ST-PR link. The values of the variance are chosen as $\sigma_e^2 = 0, 0.1, 0.3,$ and 0.8. As a validation, when $L=1$ and $\sigma_e^2=0$, it yields the result shown in (Ghasemi & Sousa 2007). And for $L=1$ and $\sigma_e^2 = 0.1, 0.3, 0.8$, it gives the results in (Musavian & Aissa 2009a). We can see that given L the ergodic capacity of the SU decreases while σ_e^2 increases. This is obvious that when the ST-PR link has more estimation errors, the secondary transmitter has to lower its transmit power to satisfy the average interference power constraint. Such that the ergodic capacity degrades. The simulation results also indicate that increasing the degrees of receive MRC will improve the ergodic capacity and compensate the capacity loss caused by imperfect channel estimation. Furthermore, when the number of MRC branches is large enough, the SU is able to achieve higher ergodic capacity under imperfect channel estimation than in estimation error free case $\sigma^2 = 0$.

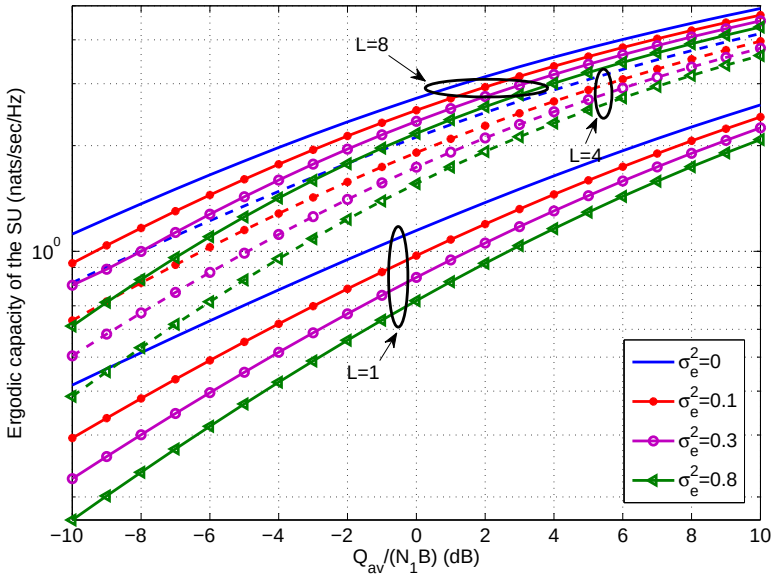

Figure 29. Ergodic capacity of the SU with different degrees of MRC diversity under AIP constraint and different estimation error variances of ST-PR link.

Figures 30, 31 and 32 depict how the ergodic capacity of the SU behaves toward the degrees of MRC and AIP constraint given the estimation error variance. Again the more diversity the SU has, the higher ergodic capacity is obtained. In addition, with a looser AIP constraint, for example $Q_{av}/(N_1B)$ is large, the SU achieves more improvement on ergodic capacity.

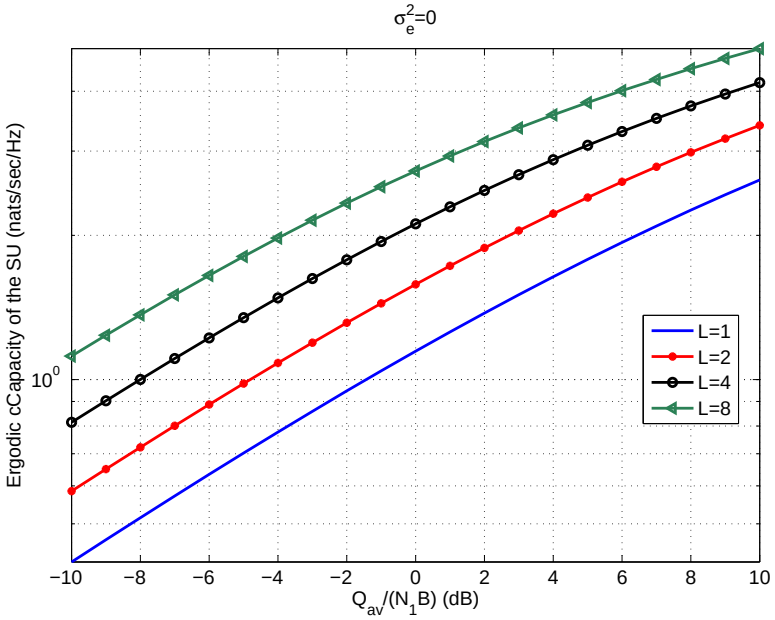

Figure 30. Ergodic capacity comparison with different degrees of MRC diversity at the SU Receiver, L=1, 2, 4, 8, under the AIP constraint and perfect channel estimation of ST-PR link, i.e. $\sigma_e^2 = 0$.

4.5 Conclusion

This chapter studies the ergodic capacity of a cognitive-shared channel with maximal ratio combining at the secondary receiver in a Rayleigh fading environment. The secondary user does have the perfect channel information of the ST-PR link, where the estimation error is considered. Our analytical analysis and numerical results show that with receive MRC equipped at the secondary receiver, the ergodic capacity is improved. In addition, the estimation error degrades the ergodic capacity of the ST-SR channel. Furthermore, the MRC technique is able to compensate the channel estimation error. We illustrate that when the estimation error variance is large, for example $\sigma_e^2 = 0.8$, increasing the degrees of MRC diversity, for instance $L = 8$, is able to achieve higher ergodic capacity than the estimation error free case.

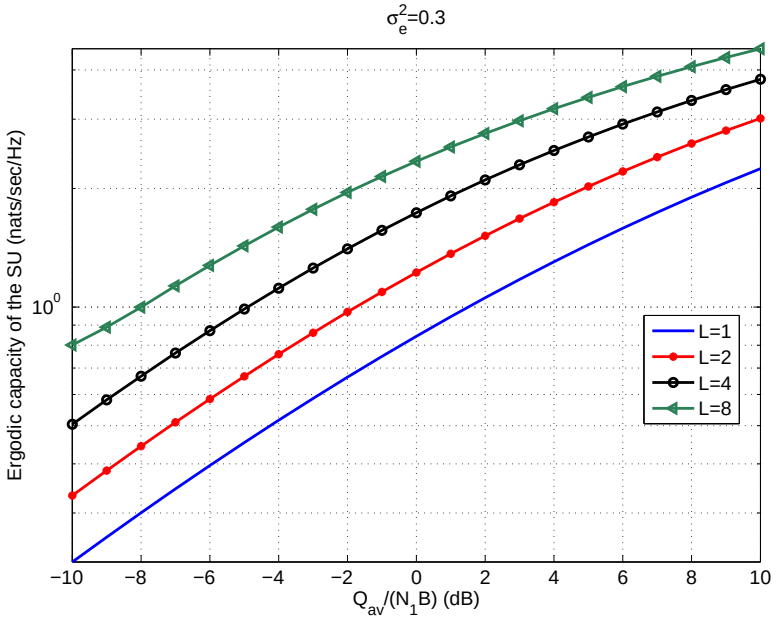

Figure 31. Ergodic capacity comparison with different degrees of MRC diversity at the SU Receiver, L=1, 2, 4, 8, under the AIP constraint and imperfect channel estimation of ST-PR link, i.e. $\sigma_e^2 = 0.3$.

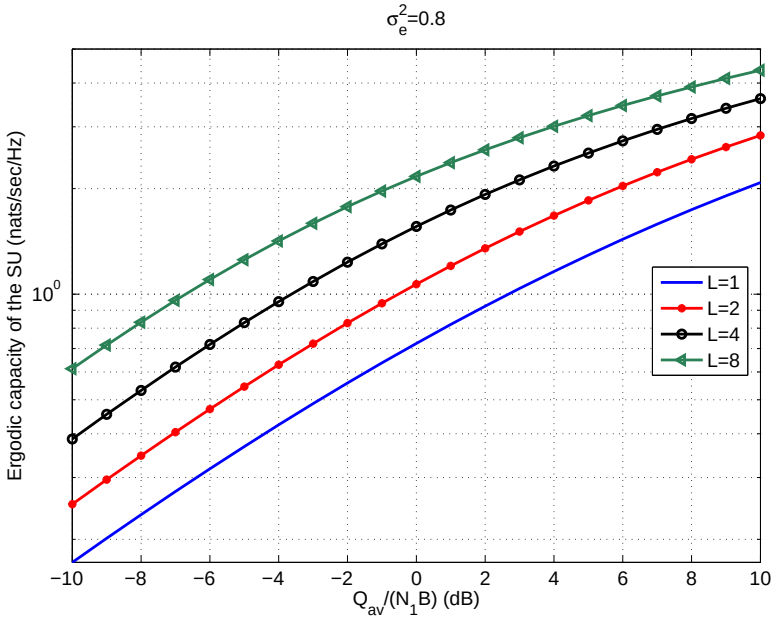

Figure 32. Ergodic capacity comparison with different degrees of MRC diversity at the SU Receiver, L=1, 2, 4, 8, under the AIP constraint and imperfect channel estimation of ST-PR link, i.e. $\sigma_e^2 = 0.8$.

5 PERFORMANCE ANALYSIS WITH GSC DIVERSITY UNDER PRIMARY OUTAGE PROBABILITY*

This chapter focuses on a cognitive-shared system that employs generalized selection combining in Rayleigh block fading. The closed-form expressions of the ergodic capacity and the symbol error probability of a cognitive-shared channel are proposed. The results show that the channel from the secondary transmitter to the primary receiver is of prominence on the performance of the secondary user.

5.1 Introduction

The radio spectrum is one of the most important resources for wireless communication. For accessing the spectrum, the secondary users (SUs) may be allowed to coexist in the shared bands. However, the SUs need to regulate the transmit power in order to satisfy the interference constraints imposed by the primary users while trying to maximize their own maximum achievable rate. Thereafter, many research, e.g. (Gastpar 2007; Ghasemi & Sousa 2007; Kang *et al.* 2009), have been done to study the ergodic capacity of the secondary user in a fading environment.

In order to improve the performance, multiple-antenna technology has been considered for communication systems (Telatar 1999). Duan et al. in (2010a) analyzed the ergodic capacity of the secondary system where the maximal ratio combining (MRC) diversity technique was considered at the secondary receiver. The performance in terms of ergodic capacity of implementing the transmit antenna selection (TAS) and the MRC techniques has been studied in (Blagojevic & Ivanis 2012).

Generalized selection combining (GSC) has received considerable attention in literature (Eng *et al.* 1996; Simon & Alouini 2005; Win & Winters 2001; Wu *et al.* 2012). The GSC combines coherently K branches with the largest signal to noise ratios (SNR) of total M branches, so that it enhances the accuracy of the channel estimation (Simon & Alouini 2005). Moreover, through changing the number of selected antenna branches, one can tradeoff performance for receiver complexity,

*Reprinted with permission from "Performance Analysis of a Cognitive-shared channel with GSC Diversity under Primary Outage Probability" by Ruifeng Duan and M. Elmusrati, to appear in *Proc. International Conference on Computing, Networking and Communications (ICNC)*, pp. 1-5, Copyright [2014] by the IEEE.

and reduce the power consumption and the cost of the radio frequency part at the receiver (Win & Winters 2001).

In this chapter we study the ergodic capacity and the symbol error probability (SEP) of a cognitive-shared channel with GSC under the constraint of the primary outage probability. This means that the transmission power of the secondary transmitter is regulated in order to maintain the outage probability of the primary user below a predefined threshold. The outage probability of the primary user is defined as the probability that the received signal to noise ratio (SNR) drops below a threshold. Recently, Wu et al in (Wu *et al.* 2012) studied the effective capacity of cognitive radio systems with GSC diversity under imperfect channel knowledge under the peak interference power constraint at the primary receiver. To the best of our knowledge, the closed-form expressions of the ergodic capacity and the SEP of a spectrum-sharing channel with GSC diversity under the primary outage probability have not been investigated in the literature. We present those results in this chapter.

The remainder of this chapter is organized as follows. In Section 5.2, we illustrate the system and channel models. The composite channel probability density function (p.d.f.) of the cognitive channel is also reviewed. In Section 5.3, we first derive the p.d.f. of the signal-to-noise ratio at the secondary receiver. Then a closed-form expression of the ergodic capacity of the secondary user is obtained. Analytical and simulated results are then presented in Section 5.5. The last section concludes this chapter.

We use $\log(\cdot)$ to denote the natural logarithm in this chapter, P_p denotes the transmit power of the primary transmitter, P_s represents the transmit power of the ST, N_0 is the additive white Gaussian noise (AWGN) power density at the PR, B_0 denotes the bandwidth of the primary user, N_1 is the AWGN power density at the SR, B_1 denotes the bandwidth of the secondary user, R_p is the required rate of the PU, and ε_p is the predefined outage probability of the PU.

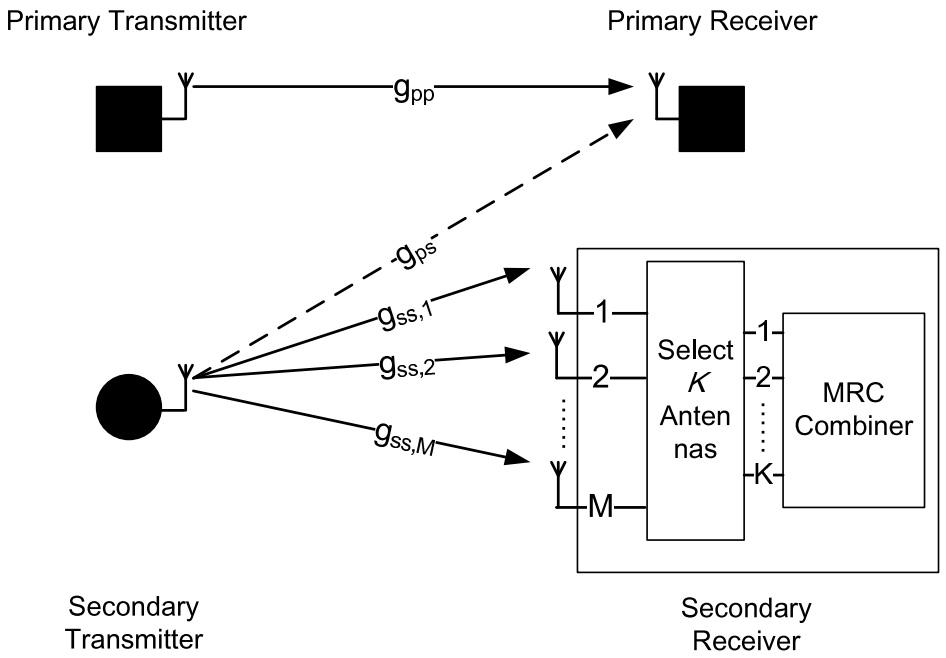

Figure 33. System Model: K branches are selected at the secondary transmitter.

5.2 System and Channel Model

This chapter focuses on the spatial diversity scheme for a cognitive-shared channel shown in Fig. 33. At the secondary receiver (SR), the GSC technique is considered, where the SR is equipped with M branches of which K branches with largest SNR are combined coherently using maximal ratio combining (MRC). The perfect channel state information is assumed to be available at the secondary receiver. However, the ST is provided only the channel statistics about the secondary link (ST-SR) and the channel from the ST to the primary receiver (PR). The ST is equipped with single antennas and the primary receiver (PR) has one antenna. We assume that the channels from the secondary transmitter to the ith branch of the secondary receiver are identical and independent (i.i.d.) Rayleigh block fading, while the ST-PR channel is independent from the secondary channels. Let g_{pp} denote the channel power gain from the primary transmitter (PT) to the PR, g_{ps} represent the channel power gain from the ST to the PR, and $g_{ss,i}$ be the channel power gain of the link from the ST to the ith antenna element at the SR. The wireless channels experience block Rayleigh fading assumed to be ergodic. Thus, the channel state does not change during each block, and the channel states are uncorrelated between blocks (Ozarow *et al.* 1994). In Rayleigh fading the channel power gain follows exponential distribution. Let $\overline{g}_{pp}$, $\overline{g}_{ps}$, and $\overline{g}_{ss}$ denote the aver-

age values of g_{pp}, g_{ps}, and $g_{ss,i}, i = 1, \cdots, M$, respectively. Here we use $\overline{g}_{ss}$ instead of $\overline{g}_{ss,i}$ to denote the average value of $g_{ss,i}$ since we assume that the channels from the secondary transmitter to the ith branch of the SR are i.i.d.. For an exponential distributed random variable X with mean $\bar{x}$, the probability density function (p.d.f.), $f_X(x)$, is given by

$$f_X(x) = \frac{1}{\bar{x}} e^{-x/\bar{x}}, \quad x \geq 0 \tag{5.1}$$

The corresponding cumulative distribution function (c.d.f.) is

$$F_X(x) = 1 - e^{-x/\bar{x}}, \quad x \geq 0 \tag{5.2}$$

For a general selection combining scheme (GSC), the best K diversity branches at the SR with the largest instantaneous SNR's are selected and then coherently combined with a maximal ratio combiner, where $K \leq M$ and M is the total number of diversity branches available at the SR. We first arrange the channel power gain from the ST to each branch at the SR, $\{g_{ss,i:M}\}_{i=1}^{M}$, in a decreasing order that $g_{ss,1:M} \geq g_{ss,2:M} \geq g_{ss,M:M}$. Then the combined channel gain, $g_{\mathrm{GSC},K}$, with K selected branches to be coherently combined through the MRC combiner can be represented as

$$g_{\mathrm{GSC},K} = \sum_{k=1}^{K} g_{ss,k:M} \tag{5.3}$$

Therefore, the corresponding p.d.f. of $g_{\mathrm{GSC},K}$ is given by (Alouini & Simon 2000; Wu *et al.* 2012)

$$\begin{aligned} f_{g_{\mathrm{GSC},K}}(g) = \binom{M}{K} \Bigg\{ & \frac{g^{K-1}}{\overline{g}_{ss}^{K}(K-1)!} \exp\left(-\frac{g}{\overline{g}_{ss}}\right) \\ & + \frac{1}{\overline{g}_{ss}} \sum_{n=1}^{M-K} (-1)^{K+n-1} \binom{M-K}{n} \left(\frac{K}{n}\right)^{K-1} \exp\left(-\frac{g}{\overline{g}_{ss}}\right) \\ & \times \left[\exp\left(-\frac{ng}{K\overline{g}_{ss}}\right) - \sum_{m=0}^{K-2} \frac{1}{m!} \left(-\frac{ng}{K\overline{g}_{ss}}\right)^{m} \right] \Bigg\} \end{aligned} \tag{5.4}$$

where $\binom{M}{K} = \frac{M!}{K!(M-K)!}$ denotes the binomial coefficient.

In order to share the same spectrum with the primary user, the interference by the secondary user to the primary user must be regulated (Haykin 2005). In this chapter we consider the primary user outage probability constraint, where the outage probability is defined that the instantaneous achievable rate of the primary user is less than the predefined threshold. The outage probability of the primary user without the interference from the secondary user is given by

$$\Pr\left\{\log\left(1+\frac{P_p g_{pp}}{N_0 B_0}\right) < R_p\right\} \leq \varepsilon_0 \tag{5.5}$$

where P_p is the transmit power of the primary user which is assumed to be fixed, g_{pp} denotes the channel power gain of PT-PR, N_0 is the AWGN power density at the primary receiver, B_0 denotes the bandwidth of the primary receiver, R_p represents the required instantaneous achievable rate, and ε_0 defines the threshold. Then considering the maximum allowed outage probability and g_{pp} is exponentially distributed, we have

$$\varepsilon_0 = 1 - \exp\left(-\frac{e^{R_p}-1}{P_p \overline{g}_{pp}/N_0 B_0}\right) \tag{5.6}$$

Let P_s be the transmit power of the secondary user, and then the primary user outage probability with the interference of the secondary user can be represented as

$$\Pr\left\{\log\left(1+\frac{P_p g_{pp}}{P_s g_{ps}+N_0 B_0}\right) < R_p\right\} \leq \varepsilon_p \tag{5.7}$$

where $\varepsilon_p \geq \varepsilon_0$ is a new threshold that the primary may accept in order to share the spectrum to the secondary user. The expression for the transmission power of the SU can be obtained over Rayleigh fading as (Rezki & Alouini 2012; Zou *et al.* 2010)

$$P_s \leq \frac{\overline{g}_{pp} P_p}{\overline{g}_{ps}\left(e^{R_p}-1\right)}\left[\frac{1}{1-\varepsilon_p}\exp\left(-\frac{e^{R_p}-1}{\overline{g}_{pp} P_p/N_0 B_0}\right)-1\right] \tag{5.8}$$

The transmit power should be positive, and then we write the maximum transmit power of the ST as follows

$$P_s = \left(\frac{\overline{g}_{pp} P_p}{\overline{g}_{ps}\left(e^{R_p}-1\right)}\left[\frac{1}{1-\varepsilon_p}\exp\left(-\frac{e^{R_p}-1}{\overline{g}_{pp} P_p/N_0 B_0}\right)-1\right]\right)^+ \tag{5.9}$$

From this expression we can observe that the secondary transmitter will transmit using fixed power. In addition, the SU is able to transmit if the average SNR of the PU without interference from the SU satisfies $\frac{\overline{g}_{pp}P_p}{N_0B_0} \geq \frac{e^{R_p}-1}{-\log(1-\varepsilon_p)}$. We define the outage probability increment as $\Delta\varepsilon = \varepsilon_p - \varepsilon_0$. We admit that the secondary user could achieve higher capacity if it has the channel information of ST-PR, where the SU is able to exploit opportunistic transmission. Thus the transmit power of the SU obtained here is the maximum transmit power the SU can adopt with the mean value of the interference channel. We leave the opportunistic transmission with the instantaneous interference channel information and with the interference of the primary user as our future work.

5.3 Closed-form Expression of Ergodic Capacity

In this section we derive the ergodic capacity of the secondary user, where the transmit power of the ST is given by (5.9). First we derive the p.d.f. expression of the received SNR, $f_{\gamma_{\mathrm{GSC},K}}(\gamma)$, at the secondary receiver as follows

$$
\begin{aligned}
(5.10) \qquad f_{\gamma_{\mathrm{GSC},K}}(\gamma) =& f_{g_{\mathrm{GSC},K}}\left(g=\frac{\gamma N_1B_1}{P_s}\right)/\frac{P_s}{N_1B_1} \\
=& \binom{M}{K}K^K\left\{\frac{\gamma^{K-1}}{\overline{\gamma}^K(K-1)!}\exp\left(-\frac{K\gamma}{\overline{\gamma}}\right)\right. \\
&+\frac{1}{\overline{\gamma}}\sum_{n=1}^{M-K}(-1)^{K+n-1}\binom{M-K}{n}\left(\frac{1}{n}\right)^{K-1}\exp\left(-\frac{K\gamma}{\overline{\gamma}}\right) \\
&\left.\times\left[\exp\left(-\frac{n\gamma}{\overline{\gamma}}\right)-\sum_{m=0}^{K-2}\frac{1}{m!}\left(-\frac{n\gamma}{\overline{\gamma}}\right)^m\right]\right\}
\end{aligned}
$$

where $\overline{\gamma} = K\frac{\overline{g}_{ss}P_s}{N_1B_1}$ denotes the average SNR of the MRC combiner at the secondary receiver.

In order to obtain the closed-form of the ergodic capacity of the SU, we use an alternative expression of $\log(1+z)$ (Gradshteyn & Ryzhik 2007: eqn. 9.121-6)

$$
(5.11) \qquad \log(1+z) = z\,{}_2F_1(1,1;2;-z)
$$

where ${}_2F_1(\alpha,\beta;\sigma;-z)$ is the Hypergeometric function (Gradshteyn & Ryzhik 2007: ch. 9.1). The MacRobert's function, $E\left(\begin{matrix}a_1,\ldots,a_p\\ b_1,\ldots,b_q\end{matrix}\middle| z\right)$, and the relation to

the Meijer-G function is given by (Erdélyi *et al.* 1953: 5.6 (2))

$$E\left(\begin{matrix}a_1,\ldots,a_p\\ b_1,\ldots,b_q\end{matrix}\middle| z\right) = G^{p,1}_{q+1,p}\left(\begin{matrix}1,b_1,\ldots,b_q\\ a_1,\ldots,a_p\end{matrix}\middle| z\right) \tag{5.12}$$

Theorem 5.1. *The ergodic capacity of a cognitive-shared channel with GSC diversity at the secondary receiver shown in Fig. 33 over Rayleigh fading under the primary outage probability constraint is given by, (see Appendix 3 for details),*

(5.13)

$$C = \binom{M}{K}\left\{\frac{\overline{\gamma}}{K!}G^{3,1}_{2,3}\left(\begin{matrix}1,2\\ 1,1,K+1\end{matrix}\middle|\frac{K}{\overline{\gamma}}\right) + K^K\overline{\gamma}\sum_{n=1}^{M-K}(-1)^{K+n-1}\binom{M-K}{n}\left(\frac{1}{n}\right)^{K-1} \times\left[\frac{G^{3,1}_{2,3}\left(\begin{matrix}1,2\\ 1,1,2\end{matrix}\middle|\frac{K+n}{\overline{\gamma}}\right)}{(K+n)^2} - \sum_{m=0}^{K-2}\frac{1}{m!}(-n)^m\frac{G^{3,1}_{2,3}\left(\begin{matrix}1,2\\ 1,1,m+2\end{matrix}\middle|\frac{K}{\overline{\gamma}}\right)}{K^{m+2}}\right]\right\}$$

where $\overline{\gamma} = K\frac{\overline{g}_{ss}P_s}{N_1B_1}$.

Proof. □

For $M = K = 1$, the expression (5.13) can be simplified as

$$C_{M=1} = \overline{\gamma}G^{3,1}_{2,3}\left(\begin{matrix}1,2\\ 1,1,2\end{matrix}\middle|\frac{1}{\overline{\gamma}}\right) = G^{3,1}_{2,3}\left(\begin{matrix}0,1\\ 0,0,1\end{matrix}\middle|\frac{1}{\overline{\gamma}}\right) = G^{2,1}_{1,2}\left(\begin{matrix}0\\ 0,0\end{matrix}\middle|\frac{1}{\overline{\gamma}}\right) \tag{5.14}$$

which is identical to the result of the direct derivation of the ergodic capacity over Rayleigh fading channel, i.e.,

$$C_{M=1} = \int_0^\infty \log(1+\gamma)\frac{1}{\overline{\gamma}}e^{-\frac{\gamma}{\overline{\gamma}}}d\gamma = e^{\frac{1}{\overline{\gamma}}}\Gamma\left(0,\frac{1}{\overline{\gamma}}\right) = G^{2,1}_{1,2}\left(\begin{matrix}0\\ 0,0\end{matrix}\middle|\frac{1}{\overline{\gamma}}\right) \tag{5.15}$$

where we are with the help of (Gradshteyn & Ryzhik 2007: eqn. (4.337-2), eqn. (8.359-1), eqn. (9.301), and eqn. (9.31-5)).

5.4 SEP Analysis

A general symbol error probability (SEP) expression for all general modulation formats with respect to the received SNR, γ, was provided in (McKay *et al.* 2007) that

$$P_e = E_\gamma\left[aQ\left(\sqrt{2b\gamma}\right)\right] = \frac{a}{2}E_\gamma\left[\mathrm{erfc}\left(\sqrt{b\gamma}\right)\right] \tag{5.16}$$

where $Q(\cdot)$ is the Gaussian Q-function, and a and b are modulation format based, for instance, binary phase-shift keying (BPSK), $a = 1$ and $b = 1$; binary frequency-shift keying (BFSK) with orthogonal signaling, $a = 1$ and $b = 0.5$; M-ary pulse amplitude modulation (PAM), $a = 2(M-1)/M$ and $b = 3/(M^2-1)$; M-ary phase-shift keying (PSK), $a = 2$ and $b = \sin^2(\pi/M)$. We use an alternative expression $\text{erfc}(\sqrt{x}) = \sqrt{\pi}^{-1} G_{1,2}^{2,0}\left(\begin{smallmatrix}1\\0,1/2\end{smallmatrix}\middle| x\right)$ (Wolfram 2014: eqn. 06.27.26.0006.01), and the average symbol error probability can be expressed as follows,

$$P_e = \frac{a}{2\sqrt{\pi}} E_\gamma \left[G_{1,2}^{2,0}\left(\begin{smallmatrix}1\\0,1/2\end{smallmatrix}\middle| b\gamma\right)\right] \tag{5.17}$$

In our case we replace γ with $\gamma_{\text{GSC},K}$, and then substituting the p.d.f. of $\gamma_{\text{GSC},K}$ (5.10) into (5.17), after some manipulations we obtain the closed-form of the symbol error probability as follows

$$\begin{aligned} P_e = \frac{aK^K}{2\sqrt{\pi}} \binom{M}{K} \Bigg\{ & \frac{1}{\overline{\gamma}^{K-1} K! b^{K-1}} G_{2,2}^{2,1}\left(\begin{smallmatrix}0,K\\K-1,K-1/2\end{smallmatrix}\middle| \frac{b\overline{\gamma}}{K}\right) \\ & + \sum_{n=1}^{M-K} (-1)^{K+n-1} \binom{M-K}{n} \left(\frac{1}{n}\right)^{K-1} \\ & \times \Bigg[\frac{1}{K+n} G_{2,2}^{2,1}\left(\begin{smallmatrix}0,1\\0,1/2\end{smallmatrix}\middle| \frac{b\overline{\gamma}}{K+n}\right) \\ & - \sum_{m=0}^{K-2} \frac{1}{m! K b^m} \left(-\frac{n}{\overline{\gamma}}\right)^m G_{2,2}^{2,1}\left(\begin{smallmatrix}0,m+1\\m,m+1/2\end{smallmatrix}\middle| \frac{b\overline{\gamma}}{K}\right) \Bigg] \Bigg\}. \end{aligned} \tag{5.18}$$

Proof. The details are shown in Appendix 3. □

For $M = K = 1$, the expression can be simplified as

$$P_{e,M=1} = \frac{a}{2\sqrt{\pi}} G_{2,2}^{2,1}\left(\begin{smallmatrix}0,1\\0,1/2\end{smallmatrix}\middle| b\overline{\gamma}\right) \tag{5.19}$$

5.5 Simulation Results

This section presents the analytical and simulation results for the ergodic capacity, where K of total $M = 6$ antennas are selected for the MRC combiner at the secondary receiver. We assume that Rayleigh block fading channels. In the simulation we aim to illustrate the effect of the mean channel gain ratio $\rho = \frac{\overline{g}_{ps}}{\overline{g}_{ss}}$ and the allowed outage increment $\Delta\varepsilon$ of the primary user on the performance

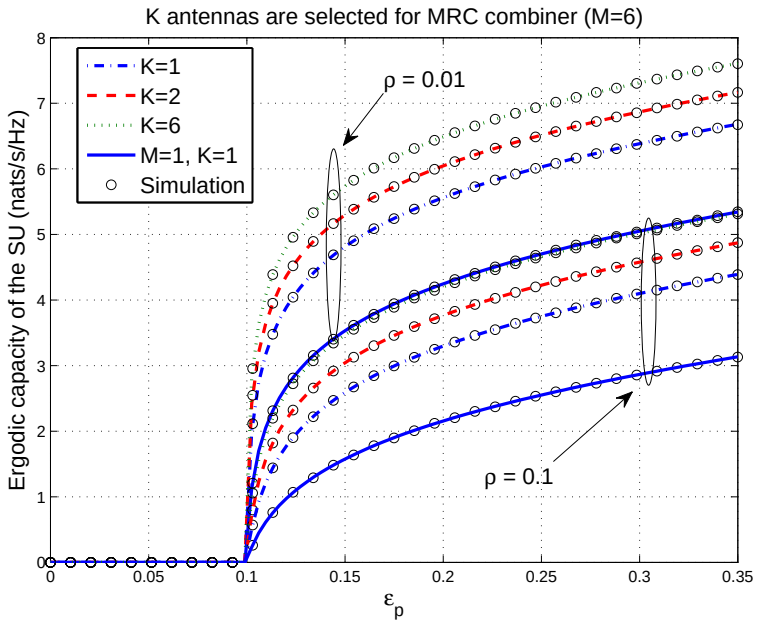

Figure 34. Ergodic capacity of the SU versus ε_p.

of the secondary user. Without loss of generality, the simulation parameters are $N_0B_0 = 1$, $N_1B_1 = 1$, $\overline{g}_{pp} = 1$, $\overline{g}_{ss} = 1$, and the required rate for the primary user $R_P = 0.1$nats/sec/Hz.

Fig. 34 depicts the analytically derived and simulated ergodic capacity of the SU versus the primary user outage probability defined by (5.5). As we discussed in previous section, the secondary user is not allow to transmit when the primary user the target can not be achieved. In addition, the GSC improves the ergodic capacity of the SU dramatically through comparing the results with the single antenna scenario ($M = K = 1$). In Fig. 35, the ergodic capacity of the SU is plotted versus the increment of the primary user outage probability. From the obtained results, we can see that the ergodic capacity of the SU is influenced dramatically by the interference channel of ST-PR, which is consistent with the results drawn in (Kang *et al.* 2009).

Fig. 36 shows the analytically derived and simulated ergodic capacity of the SU versus the channel mean ratio defined by $\rho = \frac{\overline{g}_{ps}}{\overline{g}_{ss}}$. We can see again the improvement of using GSC at the SR. The ergodic capacity of the SU decreases while the mean value of the interference channel from the ST to PR is increasing, for instance, the secondary transmitter is approaching the primary receiver. In Fig. 37,

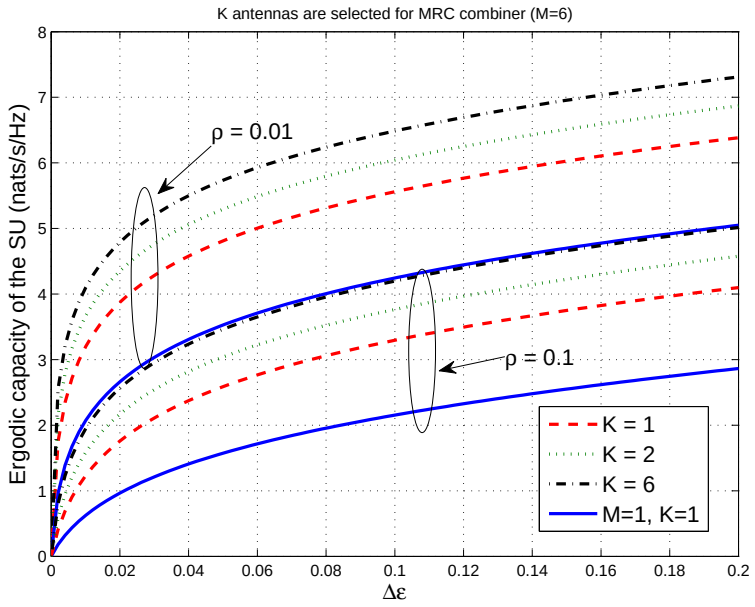

Figure 35. Ergodic capacity of the SU versus the increment of the primary user outage probability, $\Delta\varepsilon$.

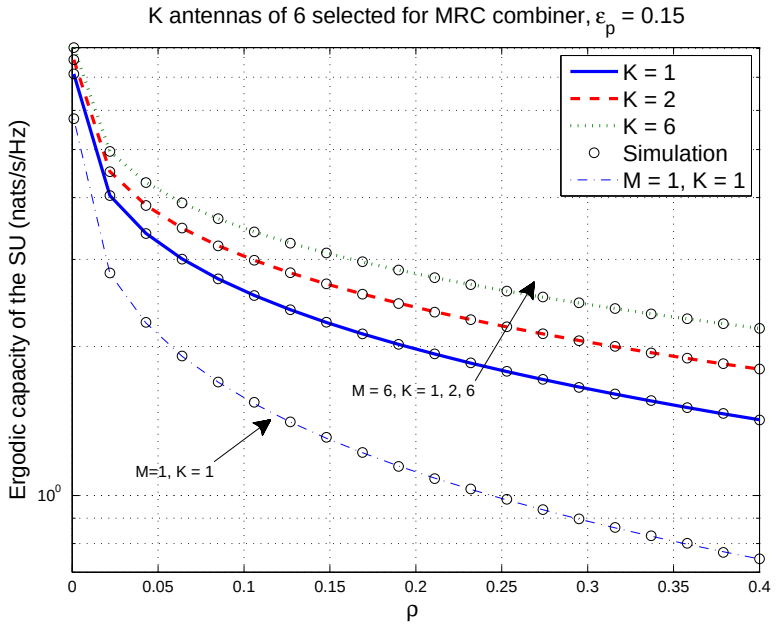

Figure 36. Ergodic capacity of the SU versus ρ given $\varepsilon_p = 0.15$.

the ergodic capacity of the SU is plotted versus ρ for different values of the increment of the primary user outage probability. When the increment of the primary outage probability is fixed, the values of ρ have different influence on the ergodic

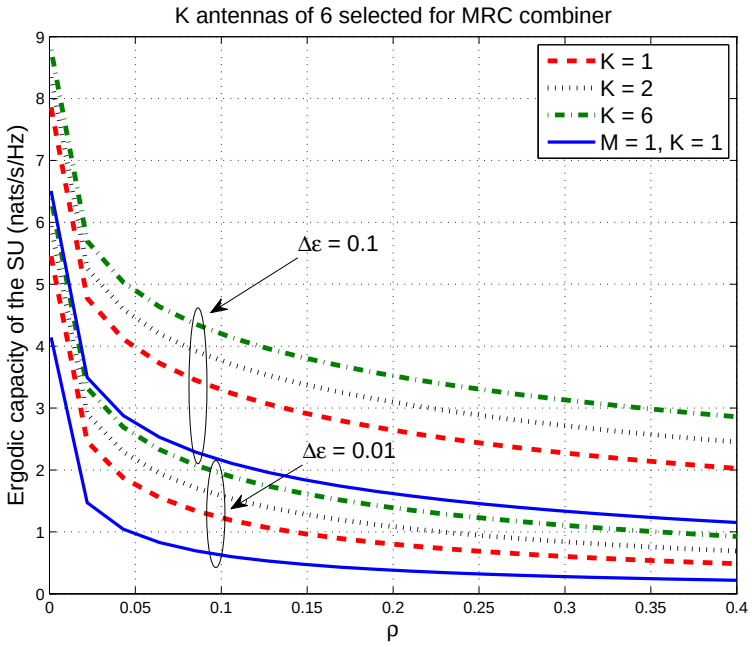

Figure 37. Ergodic capacity of the SU versus ρ for $\Delta\varepsilon = 0.01$ and $\Delta\varepsilon = 0.1$.

capacity. In the small value range of ρ, the ergodic capacity is sensitive to ρ; in the large value range of ρ, the ergodic capacity is sensitive to it.

In Fig. 38 we show analytical results of the symbol error probability for 8-PSK modulation of the secondary user versus primary user outage probability for different number of selected branches. In this case, $a = 2$ and $b = \sin^2\left(\frac{\pi}{8}\right)$. The SEP is dramatically improved by implementing GSC through comparing to the case of $M = K = 1$. Fig. 39 illustrates the SEP versus the increment of the primary user outage probability. Once more the ST-PR channel influences the SEP dramatically.

5.6 Conclusion

In this chapter, we have studied and derived an expression for the ergodic capacity of a cognitive-shared channel with generalized selection combining diversity under the primary outage probability in Rayleigh block fading environment. Closed-form expressions of the ergodic capacity and the symbol error probability for the proposed model are obtained. The results are verified analytically and through simulations.

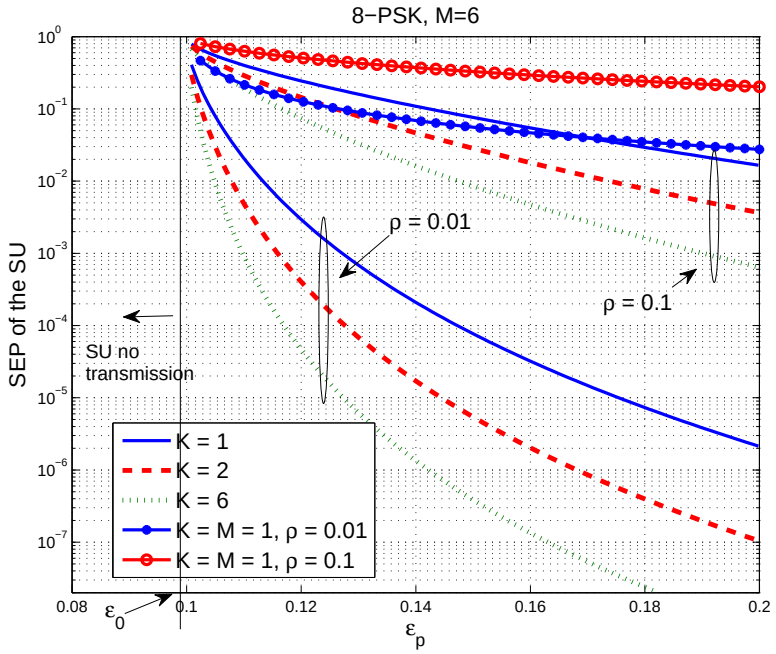

Figure 38. Symbol error probability versus primary user outage probability. ε_0 is given by (eqn. 5.6).

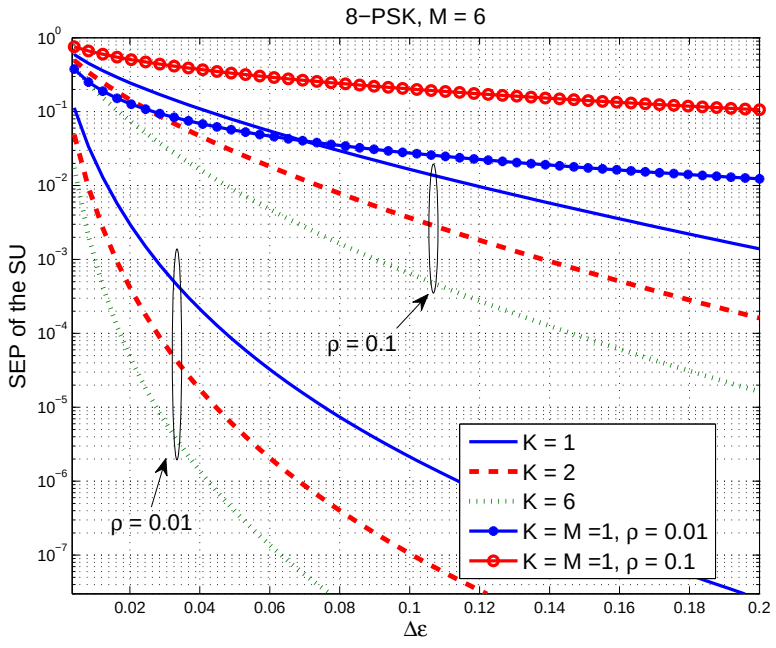

Figure 39. Symbol error probability versus the increment of the primary user outage probability, $\Delta\varepsilon$.

6 EFFECTIVE CAPACITY OF COGNITIVE RADIOS WITH TAS AND MRC

We investigate the effective capacity of a cognitive-shared channel with implementing transmit antenna selection at the secondary transmitter and maximal ratio combining at the secondary receiver under different transmit antenna selection schemes, minimum interference selection (Sel (1)), maximum secondary composite channel gain selection (Sel (2)), and the maximum channel ratio selection (Sel (3)). Closed-form expressions for the effective capacity are presented and validated through simulations.

6.1 Introduction

As what we have seen from previous chapters and references therein that the ergodic capacity has no transmission delay limitation, while the outage capacity does not allow any delay. To this point, the concept of effective capacity (EC) was developed in (Wu & Negi 2003) to define the maximum arrival data rate that can be supported by the channel subject to the required communication delay. It is a link-layer channel model and can be interpreted as the dual of effective bandwidth (Chang & Thomas 1995). The quality of service (QoS) is represented by a term, named QoS exponent. When the QoS exponent $\theta \to 0$, it means that there is no delay limitation, and the effective capacity equals the ergodic capacity. On the other hand, the link cannot tolerate any delay as $\theta \to \infty$. This concept has received much attention in the point-to-point case, e.g., (Tang & Zhang 2007a;b), as well as in cognitive radio, e.g., (Akin & Gursoy 2010; Musavian & Aissa 2010) and references therein.

A combined transmitter antenna selection and receiver maximal ratio combing sche-me was proposed in (Thoen *et al.* 2001). The authors investigated the system performance in terms of the average bit-error rate, and proved that the diversity order of the product of the number of transmit and receive antennas could be achieved, so that this scheme significantly improves the diversity. On one hand, this combined scheme provides not only the diversity gain as the selection combining at the transmitter and the selection combining at the receiver (SC/SC) but also provides the combining gain which the SC/SC does not have. On the other hand, using the SC at the transmitter reduces the complexity of the transmitter and transmit power so that it is suitable in the uplink communication (Thoen *et al.* 2001).

Thereafter, the transmit antenna selection (TAS) and the maximal ratio combining (MRC) techniques have been extensively studied in the literature for traditional wireless communication systems, e.g. (Chen *et al.* 2009; 2005; Hung *et al.* 2010). In (Chen *et al.* 2009; 2005), the authors investigated the outage probability and bit error rate of TAS/MRC in Rayleigh and Nakagami-*m* fading channels, respectively. In (Hung *et al.* 2010), the authors proposed the expressions of the outage probability of multiuser diversity for a TAS/MRC system in independent and identically distributed Nakagami-*m* channels. The full diversity is achieved at high SNR regime.

Recently, the authors in (Blagojevic & Ivanis 2012) studied the ergodic capacity of a spectrum sharing secondary user link with TAS/MRC, in the Rayleigh fading environment. The closed-form expression of the ergodic capacity of the secondary user with peak interference power constraint was derived, while the case with additional peak transmit power for the SU was simulated. The ergodic capacity depends only on the product of the numbers of transmit and receive antennas and the product of the peak signal-to-noise ratio (SNR) and the mean channel power gain ratio. To the best of our knowledge, the EC of a cognitive-shared channel with TAS/MRC in a Rayleigh fading environment and the comparison of the EC with different transmit antenna selection schemes have not been studied in the literature. We investigate this problem under different selection schemes in this chapter.

The remainder of this chapter is organized as follows. In Section 6.2, we present the system and channel model, and the transmit selection schemes investigated in this chapter, as well as the probability density function (p.d.f) and cumulative distribution function (c.d.f) of the SNR at the secondary receiver. In Section 6.3, the EC of the SU under peak interference power (PIP) constraint is studied with different antenna selection techniques. In Section 6.4, the EC of the secondary user under average interference power (AIP) constraint is analyzed. The results are then depicted in Section 6.5. The last Section concludes this chapter.

6.2 System and Channel Model

The spatial diversity scheme for a cognitive-shared channel investigated in this chapter is depicted in Figure 40. This model forms a combination of transmit antenna selection (TAS) at the secondary transmitter (ST) and maximal ratio combining (MRC) at the secondary receiver (SR). The ST is equipped with M antennas

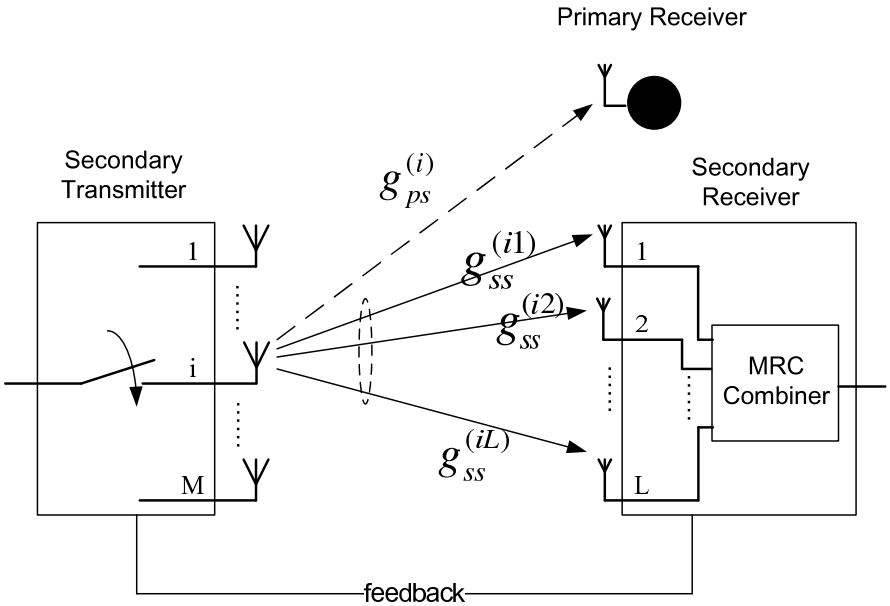

Figure 40. System Model: the *i*th transmit antenna is selected.

and the SR employs L receiving branches that are assumed to be independent from each other. The primary receiver (PR) has one antenna. We assume that the secondary system is far away from the primary transmitter (PT), so that the interference from the PT to the SR is ignored. This pattern has been adopted widely in the research of performance analysis of cognitive radio (Ghasemi & Sousa 2007; Jovicic & Viswanath 2009; Kang *et al.* 2009; Musavian & Aissa 2009b; 2010; Peha 2009; Suraweera *et al.* 2010; Zhang *et al.* 2010). In this scenario, the secondary transmitter aims to maximize its effective capacity, where the interference caused at the primary receiver must be regulated by the predefined interference constraint. Therefore, the ST will select one of its transmit antennas by using proper transmit power to maximize its effective capacity. in order to see how the different transmit antenna selection schemes influence the capacity, we study three scenario: minimum interference selection (Sel (1)), maximum secondary composite channel gain selection (Sel (2)), and the maximum channel ratio selection (Sel (3)).

Let $g_{ss}^{(il)}$, which is assumed to be i.i.d $\forall l = 1, \cdots, L$, be the channel power gain from the *i*th antenna element of the ST to the *l*th antenna element of the SR with mean $\overline{g}_{ss}$, $g_{ss}^{(i)}$ denote the composite channel power gain from the *i*th antenna element of the ST to the SR, and $g_{ps}^{(i)}$ represents the channel power gain from the *i*th antenna element of the ST to the PR. In our analysis, we assume that the wireless channels

experience block Rayleigh fading assumed to be ergodic and stationary. Thus, the channel state does not change during each block, and the channel states are uncorrelated between blocks (Ozarow *et al.* 1994). Let T denote the time duration of a block. In consequence, in a Rayleigh fading the channel power gain $g_{ps}^{(i)}$ follows exponential distribution with mean value $\overline{g}_{ps}$. The compound channel power gain $g_{ss}^{(i)}$ is characterized by a Chi-square distribution with $2L$ degrees of freedom, and the corresponding p.d.f. and c.d.f. of $g_{ss}^{(i)}$ are given as follows (Proakis & Salehi 2008):

$$f_{g_{ss}^{(i)}}(h) = \frac{h^{L-1}\exp\left(-h/\overline{g}_{ss}\right)}{\overline{g}_{ss}^{L}(L-1)!}, \quad h \geq 0, \quad 1 \leq i \leq M \tag{6.1}$$

$$F_{g_{ss}^{(i)}}(h) = \frac{1}{(L-1)!}\gamma\left(L, \frac{h}{\overline{g}_{ss}}\right) = 1 - \exp\left(-\frac{h}{\overline{g}_{ss}}\right)\sum_{l=0}^{L-1}\frac{1}{l!}\left(\frac{h}{\overline{g}_{ss}}\right)^{l} \tag{6.2}$$

where the noise at each branch is assumed to be uncorrelated additive white Gaussian noise (AWGN). The p.d.f. of $g_{ps}^{(i)}$ is represented by

$$f_{g_{ps}^{(i)}}(g) = \frac{1}{\overline{g}_{ps}} e^{-g/\overline{g}_{ps}}, \quad g \geq 0, \quad 1 \leq i \leq M. \tag{6.3}$$

The MRC technique requires perfect knowledge of the branch amplitudes and phases, and provides the optimal diversity. Hence, it offers the maximal capacity improvement relative to other linear combining techniques (Brennan 2003). The transmit power of the secondary transmitter is regulated by peak interference power (Q_{pk}) constraint or the average interference power (Q_{av}) constraint at the primary receiver. We investigate the following three schemes of transmit antenna selection of the secondary transmitter:

- Minimum interference selection (Sel (1)): the antenna element at the secondary transmitter is selected which causes minimum interference to the primary user. In other words, the interference channel (from the secondary transmitter to the primary receiver, ST-PR) power gain is the minimum. In this case the ST uses only the interference channel information for making selection.

- Maximum secondary composite channel gain selection (Sel (2)): the antenna element is selected to maximize the data rate of the secondary user. That is,

the antenna element which has maximum channel gain to the secondary receiver is selected (from the secondary transmitter to the secondary receiver, ST-SR).

- Maximum channel ratio selection (Sel (3)): the antenna element is selected at the secondary transmitter which has the maximal channel gain ratio of $g_{ss}^{(i)}/g_{ps}^{(i)}$.

For deriving the expressions of the effective capacity of the secondary user, we first investigate the related p.d.f. and c.d.f. expressions in the following.

6.2.1 Minimum interference selection

The transmit antenna which minimizes the interference to the primary is selected, i.e., the channel from the selected antenna to the primary user has the minimal channel gain among all antennas.

$$k = \arg_{\forall i} \min \left\{ g_{ps}^{(i)} \right\}, \quad 1 \leq i \leq M. \tag{6.4}$$

Using order theorem (David & Nagaraja 2003), the c.d.f. and the p.d.f. of $g_{ps}^{(k)}$ are given by

$$F_{g_{ps}^{(k)}}(g) = 1 - \left[\exp\left(-\frac{g}{\overline{g}_{ps}} \right) \right]^M \tag{6.5}$$

and

$$f_{g_{ps}^{(k)}}(g) = M \left[\exp\left(-\frac{g}{\overline{g}_{ps}} \right) \right]^{M-1} \frac{\exp\left(-g/\overline{g}_{ps}\right)}{\overline{g}_{ps}} = \frac{M}{\overline{g}_{ps}} \left[\exp\left(-\frac{g}{\overline{g}_{ps}} \right) \right]^M \tag{6.6}$$

Now we derive the probability distribution of the ratio, $g_{ss}^{(k)}/g_{ps}^{(k)}$. Let $z = g_{ss}^{(k)}/g_{ps}^{(k)}$ and $w = g_{ps}^{(k)}$. The Jacobian is given by

$$J_{z,w} = \det \begin{vmatrix} w & z \\ 0 & 1 \end{vmatrix} = w \tag{6.7}$$

The joint p.d.f. of z and w.

$$f_{z,w} = f_{g_{ss}^{(k)},g_{ps}^{(k)}}(h = zw, g = w)\, w \tag{6.8}$$
$$= \frac{M}{\overline{g}_{ps}}\left[\exp\left(-\frac{w}{\overline{g}_{ps}}\right)\right]^{M} \frac{(zw)^{L-1}e^{-zw/\overline{g}_{ss}}}{\overline{g}_{ss}^{L}(L-1)!}w$$

The p.d.f. of z.

$$f_z(z) = \int_0^\infty f_{z,w}(z,w)\,dw \tag{6.9}$$
$$= \frac{Mz^{L-1}}{\overline{g}_{ps}\overline{g}_{ss}^{L}(L-1)!}\int_0^\infty w^L \exp\left(-\frac{Mw}{\overline{g}_{ps}} - \frac{zw}{\overline{g}_{ss}}\right) dw$$
$$= \frac{ML\rho z^{L-1}}{(z+M\rho)^{L+1}}$$

where $\rho = \overline{g}_{ss}/\overline{g}_{ps}$. The last step is with the help of (Gradshteyn & Ryzhik 2007: eqn. 3.351-1)

The c.d.f. of z.

$$F_z(z) = \int_0^z f_z(x)\,dx = \int_0^z \frac{ML\rho x^{L-1}}{(x+M\rho)^{L+1}}\,dx = \left(\frac{z}{z+M\rho}\right)^{L} \tag{6.10}$$

6.2.2 Maximum secondary composite channel gain selection

The transmit antenna which has maximal channel gain of ST-SR is selected, i.e., the channel from the selected antenna to the secondary receiver has the maximal composite channel gain among all antennas.

$$k = \arg_{\forall i}\max\left\{g_{ss}^{(i)}\right\}, \quad 1 \le i \le M. \tag{6.11}$$

Using order theorem (David & Nagaraja 2003), the c.d.f. of the maximum channel gain, $g_{ss}^{(k)}$, can be represented as

$$
\begin{aligned}
F_{g_{ss}^{(k)}}(x) &= \prod_{l=1}^{M} F_{h_l}(x) = \prod_{l=1}^{M} \left[\frac{1}{(L-1)!} \gamma\left(L, \frac{x}{\overline{g}_{ss}}\right) \right] \\
&= \prod_{l=1}^{M} \left[1 - e^{-\frac{x}{\overline{g}_{ss}}} \sum_{k_l=0}^{L-1} \frac{1}{k_l!} \left(\frac{x}{\overline{g}_{ss}}\right)^{k_l} \right] \\
&= \sum_{n \in \theta_M} \prod_{l=1}^{M} (-1)^{n_l} \left[e^{-\frac{x}{\overline{g}_{ss}}} \sum_{k_l=0}^{L-1} \frac{1}{k_l!} \left(\frac{x}{\overline{g}_{ss}}\right)^{k_l} \right]^{n_l} \\
&= \sum_{n \in \theta_M} \prod_{l=1}^{M} (-1)^{n_l} e^{-\frac{x}{\overline{g}_{ss}} n_l} \left[\sum_{k_l=0}^{L-1} \frac{1}{k_l!} \left(\frac{x}{\overline{g}_{ss}}\right)^{k_l} \right]^{n_l} \\
&= \sum_{n \in \theta_M} e^{-\frac{x}{\overline{g}_{ss}} \sum_{l=1}^{M} n_l} \prod_{l=1}^{M} (-1)^{n_l} \sum_{k_l=0}^{L-1} \frac{L^{n_l-1}}{(k_l!)^{n_l}} \left(\frac{x}{\overline{g}_{ss}}\right)^{k_l n_l} \\
&= \sum_{n \in \theta_M} \sum_{k_1=0}^{L-1} \cdots \sum_{k_M=0}^{L-1} e^{-\frac{x}{\overline{g}_{ss}} \sum_{l=1}^{M} n_l} x^{\sum_{l=1}^{M} k_l n_l} \prod_{l=1}^{M} \left(\frac{-1}{k_l!}\right)^{n_l} \frac{L^{n_l-1}}{\overline{g}_{ss}^{k_l n_l}} \\
&= \sum_{n \in \theta_M} \sum_{k_1=0}^{L-1} \cdots \sum_{k_M=0}^{L-1} K_{n,k} e^{-xB_n} x^{A_{n,k}}
\end{aligned}
\tag{6.12}
$$

where θ_M is defined as the binary number set with M elements

$$
K_{n,k} = \prod_{l=1}^{M} \left(\frac{-1}{k_l!}\right)^{n_l} \frac{L^{n_l-1}}{\overline{g}_{ss}^{k_l n_l}} \tag{6.13}
$$

$$
B_n = \frac{1}{\overline{g}_{ss}} \sum_{l=1}^{M} n_l \tag{6.14}
$$

$$
A_{n,k} = \sum_{l=1}^{M} k_l n_l \tag{6.15}
$$

The above proof follows the Lemma in (Yilmaz *et al.* 2011) and (Yilmaz *et al.* 2013). The p.d.f. can be obtained as following

$$
\begin{aligned}
f_{g_{ss}^{(k)}}(x) &= \frac{d}{dx} F_{h_{\max}}(x) \\
&= \sum_{n \in \theta_M} \sum_{k_1=0}^{L-1} \cdots \sum_{k_M=0}^{L-1} K_{n,k} e^{-xB_n} x^{A_{n,k}-1} \left[A_{n,k} - xB_n \right]
\end{aligned}
\tag{6.16}
$$

Let $z = g_{ss}^{(k)}/g_{ps}^{(k)}$ and $w = g_{ps}^{(k)}$. The Jacobian is given by

$$J_{z,w} = \det \begin{vmatrix} w & z \\ 0 & 1 \end{vmatrix} = w \tag{6.17}$$

The joint p.d.f. of z and w can be obtained by

$$\begin{aligned} f_{z,w} &= f_{g_{ss}^{(k)}, g_{ps}^{(k)}}(h = zw, g = w)\, w \\ &= \frac{1}{\overline{g}_{ps}} e^{-w/\overline{g}_{ps}} \sum_{n \in \theta_M} \sum_{k_1=0}^{L-1} \cdots \sum_{k_M=0}^{L-1} K_{n,k} e^{-zwB_n} (zw)^{A_{n,k}-1} \left[A_{n,k} - zwB_n\right] w \end{aligned} \tag{6.18}$$

The p.d.f. of z can be expressed as

(6.19)

$$\begin{aligned} f_z(z) &= \int_0^\infty f_{z,w}(z,w)\, dw \\ &= \frac{1}{\overline{g}_{ps}} \sum_{n \in \theta_M} \sum_{k_1=0}^{L-1} \cdots \sum_{k_M=0}^{L-1} K_{n,k} z^{A_{n,k}-1} \int_0^\infty e^{-w/\overline{g}_{ps} - zwB_n} w^{A_{n,k}} \left[A_{n,k} - zwB_n\right] dw \\ &= \sum_{n \in \theta_M} \sum_{k_1=0}^{L-1} \cdots \sum_{k_M=0}^{L-1} K_{n,k} \overline{g}^{A_{n,k}} \\ &\quad \times \left(\frac{A_{n,k}\Gamma(A_{n,k}+1) z^{A_{n,k}-1}}{\left(1 + B_n \overline{g}_{ps} z\right)^{A_{n,k}+1}} - \frac{B_n \overline{g}_{ps} \Gamma(A_{n,k}+2) z^{A_{n,k}}}{\left(1 + B_n \overline{g}_{ps} z\right)^{A_{n,k}+2}} \right) \end{aligned}$$

where in the last step we have used (Gradshteyn & Ryzhik 2007: eqn. 3.381-4).

It is obvious that if $B_n = 0$, i.e. $n \in \mathbf{0}_M$ we also have $A_{n,k} = 0$, then $f_z(z) = 0$. In the following, without loss of generality we assume that $n \in \theta_M$ represents $n \in \theta_M$ and $n \neq \mathbf{0}_M$, where $\mathbf{0}_M$ is binary set with M zero elements.

6.2.3 Maximum channel ratio selection

The transmit antenna which maximizes $z_i \triangleq \frac{g_{ss}^{(i)}}{g_{ps}^{(i)}}$ is selected, i.e.,

$$k = \arg_{\forall i} \max \left\{ \frac{g_{ss}^{(i)}}{g_{ps}^{(i)}} \right\}, \quad 1 \leq i \leq M. \tag{6.20}$$

The p.d.f. of z_i can be obtained as follows.

$$f_{z_i}(x) = \frac{L\rho x^{L-1}}{(x+\rho)^{L+1}} \tag{6.21}$$

where $\rho = \overline{g}_{ss}/\overline{g}_{ps}$.

Proof. Let $z_i = \frac{g_{ss}^{(i)}}{g_{ps}^{(i)}}$ and $w = g_{ps}^{(i)}$. Then the Jacobian, $J(z_i, w)$, is given by

$$J_{z_i,w}(z,w) = \det \begin{vmatrix} w & z \\ 0 & 1 \end{vmatrix} = w \tag{6.22}$$

$$\begin{aligned} f_{z_i,w}(z,w) &= f_{g_{ss}^{(i)}}(h = zw) f_{g_{ps}^{(i)}}(g = w) w \\ &= \frac{(zw)^{L-1} e^{-zw/\overline{g}_{ss}}}{\overline{g}_{ss}^{L}(L-1)!} \frac{1}{\overline{g}_{ps}} e^{-w/\overline{g}_{ps}} w \end{aligned}$$

Then the marginal distribution of z_i can be obtained by integrating $f_{z,w}(z,w)$ over w.

$$\begin{aligned} f_{z_i}(z) &= \int_0^\infty f_{z_i,w}(z,w)dw = \int_0^\infty \frac{(zw)^{L-1} e^{-zw/\overline{h}}}{\overline{h}^{L}(L-1)!} \frac{1}{\overline{g}} e^{-w/\overline{g}} w dw \\ &= \frac{L\rho z^{L-1}}{(z+\rho)^{L+1}} \end{aligned}$$

□

The c.d.f. can be obtained as

$$F_{z_i}(z) = \int_0^z f_{z_i}(x)dx = \int_0^z \frac{L\rho x^{L-1}}{(x+\rho)^{L+1}} dv = \left(\frac{z}{z+\rho}\right)^L \tag{6.23}$$

Then according to the order theorem the p.d.f. of z_k can be obtained as

$$f_{z_k}(z) = M(F_{z_i}(z))^{M-1} f_{z_i}(z) = ML\rho \frac{z^{ML-1}}{(z+\rho)^{ML+1}} \tag{6.24}$$

6.3 Effective Capacity Under PIP Constraint

In this section we study the effective capacity of the secondary user under peak interference power (PIP) constraint for different transmit antena selection schemes.

First, we again briefly review the concept of the effective capacity and derive a closed-form expression for the EC. The probability of the queue length $q(x)$ of a stationary ergodic arrival and service process exceeding a certain threshold T_q decays exponentially as a function of T_q (Tang & Zhang 2007b). The delay QoS exponent is defined as

$$\theta = -\lim_{T_q \to \infty} \frac{\log(\Pr\{q(\infty) > T_q\})}{T_q}. \tag{6.25}$$

It is worth noting that $\theta \to 0$ indicates that the system has no delay constraint, while $\theta \to \infty$ implies a stringent delay constraint. The effective capacity is defined in (Wu & Negi 2003: Eqn. (12)) as follows,

$$EC(\theta) = -\lim_{t \to \infty} \frac{1}{\theta t} \log\left[\mathbb{E}\left(e^{-\theta \sum_{i=0}^{t} R[i]}\right)\right], \; t \geq 0 \tag{6.26}$$

where $\{R[i], i = 1, 2, ...\}$ denotes a discrete-time service process, which is assumed to be ergodic and stationary. For a block fading channel, the EC can be reduced to (Tang & Zhang 2007b),

$$EC(\theta) = -\frac{1}{\theta} \log\left[\mathbb{E}\left(e^{-\theta R[i]}\right)\right]. \tag{6.27}$$

The maximum achievable instantaneous service rate $R[i]$ of block i can be expressed as $R[i] = TB\log\left(1 + \frac{p_s(\theta, g_{ss}^{(k)}, g_{ss}^{(k)}) g_{ss}^{(k)}}{N_1 B}\right)$, where the superscript k denotes the kth transmit antenna branch is selected, $p_s(\theta, g_{ss}^{(k)}, g_{ps}^{(k)})$ is the transmit power of the secondary transmitter, T denotes the block length duration, N_1 denotes the AWGN power density at the , and B is the channel bandwidth. In the following we derive the expressions of the effective capacity of the secondary user in different scenarios.

Notations: Let $\mathcal{B}(x, y)$ denote the Beta function given by $\int_0^1 t^{x-1}(1-t)^{y-1}dt$, and ${}_2F_1(a, b; c; z)$ be the Gauss's hypergeometric function (Abramowitz & Stegun 1964). For convenience, let $\alpha = \theta TB$.

6.3.1 Minimum interference selection

In this case, the p.d.f. of the channel power gains, z_k, is given by (6.9). The resultant effective capacity of the secondary user is given by the following theorem.

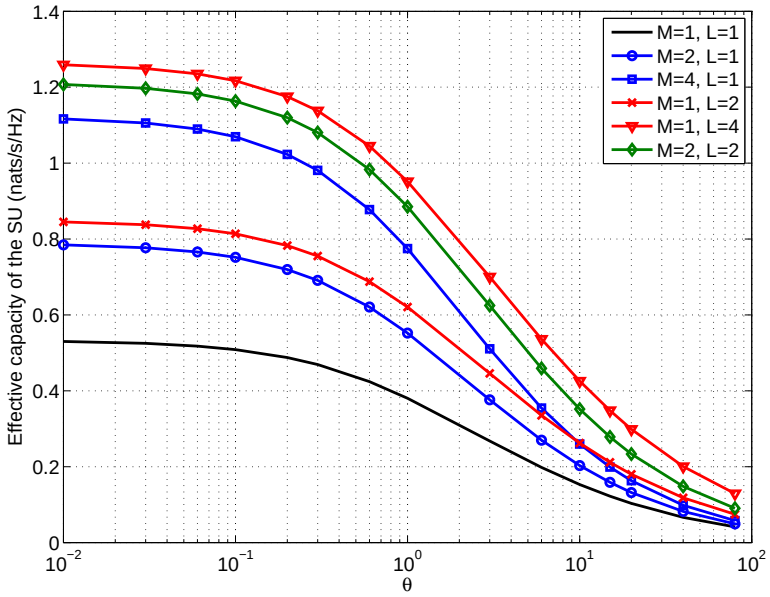

Figure 41. Effective capacity of the SU versus QoS exponent under PIP constraint and minimum interference selection, where the mean channel power gain ratio $\rho = 1$, $N_1 B = 1$, and $Q_{pk} = -5$dB.

Theorem 6.1. *The effective capacity of the cognitive-shared channel of Figure 40 under peak interference power constraint over Rayleigh fading with minimum interference selection scheme is given by*

$$EC(\theta) = -\frac{1}{\theta}\log\left[L\mathcal{B}(L,1+\alpha)_2F_1\left(\alpha,L;L+1+\alpha;1-\frac{Q_{pk}M\rho}{N_1B}\right)\right] \tag{6.28}$$

Proof.

$$\begin{aligned} EC(\theta) &= -\frac{1}{\theta}\log\left[\mathbb{E}_{z_k}\left(e^{-\alpha\log\left(1+\frac{zQ_{pk}}{N_1B}\right)}\right)\right] \\ &= -\frac{1}{\theta}\log\left[\int_0^\infty\left(1+\frac{zQ_{pk}}{N_1B}\right)^{-\alpha}\frac{ML\rho z^{L-1}}{(z+M\rho)^{L+1}}\,dz\right] \\ &= -\frac{1}{\theta}\log\left[L\mathcal{B}(L,1+\alpha)\,{}_2F_1\left(a,L;L+1+\alpha;1-\frac{Q_{pk}M\rho}{N_1B}\right)\right] \end{aligned}$$

where in the last step, we have used Eqn. (3.197-1) in (Gradshteyn & Ryzhik 2007). □

In Fig. 41 we show the effective capacity of the secondary user when the SU chooses the transmit antenna element having the minimum channel gain from the secondary transmitter to the primary receiver over different transmit and receive degrees of diversity. Without loss of generality, $N_1 B = 1$. First, it is obvious that the TAS/MRC improves the achievable effective capacity over a large range of the QoS exponent. Second, the performance of using multiple receive antennas surpasses the one using multiple transmit antennas, e.g. the performance of $M = 1, L = 2$ is better than the one of $M = 2, L = 1$, and $M = 1, L = 4$ is better than the one of $M = 4, L = 1$. Third, in this case using $M = 2$ and $L = 2$ can not achieve the full diversity, because we only utilize partial channel information, i.e. only the interference channel information. Forth, at high θ regime, $M = 1, L = 2$ is slightly better than $M = 4, L = 1$. This can be explained as that the benefit of using TAS is not able to compensate the capacity loss caused by the channel deep fading.

6.3.2 Maximum secondary composite channel gain selection

In this case, the p.d.f. of z_k is given by (6.19). The resultant effective capacity of the secondary user is given by the following theorem.

Theorem 6.2. *The effective capacity of the cognitive-shared channel of Figure 40 under peak interference power constraint over Rayleigh fading with maximum secondary composite channel gain selection is given by*

$$EC(\theta) = -\frac{1}{\theta}\log\left\{\sum_{n\in\theta_M}\sum_{k_1=0}^{L-1}\cdots\sum_{k_M=0}^{L-1}\frac{K_{n,k}}{B_n^{A_{n,k}}}\left[\mathcal{C}_1+\mathcal{C}_2\right]\right\} \tag{6.29}$$

where $\mathcal{C}_1$ *for* $B_n \neq 0$ *and* $\mathcal{C}_2$ *for* $B_n = 0$ *are given by*

$$\begin{aligned}\mathcal{C}_1 = \Bigg[&A_{n,k}\Gamma\left(A_{n,k}+1\right)\mathcal{B}(A_{n,k},\alpha+1)\\ &\times {}_2F_1\left(\alpha,A_{n,k};A_{n,k}+\alpha+1;1-\frac{Q_{pk}}{N_1 B\overline{g}_{ps}B_n}\right)\Bigg]\end{aligned} \tag{6.30}$$

and

$$\begin{aligned}\mathcal{C}_2 = \Bigg[&-\Gamma\left(A_{n,k}+2\right)\mathcal{B}(A_{n,k}+1,\alpha+1)\\ &\times {}_2F_1\left(\alpha,A_{n,k}+1;A_{n,k}+\alpha+2;1-\frac{Q_{pk}}{N_1 B\overline{g}_{ps}B_n}\right)\Bigg]\end{aligned} \tag{6.31}$$

Proof.

$$
\begin{aligned}
EC(\theta) = &-\frac{1}{\theta}\log\left[\int_0^{\infty}\left(1+\frac{Q_{pk}}{N_1 B}z\right)^{-\alpha}\frac{1}{\overline{g}_{ps}}\sum_{n\in\theta_M}\sum_{k_1=0}^{L-1}\cdots\sum_{k_M=0}^{L-1}\frac{K_{n,k}}{B_n^{A_{n,k}+1}}\right.\\
&\left.\times\left(\frac{A_{n,k}\Gamma(A_{n,k}+1)z^{A_{n,k}-1}}{\left(z+\frac{1}{B_n\overline{g}_{ps}}\right)^{A_{n,k}+1}}-\frac{\Gamma(A_{n,k}+2)z^{A_{n,k}}}{\left(z+\frac{1}{B_n\overline{g}_{ps}}\right)^{A_{n,k}+2}}\right)dz\right]\\
= &-\frac{1}{\theta}\log\left[\frac{1}{\overline{g}_{ps}}\left(\frac{Q_{pk}}{N_1 B}\right)^{-\alpha}\sum_{n\in\theta_M}\sum_{k_1=0}^{L-1}\cdots\sum_{k_M=0}^{L-1}\frac{K_{n,k}}{B_n^{A_{n,k}+1}}\int_0^{\infty}\left(\frac{N_1 B}{Q_{pk}}+z\right)^{-\alpha}\right.\\
&\left.\times\left(\frac{A_{n,k}\Gamma(A_{n,k}+1)z^{A_{n,k}-1}}{\left(z+\frac{1}{B_n\overline{g}_{ps}}\right)^{A_{n,k}+1}}-\frac{\Gamma(A_{n,k}+2)z^{A_{n,k}}}{\left(z+\frac{1}{B_n\overline{g}_{ps}}\right)^{A_{n,k}+2}}\right)dz\right]
\end{aligned}
$$

then we have the result in (6.29) by implying (Gradshteyn & Ryzhik 2007: Eqn. (3.197-1)) to the above integration. □

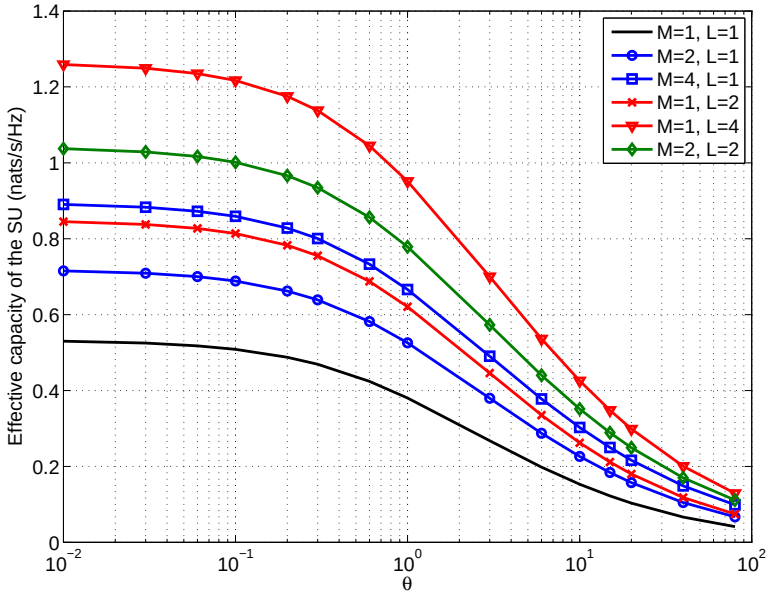

Figure 42. Effective capacity of the SU versus QoS exponent under PIP constraint and maximum MRC channel gain, where the mean channel power gain ratio $\rho = 1$, $N_1 B = 1$, and $Q_{pk} = -5$dB.

In Fig. 42 we show the effective capacity of the secondary user when the SU chooses the transmit antenna element having the maximum ST-SR channel gain

over different transmit and receive degrees of diversity. First, it is obvious that the TAS/MRC improves the achievable effective capacity over a large range of the QoS exponent. Second, in this case using more receiving antennas always (over the simulated range of θ) is superior using more transmit antennas given the same value of $M \times L$. This is different from the case of Sel (1) scheme at the high θ regime. Third, the larger value of $M \times L$, the better performance the SU has. However, the performance of the scenario of $M = 1, L = 4$ surpasses the one of $M = 2, L = 2$. This is because the former cased can use the full diversity while the later does not according to the antenna selection method.

6.3.3 Maximum Channel Ratio Selection

In this case the channel information of ST-PR and ST-SR are used to make the selection. Thus the secondary user utilizes the full diversity of multiple antennas which can be seen from the following theorem and the simulation.

Theorem 6.3. *The effective capacity of the cognitive-shared channel of Figure 40 with exploiting maximum channel ratio selection scheme under peak interference power constraint over Rayleigh fading is given by*

(6.32)
$$EC(\theta) = -\frac{1}{\theta}\log\left[ML\mathcal{B}(ML, \alpha+1)\,{}_2F_1\left(\alpha, ML; \alpha+ML+1; 1-\frac{Q_{pk}\rho}{N_1 B}\right)\right]$$

Proof.

$$\begin{aligned}
&-\frac{1}{\theta}\log\left[\mathbb{E}_{z_k}\left(e^{-\alpha\log\left(1+\frac{Q_{pk}}{N_1 B}z\right)}\right)\right] \\
&= -\frac{1}{\theta}\log\left[\int_0^\infty \left(1+\frac{Q_{pk}}{N_1 B}z\right)^{-\alpha} ML\rho\frac{z^{ML-1}}{(z+\rho)^{ML+1}}dz\right] \\
&= -\frac{1}{\theta}\log\left[ML\mathcal{B}(ML, \alpha+1){}_2F_1\left(\alpha, ML; \alpha+n+1; 1-\frac{Q_{pk}\rho}{N_1 B}\right)\right]
\end{aligned}$$

where in the last step, we have used (Gradshteyn & Ryzhik 2007: Eqn. (3.197-1)). □

It is proved that the EC depends on the diversity order $M \times L$, the QoS exponent θ, the product of the channel bandwidth and the channel coherence time (duration of fading block), the interference power constraint, the noise power and the

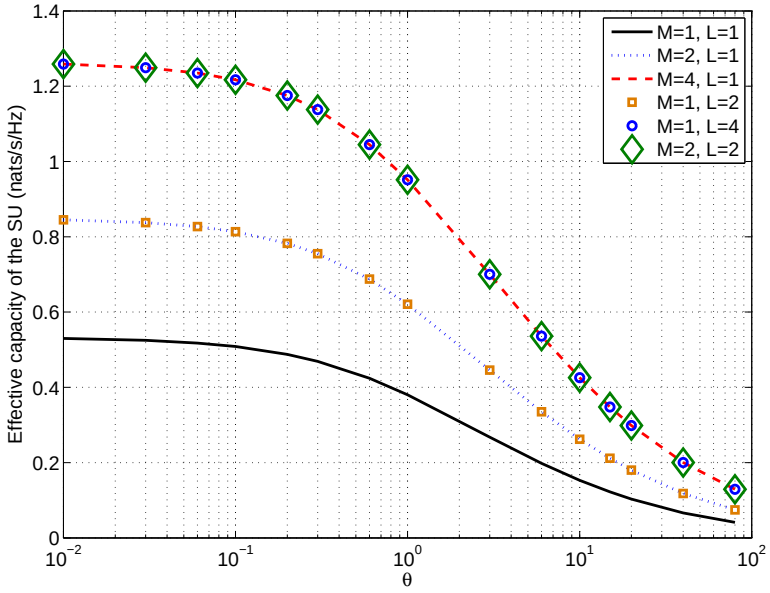

Figure 43. Effective capacity of the SU versus QoS exponent under PIP constraint and maximum channel radio selection, where the mean channel power gain ratio $\rho = 1$, $N_1 B = 1$, and $Q_{pk} = -5$dB.

mean channel power gain ratio. The simulated results are plotted in Fig. 43. We have investigated the performance of the secondary user in terms of the effective capacity under the peak interference power constraint. Next, we study the performance under average interference power constraint for the different antenna selection schemes.

6.4 Effective Capacity under AIP Constraint

In this section we study the effective capacity of the secondary user where the interference to the primary user is limited by the average interference power, Q_{av}. We may formulate the following optimization problem.

$$\text{maximize} \quad -\frac{1}{\theta}\mathbb{E}\left[e^{-\alpha \log\left(1+\frac{g_{ss}^{(k)} p_s(\theta, g_{ps}^{(k)}, g_{ss}^{(k)})}{N_1 B}\right)}\right] \tag{6.33}$$

subject to

$$\mathbb{E}\left[g_{ps}^{(k)} p_s(\theta, g_{ps}^{(k)}, g_{ss}^{(k)})\right] \leq Q_{av} \tag{6.34}$$

$$p_s(\theta, g_{ps}^{(k)}, g_{ss}^{(k)}) \geq 0 \tag{6.35}$$

This optimization problem can be equivalently written as

$$\text{minimize} \quad \mathbb{E}\left[\left(1+\frac{g_{ss}^{(k)} p_s(\theta, g_{ps}^{(k)}, g_{ss}^{(k)})}{N_1 B}\right)^{-\alpha}\right] \tag{6.36}$$

subject to (6.34), (6.35)

The power allocation can be obtained through using Lagrangian method as

$$p_s(\theta, g_{ps}^{(k)}, g_{ss}^{(k)}) = N_1 B \left[\frac{\beta^{\frac{1}{1+\alpha}}}{{g_{ss}^{(k)}}^{\frac{\alpha}{1+\alpha}} {g_{ps}^{(k)}}^{\frac{1}{1+\alpha}}} - \frac{1}{g_{ss}^{(k)}}\right]^{+} \tag{6.37}$$

where $\alpha = \theta TB$, $\beta = \frac{\alpha}{\lambda N_1 B}$, and λ is the Lagrangian multiplier associated to (6.34).

6.4.1 Minimum Interference Selection

In this case, the p.d.f. of the channel power gains, $z_k = g_{ss}^{(k)}/g_{ps}^{(k)}$, is given by (6.9). Although this case is not practical that the SU does not utilize all the channel state information (CSI) for making transmitter antenna selection, we here just study the impact of using CSI of ST-PR only on the effective capacity and the power adaptation uses all the CSI. The resultant effective capacity of the secondary user is given by the following theorem.

Theorem 6.4. *The effective capacity of the cognitive-shared channel of Figure 40 with exploiting minimum interference channel ratio selection scheme under average interference power constraint over Rayleigh fading is given by*

(6.38)
$$EC(\theta) = -\frac{1}{\theta}\log\left[\frac{1}{(M\rho\beta)^L}\,{}_2F_1\left(L+1,L;L+1;-\frac{1}{M\rho\beta}\right) + \frac{ML\rho\beta(1+\alpha)}{1+2\alpha}\,{}_2F_1\left(L+1,1+\frac{\alpha}{1+\alpha};2+\frac{\alpha}{1+\alpha};-M\rho\beta\right)\right]$$

Proof.

$$\begin{aligned}
&-\frac{1}{\theta}\log\left[\mathbb{E}_{z_k}\left(e^{-\alpha\log\left(1+p_s g_{ss}^{(k)}/N_1 B\right)}\right)\right]\\
&=-\frac{1}{\theta}\log\left[\int_0^\infty\left(1+\left[\beta^{\frac{1}{1+\alpha}}z^{\frac{1}{1+\alpha}}-1\right]^+\right)^{-\alpha}\frac{ML\rho z^{L-1}}{(z+M\rho)^{L+1}}\,dz\right]\\
&=-\frac{1}{\theta}\log\left[\int_0^{1/\beta}\frac{ML\rho z^{L-1}}{(z+M\rho)^{L+1}}\,dz+\int_{1/\beta}^\infty\beta^{-\frac{\alpha}{1+\alpha}}z^{-\frac{\alpha}{1+\alpha}}\frac{ML\rho z^{L-1}}{(z+M\rho)^{L+1}}\,dz\right]
\end{aligned}$$

we then have the result by using (Gradshteyn & Ryzhik 2007: Eqn. (3.194-1) and (3.194-2)) to the integrals. □

The Lagrangian multiplier satisfies the following condition

(6.39)
$$Q_{av} = \frac{ML\rho N_1 B\beta^2}{2}\left[\frac{2+2\alpha}{1+2\alpha}\,{}_2F_1\left(L+1,1+\frac{\alpha}{1+\alpha};2+\frac{\alpha}{1+\alpha};-M\rho\beta\right) - {}_2F_1\left(L+1,2;3;-M\rho\beta\right)\right]$$

Proof.

$$\begin{aligned}
Q_{av} &= \mathbb{E}\left[g_{ps}^{(k)}p_s(\theta,g_{ps}^{(k)},g_{ss}^{(k)})\right]\\
&=\int_0^\infty N_1 B\left[\frac{\beta^{\frac{1}{1+\alpha}}}{z^{\frac{\alpha}{1+\alpha}}}-\frac{1}{z}\right]^+ f_{z_k}(z)\,dz\\
&=\int_{1/\beta}^\infty N_1 B\left[\frac{\beta^{\frac{1}{1+\alpha}}}{z^{\frac{\alpha}{1+\alpha}}}-\frac{1}{z}\right]\frac{ML\rho z^{L-1}}{(z+M\rho)^{L+1}}\,dz\\
&=N_1 BML\rho\left[\beta^{\frac{1}{1+\alpha}}\int_{1/\beta}^\infty\frac{z^{L-\frac{\alpha}{1+\alpha}-1}}{(z+M\rho)^{L+1}}\,dz-\int_{1/\beta}^\infty\frac{z^{L-2}}{(z+M\rho)^{L+1}}\,dz\right]
\end{aligned}$$

we then have the result by employing (Gradshteyn & Ryzhik 2007: Eqn. (3.194-2)) to the last step. □

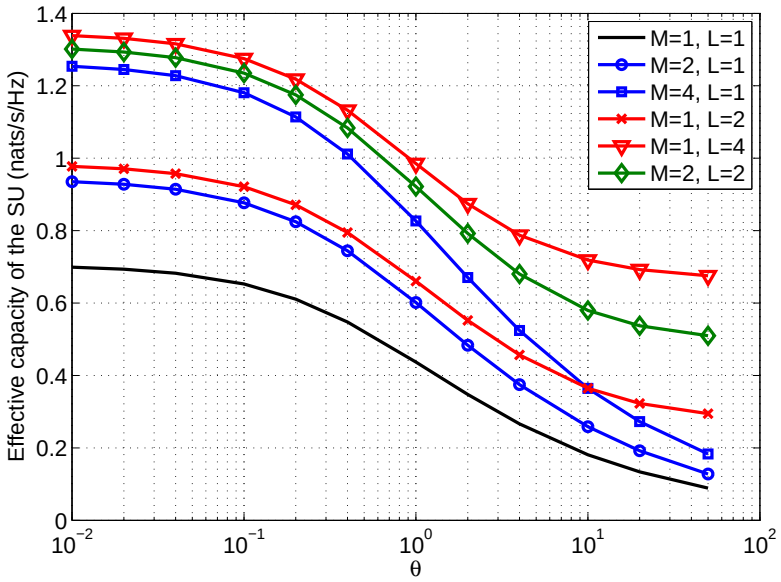

Figure 44. Effective capacity of the SU versus QoS exponent under AIP constraint and minimum interference selection, where the mean channel power gain ratio $\rho = 1$, $N_1 B = 1$, and $Q_{av} = -5$dB.

In Fig. 44 we show the effective capacity of the secondary user when the SU chooses the transmit antenna element having the minimum channel gain from the secondary transmitter to the primary receiver over different transmit and receive degrees of diversity. First, it is obvious that the TAS/MRC improves the achievable effective capacity over a large range of the QoS exponent. Second, the performance of using multiple receive antennas slightly surpasses the one using multiple transmit antennas at the range of small values of θ, e.g. the performance of $M = 1, L = 2$ is better than the one of $M = 2, L = 1$, and $M = 1, L = 4$ is better than the one of $M = 4, L = 1$. However, the gap rises when θ increases. This phenomenon is different from the one under PIP constraint. Third, in this case using $M = 2$ and $L = 2$ can not achieve the full diversity, because we only utilize partial channel information, i.e. only the interference channel information. Forth, at high θ regime, $M = 1, L = 2$ is slightly better than $M = 4, L = 1$. This can be explained as that the benefit of using TAS is not able to compensate the capacity loss caused by the channel deep fading.

6.4.2 Maximum Secondary Composite Channel Gain Selection

In this case, the p.d.f. of the channel power gains, z_k, is given by (6.19). The same as in previous subsection that the SU uses the CSI of ST-SR for making transmitter antenna selection, however, the power adaptation uses all the CSI. The resultant effective capacity of the secondary user is given by the following theorem.

Theorem 6.5. *The effective capacity of the cognitive-shared channel of Figure 40 with exploiting maximum secondary composite channel gain selection scheme under average interference power constraint over Rayleigh fading is given by*

$$EC(\theta) = -\frac{1}{\theta}\log\left\{\sum_{n\in\theta_M}\sum_{k_1=0}^{L-1}\cdots\sum_{k_M=0}^{L-1} K_{n,k}\overline{g}_{ps}^{A_{n,k}}\left[\mathfrak{I}_1+\mathfrak{I}_2\right]\right\}$$

Proof.

$$\begin{aligned}
&EC(\theta)\\
&= -\frac{1}{\theta}\log\left[\int_0^\infty\left(1+\left[\beta^{\frac{1}{1+\alpha}}z^{\frac{1}{1+\alpha}}-1\right]^+\right)^{-\alpha}\sum_{n\in\theta_M}\sum_{k_1=0}^{L-1}\cdots\sum_{k_M=0}^{L-1}K_{n,k}\overline{g}_{ps}^{A_{n,k}}\right.\\
&\quad\left.\times\underbrace{\frac{A_{n,k}\Gamma(A_{n,k}+1)z^{A_{n,k}-1}}{\left(1+B_n\overline{g}_{ps}z\right)^{A_{n,k}+1}}-\frac{B_n\overline{g}_{ps}\Gamma(A_{n,k}+2)z^{A_{n,k}}}{\left(1+B_n\overline{g}_{ps}z\right)^{A_{n,k}+2}}}_{\mathcal{G}}dz\right]\\
&= -\frac{1}{\theta}\log\left\{\sum_{n\in\theta_M}\sum_{k_1=0}^{L-1}\cdots\sum_{k_M=0}^{L-1}K_{n,k}\overline{g}_{ps}{}^{A_{n,k}}\left[\underbrace{\int_0^{1/\beta}\mathcal{G}\,dz}_{\mathfrak{I}_1}+\underbrace{\int_{1/\beta}^\infty\beta^{-\frac{\alpha}{1+\alpha}}z^{-\frac{\alpha}{1+\alpha}}\mathcal{G}\,dz}_{\mathfrak{I}_2}\right]\right\}
\end{aligned}$$

where for $A_{n,k}\neq 0$

$$\begin{aligned}
\mathfrak{I}_1 &= \frac{\Gamma(A_{n,k}+1)}{\beta^{A_{n,k}}}\,{}_2F_1\left(A_{n,k}+1,A_{n,k};A_{n,k}+2;-\frac{\overline{g}_{ps}B_n}{\beta}\right)\\
&\quad-\frac{B_n\Gamma(A_{n,k}+1)\overline{g}_{ps}}{\beta^{A_{n,k}+1}}\,{}_2F_1\left(A_{n,k}+2,A_{n,k}+1;A_{n,k}+2;-\frac{\overline{g}_{ps}B_n}{\beta}\right)\\
\mathfrak{I}_2 &= \frac{\Gamma(A_{n,k}+1)\beta\,(1+\alpha)}{\left(\overline{g}_{ps}B_n\right)^{A_{n,k}+1}(1+2\alpha)}\left[A_{n,k}\,{}_2F_1\left(A_{n,k}+1,1+\frac{\alpha}{1+\alpha};2+\frac{\alpha}{1+\alpha};-\frac{\beta}{\overline{g}_{ps}B_n}\right)\right.\\
&\quad\left.-\,(A_{n,k}+1)\,{}_2F_1\left(A_{n,k}+2,1+\frac{\alpha}{1+\alpha};2+\frac{\alpha}{1+\alpha};-\frac{\beta}{\overline{g}_{ps}B_n}\right)\right]
\end{aligned}$$

and for $A_{n,k} = 0$

$$\mathfrak{I}_1 = -\frac{B_n \overline{g}}{\beta} {}_2F_1\left(2,1;2;-\frac{\overline{g}_{ps} B_n}{\beta}\right)$$
$$\mathfrak{I}_2 = -\frac{\beta\,(1+\alpha)}{\overline{g}_{ps} B_n\,(1+2\alpha)}\left[{}_2F_1\left(2,1+\frac{\alpha}{1+\alpha};2+\frac{\alpha}{1+\alpha};-\frac{\beta}{\overline{g}_{ps} B_n}\right)\right]$$

in the above we have used (Gradshteyn & Ryzhik 2007: Eqn. (3.194-1) and (3.194-2)) and $\Gamma(1+x) = x * \Gamma(x)$. □

The Lagrangian multiplier satisfies the following condition

$$Q_{av} = N_1 B \sum_{n\in\theta_M} \sum_{k_1=0}^{L-1} \cdots \sum_{k_M=0}^{L-1} K_{n,k} \overline{g}_{ps}^{A_{n,k}} \left[\mathfrak{Q}_1 - \mathfrak{Q}_2\right] \tag{6.40}$$

where $\mathfrak{Q}_1$ is given by (6.41) and (6.43), and $\mathfrak{Q}_2$ is given by (6.42) and (6.44).

Proof.

$$Q_{av} = \mathbb{E}\left[g_{ps}^{(k)} p_s(\theta, g_{ps}^{(k)}, g_{ss}^{(k)})\right] = \int_0^\infty N_1 B \left[\frac{\beta^{\frac{1}{1+\alpha}}}{z^{\frac{\alpha}{1+\alpha}}} - \frac{1}{z}\right]^+ f_{z_k}(z)\,dz$$
$$= \int_{1/\beta}^\infty N_1 B \left[\frac{\beta^{\frac{1}{1+\alpha}}}{z^{\frac{\alpha}{1+\alpha}}} - \frac{1}{z}\right] \sum_{n\in\theta_M} \sum_{k_1=0}^{L-1} \cdots \sum_{k_M=0}^{L-1} K_{n,k} \overline{g}_{ps}^{A_{n,k}}$$
$$\times \left(\frac{A_{n,k}\Gamma(A_{n,k}+1) z^{A_{n,k}-1}}{\left(1+B_n \overline{g}_{ps} z\right)^{A_{n,k}+1}} - \frac{B_n \overline{g}_{ps} \Gamma(A_{n,k}+2) z^{A_{n,k}}}{\left(1+B_n \overline{g}_{ps} z\right)^{A_{n,k}+2}}\right) dz$$
$$= N_1 B \sum_{n\in\theta_M} \sum_{k_1=0}^{L-1} \cdots \sum_{k_M=0}^{L-1} K_{n,k} \overline{g}_{ps}^{A_{n,k}}$$
$$\times \Bigg\{ \underbrace{\beta^{\frac{1}{1+\alpha}} \Gamma(A_{n,k}+1) \int_{\frac{1}{\beta}}^\infty \left[\frac{A_{n,k} z^{A_{n,k}-\frac{\alpha}{1+\alpha}-1}}{\left(1+B_n \overline{g}_{ps} z\right)^{A_{n,k}+1}} - \frac{B_n \overline{g}_{ps} (A_{n,k}+1) z^{A_{n,k}+\frac{1}{1+\alpha}-1}}{\left(1+B_n \overline{g}_{ps} z\right)^{A_{n,k}+2}}\right] dz}_{\mathfrak{Q}_1}$$
$$\underbrace{- \left[\Gamma(A_{n,k}+1) \int_{1/\beta}^\infty \frac{A_{n,k} z^{A_{n,k}-2}}{\left(1+B_n \overline{g}_{ps} z\right)^{A_{n,k}+1}} - \frac{B_n \overline{g}_{ps} (A_{n,k}+1) z^{A_{n,k}-1}}{\left(1+B_n \overline{g}_{ps} z\right)^{A_{n,k}+2}} dz\right]}_{\mathfrak{Q}_2} \Bigg\}$$

For $A_{n,k} \neq 0$, we by using (Gradshteyn & Ryzhik 2007: Eqn. (3.194-2)) have

$$\mathcal{Q}_1 = \frac{\beta^2 \Gamma(A_{n,k}+1)(1+\alpha)}{\left(\overline{g}_{ps} B_n\right)^{A_{n,k}+1}(1+2\alpha)} \times \left[A_{n,k}\, {}_2F_1\left(A_{n,k}+1, 1+\frac{\alpha}{1+\alpha}; 2+\frac{\alpha}{1+\alpha}; -\frac{\beta}{\overline{g}_{ps} B_n}\right) - (A_{n,k}+1)\, {}_2F_1\left(A_{n,k}+2, 1+\frac{\alpha}{1+\alpha}; 2+\frac{\alpha}{1+\alpha}; -\frac{\beta}{\overline{g}_{ps} B_n}\right)\right] \tag{6.41}$$

$$\mathcal{Q}_2 = \frac{\beta^2 \Gamma(A_{n,k}+1)}{2\left(\overline{g}_{ps} B_n\right)^{A_{n,k}+1}} \left[A_{n,k}\, {}_2F_1\left(A_{n,k}+1, 2; 3; -\frac{\beta}{\overline{g}_{ps} B_n}\right) - (A_{n,k}+1)\, {}_2F_1\left(A_{n,k}+2, 2; 3; -\frac{\beta}{\overline{g}_{ps} B_n}\right)\right] \tag{6.42}$$

and for $A_{n,k} = 0$

$$\mathcal{Q}_1 = -\frac{\beta^2 (1+\alpha)}{\overline{g}_{ps} B_n}\, {}_2F_1\left(2, 1+\frac{\alpha}{1+\alpha}; 2+\frac{\alpha}{1+\alpha}; -\frac{\beta}{\overline{g}_{ps} B_n}\right) \tag{6.43}$$

$$\mathcal{Q}_2 = -\frac{\beta^2}{2\overline{g}_{ps} B_n}\, {}_2F_1\left(2, 2; 3; -\frac{\beta}{\overline{g}_{ps} B_n}\right) \tag{6.44}$$

in the above we have used (Gradshteyn & Ryzhik 2007: Eqn. (3.194-2)) and $\Gamma(1+x) = x * \Gamma(x)$. □

We depict the results in Fig. 45. Besides the improvement through using multiple antennas, the performance of the scenario of $M_1, L = 2$ is not superior to the one of $M = 4, L = 1$ as in the cases using Sel (1) scheme. Moreover, the performance of the cases with larger value of $M \times L$ surpasses the ones with lower value of $M \times L$.

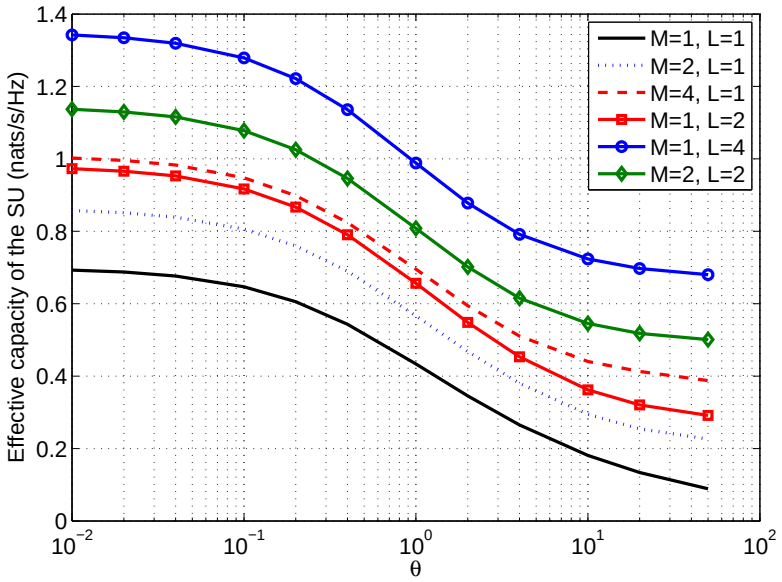

Figure 45. Effective capacity of the SU versus QoS exponent under AIP constraint and maximum MRC channel selection, where the mean channel power gain ratio $\rho = 1$, $N_1 B = 1$, and $Q_{av} = -5$dB.

6.4.3 Maximum Channel Ratio Selection

This scheme uses the all the channel state information for transmit antenna selection and for transmit power adaptation.

Theorem 6.6. *The effective capacity of the cognitive-shared channel of Figure 40 with exploiting maximum channel ratio selection scheme under peak interference power constraint over Rayleigh fading is given by*

$$EC(\theta) = -\frac{1}{\theta}\log\left[\left(\frac{1}{\rho\beta}\right)^{ML} {}_2F_1\left(ML+1, ML; 1+ML; -\frac{1}{\rho\beta}\right) + \frac{ML\rho\beta}{1+\frac{\alpha}{1+\alpha}} {}_2F_1\left(ML+1, 1+\frac{\alpha}{1+\alpha}; 2+\frac{\alpha}{1+\alpha}; -\rho\beta\right)\right] \tag{6.45}$$

Proof.

$$\begin{aligned}
EC(\theta) =& -\frac{1}{\theta}\log\left[\mathbb{E}_{z_k}\left(e^{-\alpha\log\left(1+\frac{p_s g_{ss}^{(k)}}{N_1 B}\right)}\right)\right] \\
=& -\frac{1}{\theta}\log\left[\int_0^{\infty}\left(1+\left[\beta^{\frac{1}{1+\alpha}}z^{\frac{1}{1+\alpha}}-1\right]^{+}\right)^{-\alpha}\frac{ML\rho z^{ML-1}}{(z+\rho)^{ML+1}}\,dz\right] \\
=& -\frac{1}{\theta}\log\left[\int_0^{1/\beta}\frac{ML\rho z^{ML-1}}{(z+\rho)^{ML+1}}\,dz+\int_{1/\beta}^{\infty}\beta^{-\frac{\alpha}{1+\alpha}}z^{-\frac{\alpha}{1+\alpha}}\frac{ML\rho z^{ML-1}}{(z+\rho)^{ML+1}}\,dz\right]
\end{aligned}$$

Then we obtain the expression by using (Gradshteyn & Ryzhik 2007: Eqn. (3.194-1) and (3.194-2)) to the above integrals. □

It is obviously that the EC depends on the diversity order $M \times L$, the QoS exponent θ, the product of the channel bandwidth and the channel coherence time (duration of fading block), the interference power constraint, the noise power and the mean channel power gain ratio. Fig. 46 depicts the results. The Lagrangian multiplier satisfies the following condition

$$\begin{aligned}
Q_{av} =& \frac{ML\rho N_1 B\beta^2}{2}\left[\frac{2+2\alpha}{1+2\alpha}\,{}_2F_1\left(ML+1,1+\frac{\alpha}{1+\alpha};2+\frac{\alpha}{1+\alpha};-\rho\beta\right)\right. \\
&\left. -\,{}_2F_1\left(ML+1,2;3;-\rho\beta\right)\right]
\end{aligned} \tag{6.46}$$

Proof.

$$\begin{aligned}
Q_{av} =& \mathbb{E}\left[g_{ps}^{(k)}p_s(\theta,g_{ps}^{(k)},g_{ss}^{(k)})\right] = \int_0^{\infty} N_1 B\left[\frac{\beta^{\frac{1}{1+\alpha}}}{z^{\frac{\alpha}{1+\alpha}}}-\frac{1}{z}\right]^{+} f_{z_k}(z)\,dz \\
=& \int_{1/\beta}^{\infty} N_1 B\left[\frac{\beta^{\frac{1}{1+\alpha}}}{z^{\frac{\alpha}{1+\alpha}}}-\frac{1}{z}\right]\frac{ML\rho z^{ML-1}}{(z+\rho)^{ML+1}}\,dz \\
=& N_1 BML\rho\left[\beta^{\frac{1}{1+\alpha}}\int_{1/\beta}^{\infty}\frac{z^{ML-\frac{\alpha}{1+\alpha}-1}}{(z+\rho)^{ML+1}}\,dz-\int_{1/\beta}^{\infty}\frac{z^{ML-2}}{(z+\rho)^{ML+1}}\,dz\right]
\end{aligned}$$

we then have the result by employing (Gradshteyn & Ryzhik 2007: Eqn. (3.194-2)) to the last step. □

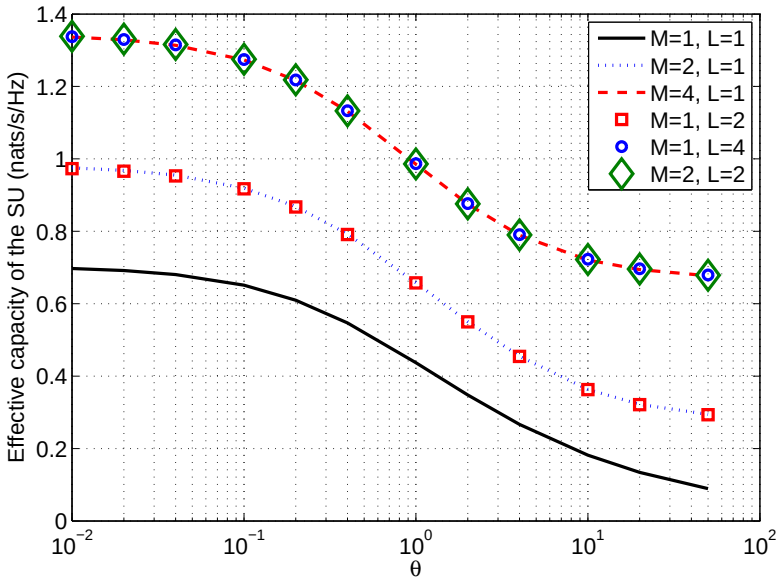

Figure 46. Effective capacity of the SU versus QoS exponent under AIP constraint and maximum channel radio selection, where the mean channel power gain ratio $\rho = 1$, and $Q_{av} = -5$dB.

6.5 Simulation Results

This section presents simulation results for the EC by comparison. The same as in previous simulations, we assume Rayleigh block fading channels, $TB = 1$, and additive white Gaussian noise power $N_1 B = 1$.

Fig. 47 and Fig. 48 compare the EC of three selection schemes versus θ under peak interference power (PIP) constraint with diversity order $M \times L = 2$ and $M \times L = 2$, respectively. From Fig. 47 we can see that Sel (1) scheme is superior to Sel (2) at the low range of delay component θ which represents delay-insensitive regime. However, along with increasing the value of θ, Sel (2) becomes better than Sel (1). Moreover, The effective capacity is capped by using full diversity order. Fig. 48 shows the similar phenomenon as in Fig. 47. We may conclude that at the stringent case, i.e. lager values of θ, with the same diversity order the receiving diversity is superior to the transmit diversity.

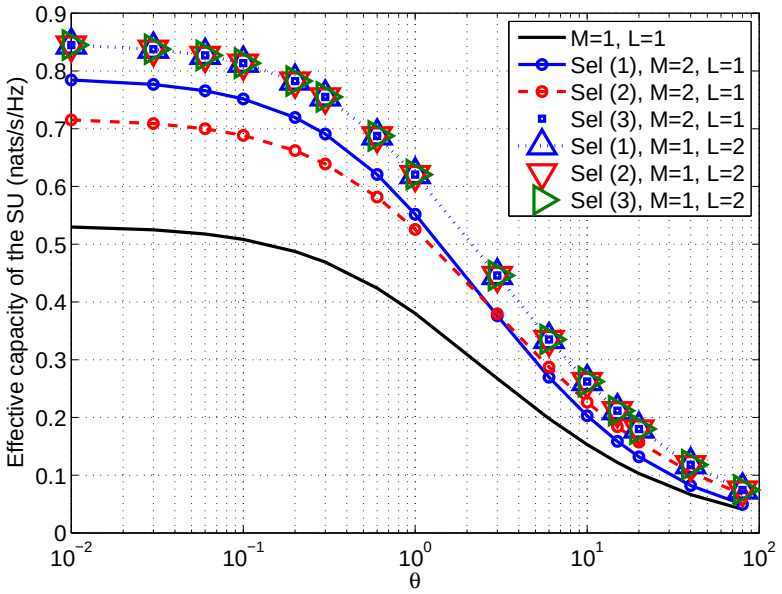

Figure 47. Effective capacity comparison under PIP constraint and different TAS schemes, where, $M \times L = 2$, the mean channel power gain ratio $\rho = 1$, and $Q_{pk} = -5$dB.

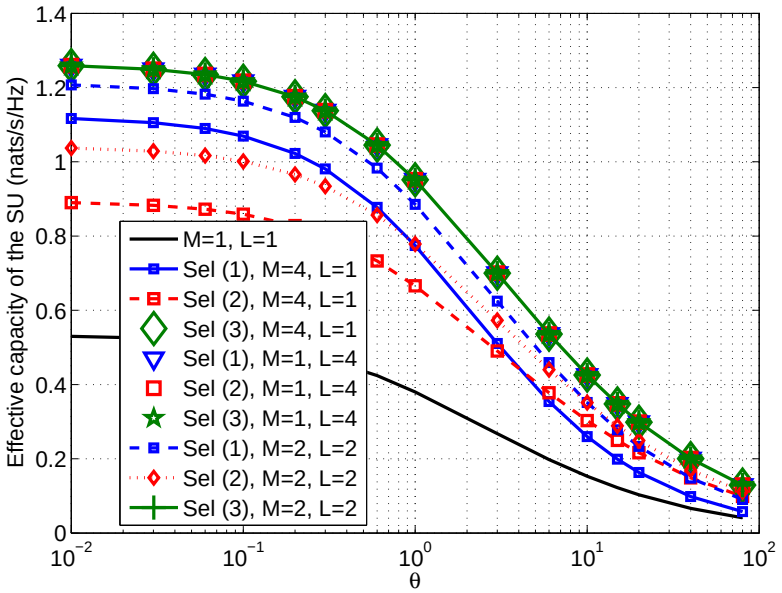

Figure 48. Effective capacity comparison under PIP constraint and different TAS schemes, where, $M \times L = 4$, the mean channel power gain ratio $\rho = 1$, and $Q_{pk} = -5$dB.

Fig. 49 and Fig. 50 show the results under average interference power constraint with diversity order $M \times L = 2$ and $M \times L = 4$, respectively. The significant difference in terms of effective capacity from the cases under peak interference power constraint is the improvement by using multiple antennas at the high θ regime.

In sum, we can see that the EC increases as the number of TAS/MRC antennas increases. And for given interference power constraint at the primary receiver, the more stringent the QoS requirement, e.g., $\theta \to \infty$, the less the effective capacity is. This is because of the delay limitation. Different selection schemes have different amount of advantages at various range of the delay exponent θ.

6.6 Conclusion and Discussion

In this chapter, we have studied and derived an expression for the effective capacity of a cognitive-shared channel with transmit antenna selection and maximal ratio combining under peak or average interference power constraint. The results are compared for using different transmit antenna selection strategies, minimum interference selection, maximum secondary channel gain selection, and maximum channel gain ratio selection. The multiple antenna techniques improve the communication quality significantly.

However, we have more work to do in the future. In the previous study, we considered only the perfect channel state information cases. Thus the influence on the effective capacity of being provided imperfect channel state information, e.g. delayed channel information, channel information with measurement errors, or both, are also important for understanding cognitive radio systems. Moreover, we need to investigate the multiple users scenarios, for instance, multiple primary users, multiple secondary users, or both. Furthermore, some new selection schemes are needed to be developed and studied if we only have the channel statistics information without the instantaneous channel state information, for instance, mean values. We will leave these as our future work.

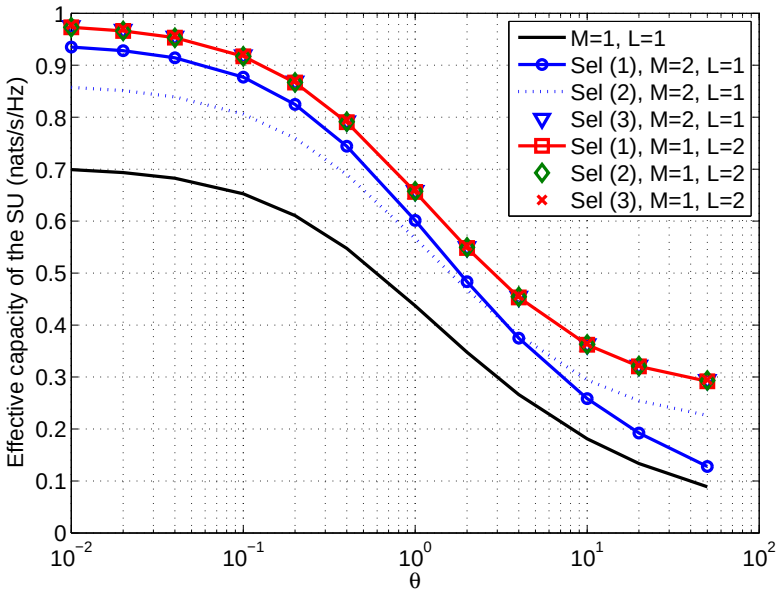

Figure 49. Effective capacity comparison under AIP constraint and different TAS schemes, where, $M \times L = 2$, the mean channel power gain ratio $\rho = 1$, and $Q_{av} = -5$dB.

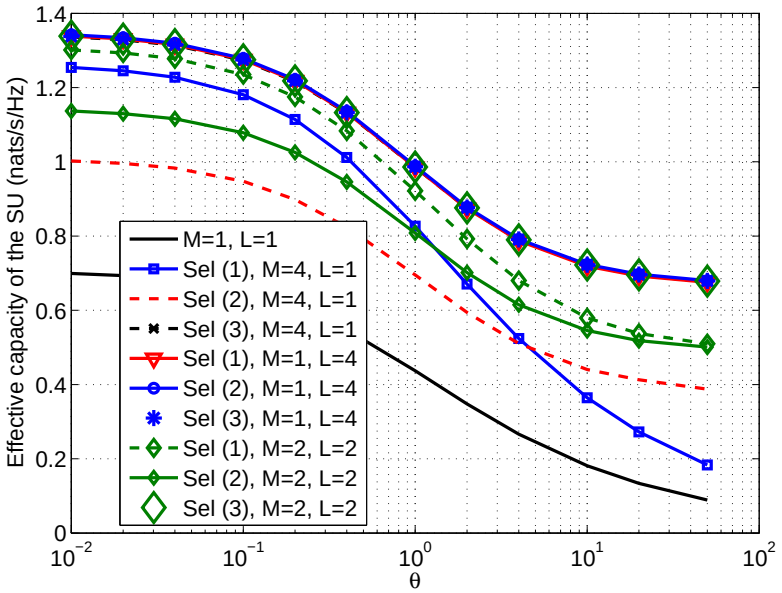

Figure 50. Effective capacity comparison under AIP constraint and different TAS schemes, where, $M \times L = 4$, the mean channel power gain ratio $\rho = 1$, and $Q_{av} = -5$dB.

7 MULTIOBJECTIVE DISTRIBUTED POWER CONTROL FOR COGNITIVE RADIOS*

We have discussed the optimal power allocation schemes which are information-theoretic based. In this chapter we propose an multiobjective distributed power control algorithm for spectrum-sharing cognitive radios (MODPCCR). As we know from literature that for spectrum sharing cognitive radios the most important factor is the strict limited interference caused to the primary users. Our proposed MODPCCR algorithm is able to achieve certain signal to interference and noise ratio (SINR) under the interference power constraint to primary users. On this problem, we assume that there is no perfect channel state information (CSI) of the secondary-primary (ST-PR) links to be provided to the secondary transmitters. Implementing MODPCCR algorithm on the secondary users could protect the primary users and achieve certain SINR for the secondary users.

7.1 Introduction

Power control scheme is an efficient approach to manage the interference problem, which have been extensively studied for code division multiple access (CDMA) networks. However, many new challenges exist on power control of cognitive radio networks. In (Zayen *et al.* 2008), a scheme based on outage probability of the primary system was proposed. The outage probability can be broadcasted to the secondary user (SU), and the SU makes the decision before starting the communication. In (Wang *et al.* 2007), an optimal power control problem was modeled as a concave minimization problem, where the authors investigated the optimal power control with and without interference temperature constraints based on the Shannon capacity. However, in (Wang *et al.* 2007) no SU is allowed to transmit before receiving authorization from the manager, thus heavy signaling is really possible. In (Qian *et al.* 2007), the power control scheme for cognitive radio ad hoc networks was studied using a genie-aided distributed power control scheme to maximize the energy efficiency of the SUs. The quality of service (QoS) of both PUs and SUs were guaranteed. In (Im *et al.* 2008), a fully distributed power control algorithm was presented without an additional process for the CR network. Specifically, the

*Reprinted with permission from "Multi-objective Distributed Power Control for Spectrum-sharing Cognitive Radios" by Ruifeng Duan and Mohammed Elmusrati, 2011, Proc. of the 7th International Wireless Communications and Mobile Computing Conference, Istanbul, Turkey, July 5-8, 2011, Copyright [2011] by the IEEE.

sum interference constraint on the PU by all SUs in the network is replaced by a new individual constraint limiting the individual transmission power. Multiobjective (MO) distributed power control algorithm for CDMA wireless communication systems was extensively studied in (Elmusrati *et al.* 2008; 2007), where the authors formulated the power control issue as an optimization problem with multiple possibly conflicted objectives, for instance, minimizing the transmit power, minimizing the outage, and maximizing the throughput. In this chapter we extend the multiobjective distributed power control algorithm for cognitive radio (MODPCCR) networks.

The remainder of this chapter describes the MODPCCR algorithm analytically and through simulations.

7.2 MODPCCR Algorithm

Generally, a multiobjective optimization problem consists of a set of objective functions which are usually different and conflicted. Each function represents a decision vector, which can be formulated as (Miettinen 1999):

$$\underset{\mathbf{x}\in S}{\text{minimize}} \quad \{f_1(\mathbf{x}), f_2(\mathbf{x}), ..., f_k(\mathbf{x})\} \tag{7.1}$$

where k is the amount of objective functions, and $\mathbf{x}$ is the feasible decision vector belonging to set S. The objectives are possibly conflicted. Here our goal is to simultaneously minimize all the objectives. The MO optimization technique provides Pareto optimal solutions, where a decision vector $\mathbf{x}^* \in S$ is Pareto optimal if there is no another decision vector $\mathbf{x} \in S$ such that $f_i(\mathbf{x}) \leq f_i(\mathbf{x^*})$ for all $i = 1, 2, ..., k$ and $f_j(\mathbf{x}) < f_j(\mathbf{x^*})$ for at least one index j (Elmusrati *et al.* 2007; Miettinen 1999). The decision maker could choose one solution from Pareto optimal solution set. In order to solve the MO optimization problem, we utilize the method of "Weighted Metrics" which is also adopted in (Elmusrati *et al.* 2008; 2007). Then the multiple objectives can be transformed into a single objective function, where the weights are normalized, i.e. $\sum_{i=1}^{k} \lambda_i = 1$ (Miettinen 1999).

For the known objectives, the optimization problem (7.1) can be rewritten as follows (Elmusrati *et al.* 2007), which is the weighted L_p-problem for minimizing distance (Miettinen 1999):

$$\text{minimize} \quad \left(\sum_{i=1}^{k} \lambda_i \left| f_i(\mathbf{x}) - z_i^* \right|^p \right)^{1/p} \tag{7.2}$$

$$\text{subject to} \quad \mathbf{x} \in S \tag{7.3}$$

where $1 \leq p \leq \infty$, z_i^* is the desired solution associated to objective i, and the trade-off factors satisfy

$$\lambda_i \geq 0, \ \forall i = 1,2,...,k, \text{ and } \sum_{i=1}^{k} \lambda_i = 1 \tag{7.4}$$

The power control problem for cognitive radio networks is more complex than that for traditional wireless systems, for example cellular networks. Here we should not only consider the required signal to interference-plus-noise ratio (SINR) and the transmit power, but also limit the interference power received at the primary users which usually is the most important factor for developing power control schemes for spectrum-sharing cognitive radios. In this chapter, a power control approach for the cognitive users is presented consisting of three objectives: minimizing the transmit power, keeping the SINR as close as possible to the target SINR, and limiting the instantaneous interference power at the primary receiver to some predefined constraint (here it is referred to the peak interference power constraint). These objectives of user i can be interpreted mathematically by the following error function:

$$e_i(t) = \lambda_{i,1} \left| P_i(t) - P_{\min} \right| + \lambda_{i,2} \left| \Gamma_i(t) - \Gamma_i^T \right| + \lambda_{i,3} \left| P_i(t) g_{0i} - \frac{Q_{pk}}{M} \right|, \quad \forall i \tag{7.5}$$

where the trade-off factors, $\lambda_{i,k}, k = 1,2,3$, satisfy $0 \leq \lambda_{i,k} \leq 1$ and $\sum_{k=1}^{3} \lambda_{i,k} = 1$, P_{min} is the minimum transmit power, $P_i(t)$ is the transmit power of user i at time slot t, g_{0i} is the channel power gain from the secondary transmitter i to the primary receiver, Γ_i^T is the target SINR of the ith SU, $\frac{Q_{pk}}{M}$ is the received interference power constraint for each user, M is the total amount of secondary users, and $\Gamma_i(t)$ is the SINR of user i at time slot t which can be formulated as:

$$\Gamma_i(t) = \frac{P_i(t) g_{ii}}{\sum_{j \neq i} P_j(t) g_{ij} + n_1} \tag{7.6}$$

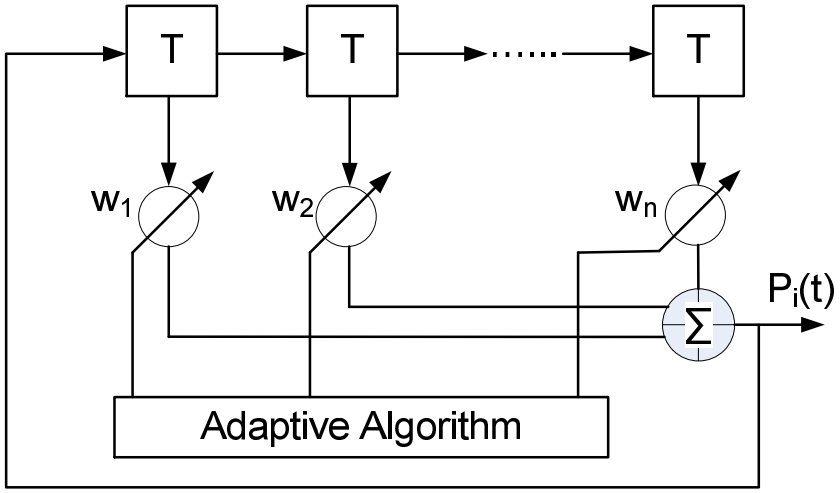

Figure 51. Autoregressive Model of Power Control

where g_{ij} is the channel gain from secondary transmitter j to secondary receiver i, and n_1 is the additive noise power. The channel information of g_{0i} may be fed back to the secondary user i by the licensee or indirectly through a band manager (Ghasemi & Sousa 2007; Peha 2009).

We formulate the following optimization problem finding the power vector, $\mathbf{P} = [P_1, P_2, ..., P_M]$, to minimize the following cost function (Elmusrati *et al.* 2007):

$$C(\mathbf{P}) = \sum_{i=1}^{M} e_i^2(t) \tag{7.7}$$

where M is the total amount of secondary users, and $e_i(t), \forall i$ are given by (7.5).

We assume that the power $P_i(t)$ is described by an autoregressive model shown in Figure 51, and then the transmission power can be represented as (Elmusrati *et al.* 2007),

$$P_i(t) = \sum_{k=1}^{n} w_i(k) P_i(t-k) \tag{7.8}$$

where n is the number of taps shown in Figure 51.

We could solve the optimization problem (7.7) for one tap, and obtain the following power control algorithm for the secondary users (see Appendix 4 for details):

$$P_i(t+1) = \frac{\lambda_{i,1}P_{\min} + \lambda_{i,2}\Gamma_i^T + \lambda_{i,3}\frac{Q_{pk}}{M}}{\lambda_{i,1}P_i(t) + \lambda_{i,2}\Gamma_i(t) + \lambda_{i,3}g_{0i}P_i(t)} \cdot P_i(t) \tag{7.9}$$

In practice, the transmission power should be bounded by the maximum transmission power, $P_{\max}$, and the minimum transmission power, $P_{\min}$. Let $\lambda_{i,1} = \lambda_{i,2} = 0$ in (7.9), we have $P_i(t+1) = \frac{Q_{pk}}{Mg_{0i}}$, which is the allowed maximum transmission power for secondary user i. Consequently, the MODPCCR algorithm becomes

$$\hat{P}_i(t+1) = \max\left(P_{\min}, \min\left(P_{\max}, P_i(t+1)\right)\right) \tag{7.10}$$

By setting different values to the tradeoff factors, $\lambda_{i,k}, k = 1,2,3$, we obtain associated Pareto optimum solutions. If we set $\lambda_{i,1} = \lambda_{i,3} = 0$, the MODPCCR algorithm becomes the distributed power control (DPC) algorithm proposed in (Grandhi *et al.* 1994). And let $\lambda_{i,1} = 1, \lambda_{i,2} = \lambda_{i,3} = 0$, the proposed algorithm becomes a non-power controlled algorithm, where user i transmits at the minimum power. In addition, for $\lambda_{i,1} = \lambda_{i,2} = 0, \lambda_{i,3} = 1$, we obtain the power control approach for the scenario that only the interference constraint is considered. The decision makers could choose the trade-off factors for certain requirements, or the values of trade-off factors can be dynamically adjusted.

7.3 Numerical Study

In this chapter we formulate the channels from the secondary transmitters to the primary receiver and from secondary transmitters to the corresponding receivers as fading channels, where the path loss and shadowing fading are considered. Also the shadowing is formulated in a discrete-time way as a Gauss-Markov process (Liang & Haas 2003; Stüber 2001) based on Gudmundson's model (Gudmundson 1991), saying $S(k+1) = \rho S(k) + \sqrt{1-\rho^2}W(k)$, where ρ is the correlation coefficient and $W(k)$ has a normal distribution with mean zero and variance σ^2. In addition, we consider the channel estimation error which means that there is no perfect channel information for the secondary transmitters of the $\text{SU}_{i,tx}$-PU_{rx} links. The CR transmitters are only provided with partial channel information of complex channel gain $c_{i,ps}$, namely $\tilde{c}_{i,ps}$, where $c_{i,ps}$ and $\tilde{c}_{i,ps}$ are jointly ergodic and stationary Gaussian processes. The secondary user performs

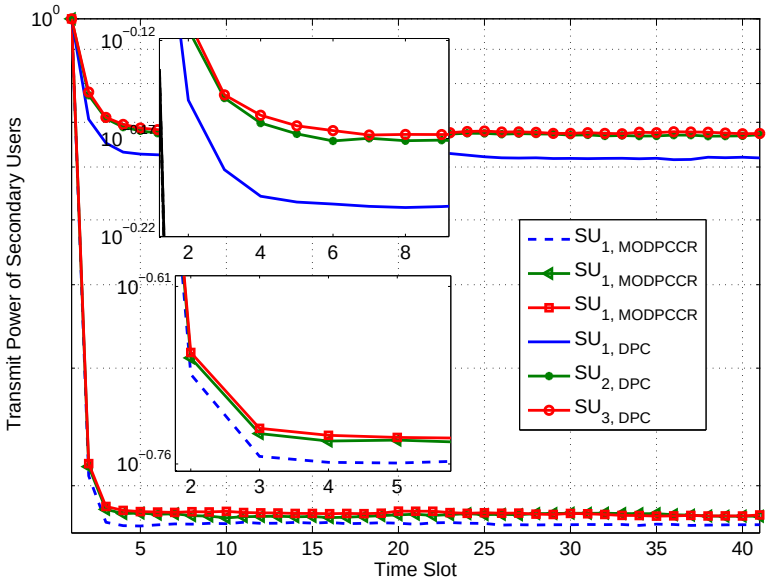

Figure 52. Average transmission power of the SUs with tradeoff factors $\lambda_1 = 0.01$, $\lambda_2 = 0.0001$, $\lambda_3 = 0.9899$, and $\sigma_e^2 = 1$dB.

minimum mean square error estimation (MMSE) of $c_{i,ps}$ given $\tilde{c}_{i,ps}$, such that $\hat{c}_{i,ps}[n] = \mathcal{E}\left\{c_{i,ps}[n] \,|\, \tilde{c}_{i,ps}[n], \tilde{c}_{i,ps}[n-1], \ldots\right\}$, where $[n]$ denotes the time index. The MMSE estimation error can be presented as $\breve{c}_{ps}[n] = c_{ps}[n] - \hat{c}_{ps}[n]$, where $\breve{c}_{i,ps}[n]$ and $\hat{c}_{i,ps}[n]$ are zero mean circularly symmetric complex Gaussian distributed variables with variances $\frac{1-\sigma^2}{2}$ and $\frac{\sigma^2}{2}$ respectively. So the associated channel power gain can be presented as $g_{0i} = \left|c_{i,ps}\right|^2$, $\hat{g_{0i}} = \left|\hat{c}_{i,ps}\right|^2$, and the channel power gain estimation error by $\breve{g_{0i}} = \left|\breve{c}_{i,ps}\right|^2$.

In the following simulations, 10^5 channel realizations are used. The variance of the shadowing is 6 dB, and the time correlation is 0.94. And the variance of channel estimation error $\sigma_e^2 = 1$dB in scenarios 1 and 2, and $\sigma_e^2 = 4$dB in case 3.

Case 1: The three tradeoff factors are $\lambda_1 = 0.01$, $\lambda_2 = 0.0001$, and $\lambda_3 = 0.9899$. Figure 52 depicts the average transmit power of the secondary transmitters. Figure 53 illustrates the corresponding average received SINR at secondary receivers. Figure 54 and Figure 55 show the average interference power at the primary user and the related distribution function. In this scenario, we compare the proposed MODPCCR algorithm to the well known DPC algorithm proposed in (Grandhi *et al.* 1994). From these figures, we can see that our algorithm uses lower transmission power compared to DPC and achieves similar SINR, then consequently

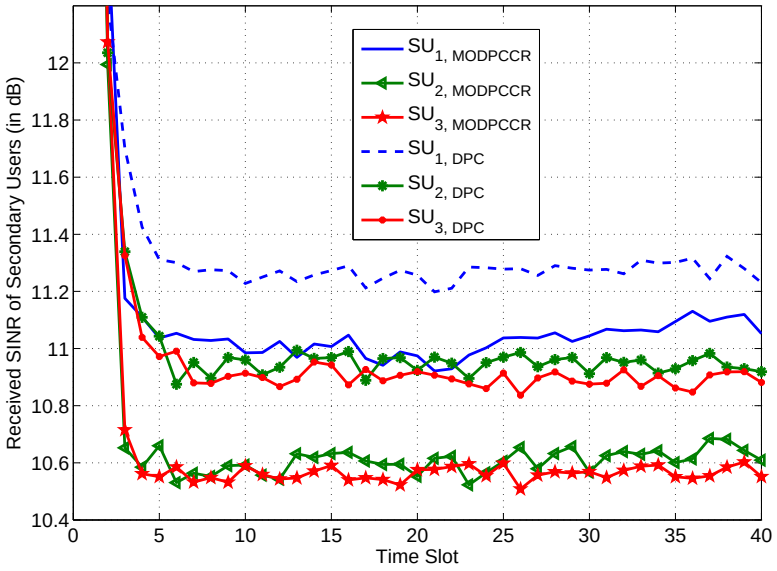

Figure 53. Average received SINR of the SUs with tradeoff factors $\lambda_1 = 0.01$, $\lambda_2 = 0.0001$, $\lambda_3 = 0.9899$, and $\sigma_e^2 = 1$dB.

the interference caused to the PU is under the predefined constraint which is set in our simulation as 0.01. Also, from Figure 55 it is intuitive that the probabilities of the interference under the constraint (saying 0.01) are approximately 0.85 and 0.2 for MODPCCR and DPC, respectively.

Case 2: The three tradeoff factors are $\lambda_1 = 0.0001$, $\lambda_2 = 0.0001$, and $\lambda_3 = 0.9998$, which means that we have less limitation on transmit power as in Case 1. Figures 56, 53, 54, and 55 show the average transmit power, the average received SINR of secondary users, and the average interference power and the empirical distribution function respectively. Compared to Case 1, from our simulation in this scenario the secondary users use a little higher average transmission power as expected than that in scenario 1. In consequence, the SUs achieve a little bit better average SINR compared to previous case and the resulted average interference to primary user is slightly over the constraint, saying 0.01 which is the same as in Case 1. Moreover, the probability of the interference under the constraint is approximately 0.5 which is higher than 0.85, however, it is still superior to that of using the DPC algorithm.

Case 3: In this case we keep the same tradeoff factors as in Case 1, $\lambda_1 = 0.01$, $\lambda_2 = 0.0001$, and $\lambda_3 = 0.9899$. However, we increase the estimation error variance to

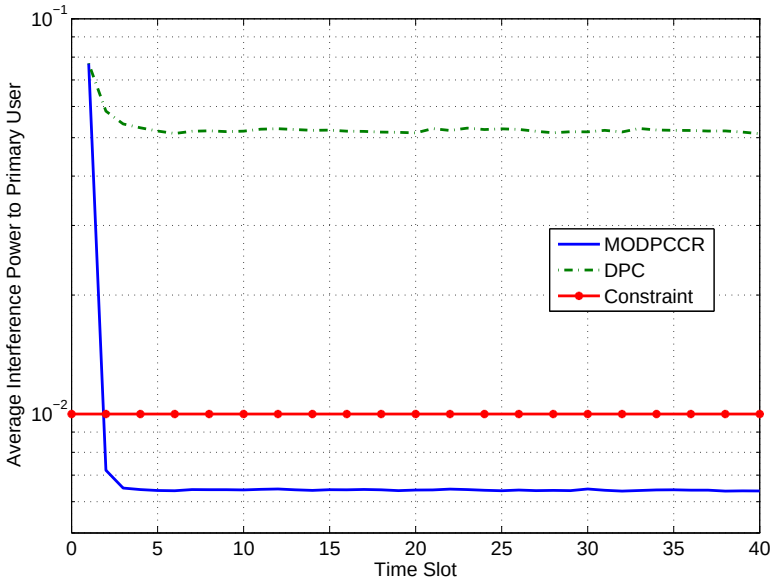

Figure 54. Average interference power at the PU with tradeoff factors $\lambda_1 = 0.01$, $\lambda_2 = 0.0001$, $\lambda_3 = 0.9899$, and $\sigma_e^2 = 1$dB.

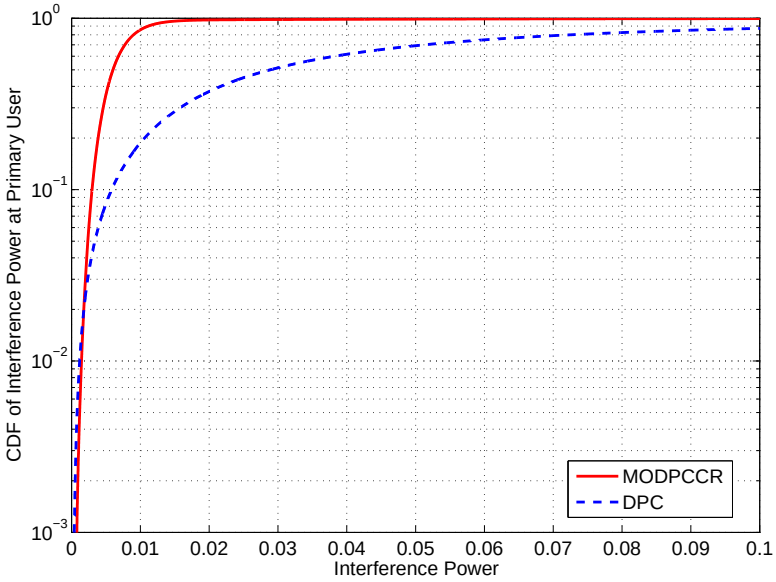

Figure 55. Cumulative distribution function of the received interference power with tradeoff factors $\lambda_1 = 0.01$, $\lambda_2 = 0.0001$, $\lambda_3 = 0.9899$, and $\sigma_e^2 = 1$dB.

4dB. The average transmit power of the secondary transmitters, the corresponding average received SINR, the average interference power to the primary user, and the

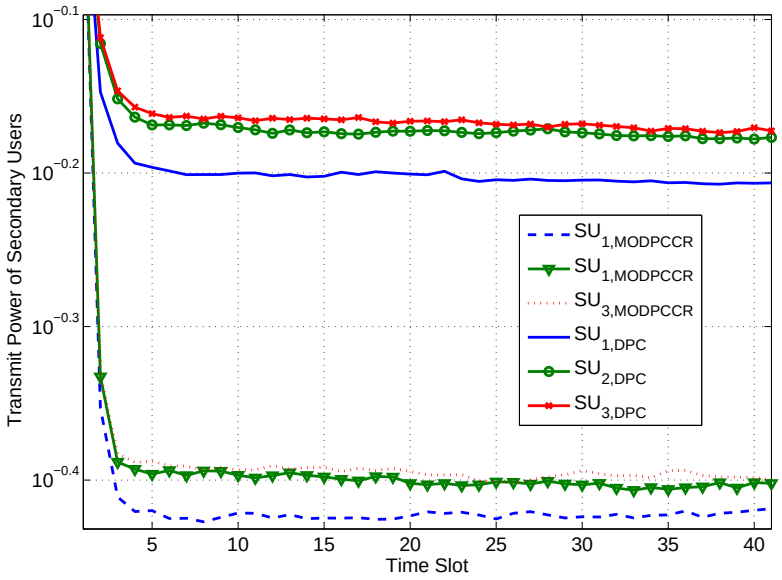

Figure 56. Average transmission power of the SUs with tradeoff factors $\lambda_1 = 0.0001$, $\lambda_2 = 0.0001$, $\lambda_3 = 0.9998$, and $\sigma_e^2 = 1$dB.

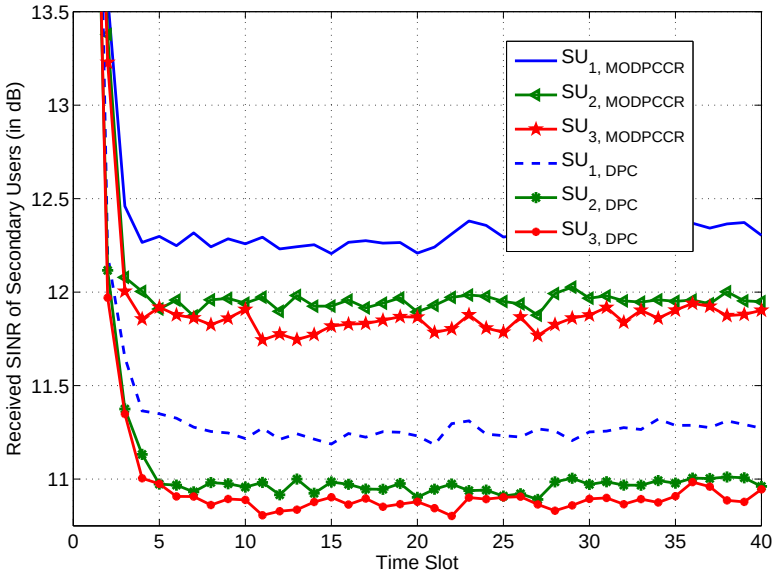

Figure 57. Average received SINR of the SUs with tradeoff factors $\lambda_1 = 0.0001$, $\lambda_2 = 0.0001$, $\lambda_3 = 0.9998$, and $\sigma_e^2 = 1$dB.

relative distribution function are shown in Figures 60, 61, 62, and 63, respectively. Compared to Case 1, there is a slight difference in transmission power, quite small

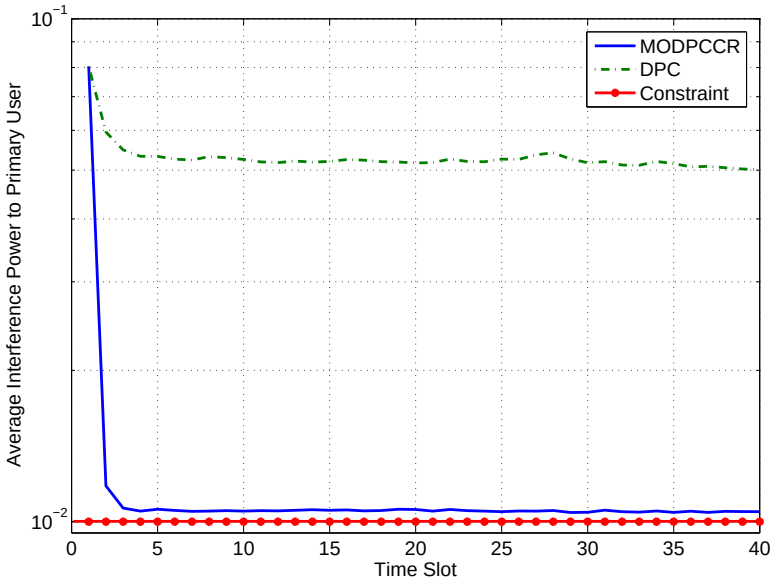

Figure 58. Average interference power at the primary user with tradeoff factors $\lambda_1 = 0.0001$, $\lambda_2 = 0.0001$, $\lambda_3 = 0.9998$, and $\sigma_e^2 = 1$dB.

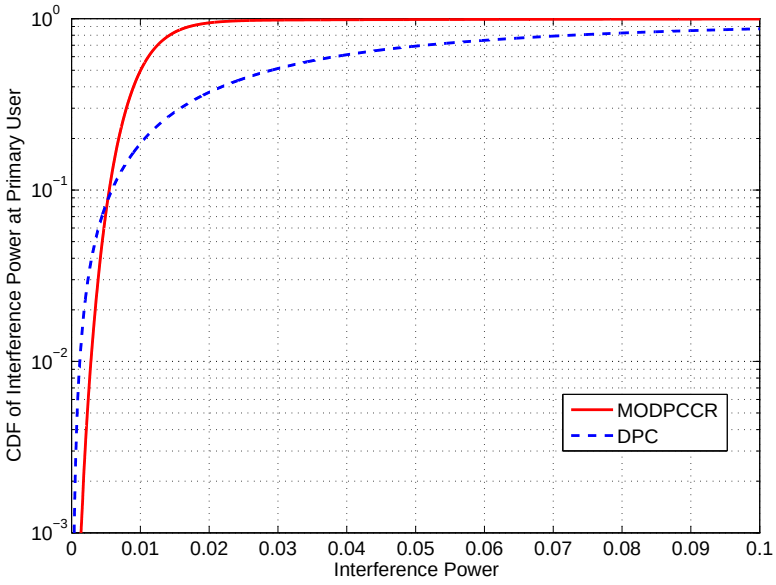

Figure 59. c.d.f. of the received interference power at the PU with tradeoff factors $\lambda_1 = 0.0001$, $\lambda_2 = 0.0001$, $\lambda_3 = 0.9998$, and $\sigma_e^2 = 1$dB.

reduce in SINR, and increase in interference. Although the probability that the interference power is over the constraint increases around 5 percent by comparison

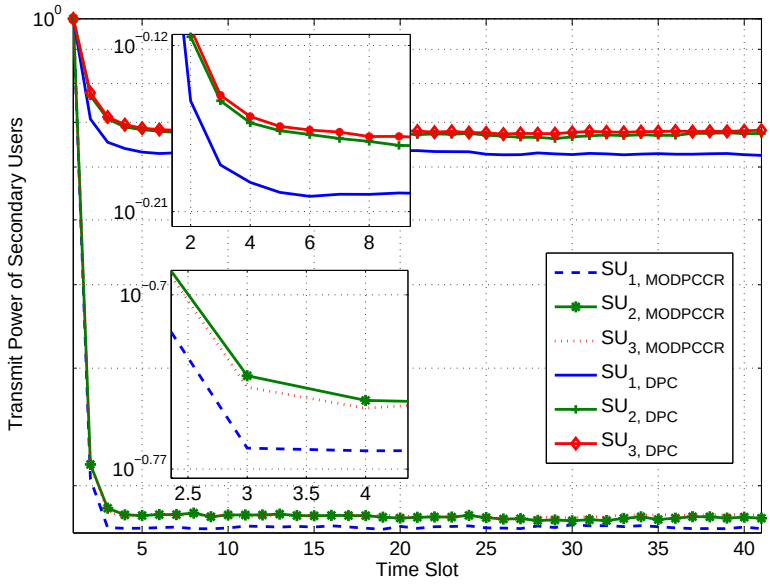

Figure 60. Average transmission power of the SUs with tradeoff factors $\lambda_1 = 0.01$, $\lambda_2 = 0.0001$, $\lambda_3 = 0.9899$, and $\sigma_e^2 = 4$dB.

between Figure 55 and Figure 63, compared to the c.d.f. of DPC algorithm it shows that our MODPCCR algorithm is still superior.

7.4 Conclusion

In this chapter, we proposed a new distributed power control algorithm for spectrum-sharing cognitive radios, called multiobjective distributed power control algorithm for spectrum-sharing cognitive radios (MODPCCR). From our analysis and simulations, we could draw the conclusion that the MODPCCR algorithm is able to achieve certain SINR under the interference power constraint to primary users. We also studied the cases that there are estimation errors of the channels from secondary transmitters to the primary receiver. Implementing MODPCCR algorithm on secondary users could protect primary users.

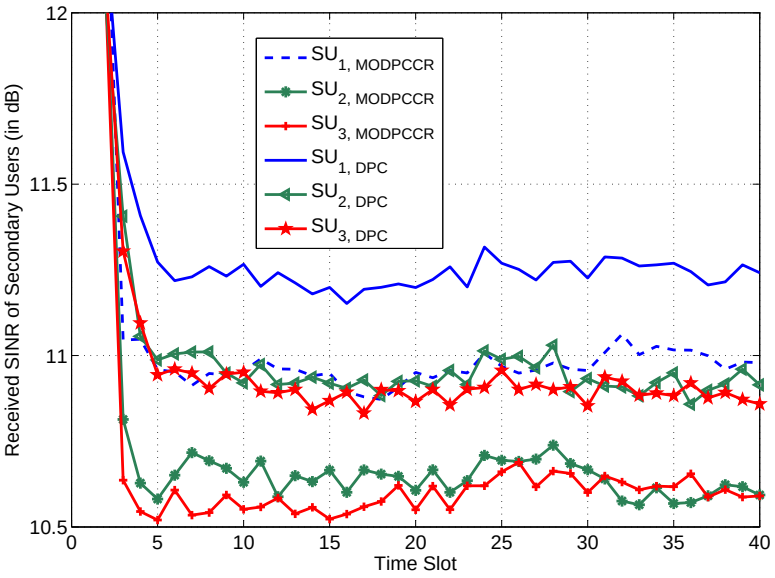

Figure 61. Average received SINR of the SUs with tradeoff factors $\lambda_1 = 0.01$, $\lambda_2 = 0.0001$, $\lambda_3 = 0.9899$, and $\sigma_e^2 = 4$dB.

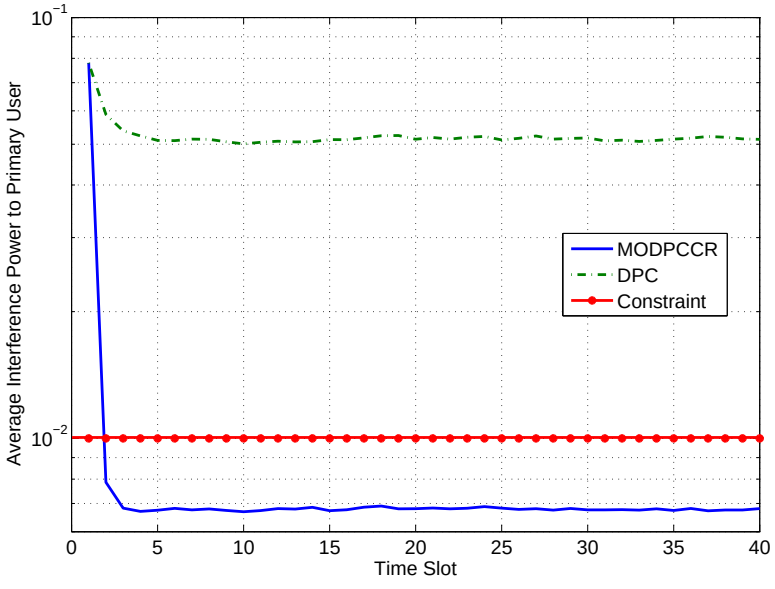

Figure 62. Average interference power at the primary user with tradeoff factors $\lambda_1 = 0.01$, $\lambda_2 = 0.0001$, $\lambda_3 = 0.9899$, and $\sigma_e^2 = 4$dB.

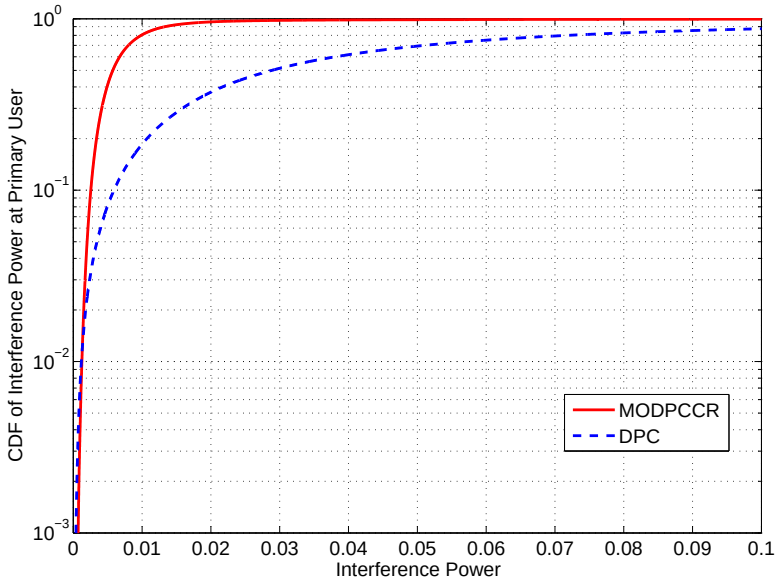

Figure 63. c.d.f. of the received interference power at the PU with tradeoff factors $\lambda_1 = 0.01$, $\lambda_2 = 0.0001$, $\lambda_3 = 0.9899$, and $\sigma_e^2 = 4$dB.

8 CONCLUSIONS AND FUTURE WORKS

In this dissertation, we investigated fundamental performance, e.g. ergodic capacity, effective capacity, and optimal power allocation, of underlay cognitive radios under certain interference constraints. Where the maximal ratio combining and generalized selection combining techniques were also considered at the secondary receiver. In chapter 2, we first reviewed the main results of the optimal power allocation schemes to achieve the ergodic capacity or effective capacity for cognitive users. We categorized the constraints of the optimization problems as long-term, short-term, or combined long- and short-constraints in this survey chapter. To improve the achievable rate of the cognitive radio, we investigated the optimal power allocation schemes and the ergodic capacity together with maximal ratio combining techniques implemented at the secondary receiver in the following chapters, i.e. chapter 3 and chapter 4. In chapter 3 we first considered a cognitive-shared channel with MRC under asymmetric fading environment. In chapter 4, we studied the case that the secondary transmitter has imperfect channel information of the interference channel, the channel from the secondary transmitter to the primary receiver. The receiving diversity techniques have not only enhanced the performance of cognitive users, but also mitigated the impact of the imperfect channel estimation. In chapter 5, we studied the ergodic capacity of a cognitive-shared channel with generalized selection combining diversity under the primary outage probability in Rayleigh block fading environment. Closed-form expressions of the ergodic capacity and the symbol error probability for the proposed model were obtained. The above chapters investigated the performance of the cognitive radios in terms of the ergodic capacity. In order to consider the delay factor, we studied the effective capacity of the cognitive radios with implementing transmit antenna selection at the secondary transmitter and the MRC at the secondary receiver. The expression for the effective capacity of the cognitive radio was obtained. In addition, for different transmit power constraints, the effective capacity was also evaluated numerically using simulations. It was proved that the QoS exponent, the diversity order, and the interference power constraints influenced the effective capacity gains. Finally, we proposed a multi-objective distributed power control algorithm for cognitive radios, which is practical and easy to be implemented, with comparison with the classic distributed power control algorithm and considering the imperfect channel estimation.

Although, we have studied the fundamentals of the cognitive radios in terms of optimal power allocation, ergodic capacity, and effective capacity, there are still many issues for the future work, for instance:

- Firstly, we need to answer the following questions of a cognitive-shared channel (single primary and secondary user): what are the optimal power allocation methods for delay-sensitive applications, both primary and secondary users? Given some QoS requirement for the secondary users (SU), what is the outage probability that the primary user will have? For different modulations, what are the bit error probabilities?
- Secondarily, we need to further investigate the fundamental performance of the spectrum-sharing systems taking multiple primary users and/or secondary users into consideration. The results will be compared to the ones of the former cases.
- Thirdly, The previous work mainly focus on the analysis from the secondary uses' point of view. Therefore, the research from the primary users' point of view should also be conducted.
- Last but not least, the applications of cognitive radios together with other technologies, for instance, ad hoc, mobile communications, smart grid, and vehicular technology.

REFERENCES

Abramowitz, M. & Stegun, I. A., eds. (1964). *Handbook of Mathematical Functions, With Formulas, Graphs, and Mathematical Tables*. 10th Printing with corrections, 1972. New York: DOVER.

Akin, S. & Gursoy, M. (2010). Effective capacity analysis of cognitive radio channels for quality of service provisioning. *IEEE Transactions on Wireless Communications* 9:11, 3354–3364.

Akyildiz, I. F., Lee, W.-Y., Vuran, M. C., & Mohanty, S. (2006). Next generation/dynamic spectrum access/cognitive radio wireless networks: a survey. *Elsevier Computer Networks* 50:13, 2127–2159.

Alouini, M.-S. & Goldsmith, A. (1999). Capacity of Rayleigh fading channels under different adaptive transmission and diversity-combining techniques. *IEEE Transactions on Vehicular Technology* 48:4, 1165–1181.

Alouini, M.-S. & Simon, M. (2000). An MGF-based performance analysis of generalized selection combining over Rayleigh fading channels. *IEEE Transactions on Communications* 48:3, 401–415.

Biglieri, E., Proakis, J., & Shamai, S. (1998). Fading channels: information-theoretic and communications aspects. *IEEE Transactions on Information Theory* 44:6, 2619–2692.

Blagojevic, V. & Ivanis, P. (2012). Ergodic capacity for TAS/MRC spectrum sharing cognitive radio. *IEEE Communications Letters* 16:3, 321–323.

Bland, R. G., Goldfarb, D., & Todd, M. J. (1981). The ellipsoid method: A survey. *Operations Research* [Web document] 29:6, 1039–1091. Available at: http://www.jstor.org/stable/170362.

Boyd, S. & Vandenberghe, L. (2004). *Convex Optimization*. New York: Cambridge University Press.

Brennan, D. (2003). Linear diversity combining techniques. *Proceedings of the IEEE* 91:2, 331–356.

Caire, G., Taricco, G., & Biglieri, E. (1999). Optimum power control over fading channels. *IEEE Transactions on Information Theory* 45:5, 1468–1489.

Chang, C.-S. & Thomas, J. (1995). Effective bandwidth in high-speed digital networks. *IEEE Journal on Selected Areas in Communications* 13:6, 1091–1100.

Chen, Y., Yu, G., Zhang, Z., Chen, H.-H, & Qiu, P. (2008). On cognitive radio networks with opportunistic power control strategies in fading channels. *IEEE Transactions on Wireless Communications* 7:7, 2752–2761.

Chen, Z., Chi, Z., Li, Y., & Vucetic, B. (2009). Error performance of maximal-ratio combining with transmit antenna selection in flat Nakagami-*m* fading channels. *IEEE Transactions on Wireless Communications* 8:1, 424–431.

Chen, Z., Yuan, J., & Vucetic, B. (2005). Analysis of transmit antenna selection/maximal-ratio combining in Rayleigh fading channels. *IEEE Transactions on Vehicular Technology* 54:4, 1312–1321.

Chiang, M., Hande, P., Lan, T., & Tan, C. W. (2008). Power control in wireless cellular networks. *Foundations and Trends®in Networking*, 2:4, 381–533.

Cover, T. M. & Thomas, J. A. (2006). *Elements of Information Theory*. 2nd edition. Hoboken, New Jersey: John Wiley & Sons.

David, H. A. & Nagaraja, H. N. (2003). *Order Statistics*. Hoboken, New Jersey: John Wiley & Sons.

Ding, H., Ge, J., Benevides da Costa, D., & Jiang, Z. (2011). Asymptotic analysis of cooperative diversity systems with relay selection in a spectrum-sharing scenario. *IEEE Transactions on Vehicular Technology* 60:2, 457–472.

Duan, R., Elmusrati, M., Jäntti, R., & Virrankoski, R. (2010a). Capacity for spectrum sharing cognitive radios with MRC diversity at the secondary receiver under asymmetric fading. In *Proceedings of IEEE Global Telecommunications Conference (2010)*.

Duan, R., Jäntti, R., Elmusrati, M., & Virrankoski, R. (2010b). Capacity for spectrum sharing cognitive radios with MRC diversity and imperfect channel information from primary user. In *Proceedings of IEEE Global Telecommunications Conference (2010)*.

Duong, T., Yeoh, P. L., Bao, V. N. Q., Elkashlan, M., & Yang, N. (2012). Cognitive relay networks with multiple primary transceivers under spectrum-sharing. *IEEE Signal Processing Letters* 19:11, 741–744.

Elmusrati, M., El-Sallabi, H., & Koivo, H. (2008). Applications of multi-objective optimization techniques in radio resource scheduling of cellular communication systems. *IEEE Transactions on Wireless Communications* 7:1, 343–353.

Elmusrati, M., Jantti, R., & Koivo, H. (2007). Multiobjective distributed power control algorithm for CDMA wireless communication systems. *IEEE Transactions on Vehicular Technology* 56:2, 779–788.

Eng, T., Kong, N., & Milstein, L. (1996). Comparison of diversity combining techniques for Rayleigh-fading channels. *IEEE Transactions on Communications* 44:9, 1117–1129.

Erdélyi, A., Magnus, W., Oberhettinger, F., & Tricomi, F. G. (1953). *Higher Transcendental Functions*, 1. New York: McGraw Hill.

Etkin, R., Parekh, A., & Tse, D. (2007). Spectrum sharing for unlicensed bands. *IEEE Journal on Selected Areas in Communications* 25:3, 517–528.

FCC (2002). Spectrum policy task force report. Technical Report 02-135, Federal Communications Commission [Web document] [Aug. 2012]. Available at: http://hraunfoss.fcc.gov/edocs_public/attachmatch/DOC-228542A1.pdf.

FCC (2003a). Notice of inquiry and notice of proposed rulemaking. ET Docket No. 03-237, Federal Communications Commission [Web document] [Aug. 2012]. Available at: http://hraunfoss.fcc.gov/edocs_public/attachmatch/FCC-03-289A1.pdf.

FCC (2003b). Notice of proposed rule making and order. ET Docket No. 03-322., Federal Communications Commission [Web document] [Aug. 2012]. Available at: http://hraunfoss.fcc.gov/edocs_public/attachmatch/FCC-03-322A1.pdf.

Gastpar, M. (2004). On capacity under received-signal constraints. In *Proceedings of 42nd Annual Allerton Conference on Communications, Control and Computing (2004)*.

Gastpar, M. (2007). On capacity under receive and spatial spectrum-sharing constraints. *IEEE Transactions on Information Theory* 53:2, 471–487.

Ghasemi, A. & Sousa, E. S. (2007). Fundamental limits of spectrum-sharing in fading environments. *IEEE Transactions on Wireless Communications* 6:2, 649–658.

Goldsmith, A., Jafar, S. A., Maric, I., & Srinivasa, S. (2009). Breaking spectrum gridlock with cognitive radios: An information theoretic perspective. *Proceeding of the IEEE* 97:5, 894–914.

Goldsmith, A. & Varaiya, P. (1997). Capacity of fading channels with channel side information. *IEEE Transactions on Information Theory* 43:6, 1986–1992.

Grace, D., Chen, J., Jiang, T., & Mitchell, P. (2009). Using cognitive radio to deliver 'green' communications. In *International Conference on Cognitive Radio Oriented Wireless Networks and Communications (CROWNCOM)*, 1–6.

Gradshteyn, I. & Ryzhik, I. (2007). *Table of Integrals, Series, and Products, Seventh Edition*. 7th ed., Burlington: Academic Press.

Grandhi, S., Vijayan, R., & Goodman, D. (1994). Distributed power control in cellular radio systems. *IEEE Transactions on Communications* 42:234, 226–228.

Gudmundson, M. (1991). Correlation model for shadow fading in mobile radio systems. *Electronics Letters* 27:23, 2145–2146.

Gursoy, M., Qiao, D., & Velipasalar, S. (2009). Analysis of energy efficiency in fading channels under QoS constraints. *IEEE Transactions Wireless Communications* 8:8, 4252–4263.

Haykin, S. (2005). Cognitive radio: brain-empowered wireless communications. *IEEE Journal on Selected Areas in Communications* 23:2, 201–220.

Hoven, N. & Sahai, A. (2005). Power scaling for cognitive radio. In *Proceedings of International Conference on Wireless Networks, Communications and Mobile Computing* 1, 250–255.

Hung, C.-C., Chiang, C.-T., Yen, N.-Y., & Wu, R.-C. (2010). Outage probability of multiuser transmit antenna selection/maximal-ratio combining systems over arbitrary Nakagami-*m* fading channels. *IET Communications* 4:1, 63–68.

Im, S., Jeon, H., & Lee, H. (2008). Autonomous distributed power control for cognitive radio networks. In *Proceedings of IEEE Vehicular Technology Conference 2008-Fall,* 1–5.

Islam, H., Liang, Y.-C., & Hoang, A. (2008). Joint power control and beamforming for cognitive radio networks. *IEEE Transactions on Wireless Communications* 7:7, 2415–2419.

Jafar, S. A. & Srinivasa, S. (2007). Capacity limits of cognitive radio with distributed and dynamic spectral activity. *IEEE Journal on Selected Areas in Communications* 25:3, 529–537.

Jakes, W. C., ed. (1994). *Microwave Mobile Communications*. New York: Wiley-IEEE Press.

Jovicic, A. & Viswanath, P. (2009). Cognitive radio: An information-theoretic perspective. *IEEE Transactions on Information Theory* 55:9, 3945–3958.

Kang, X., Liang, Y.-C., Nallanathan, A., Garg, H., & Zhang, R. (2009). Optimal power allocation for fading channels in cognitive radio networks: Ergodic capacity and outage capacity. *IEEE Transactions on Wireless Communications* 8:2, 940–950.

Kaya, O. & Ulukus, S. (2004). Optimum power control for CDMA with deterministic sequences in fading channels. *IEEE Transactions on Information Theory* 50:10, 2449–2462.

Khojastepour, M. & Aazhang, B. (2004). The capacity of average and peak power constrained fading channels with channel side information. In *Proceedings of IEEE Wireless Communications and Networking Conference* 1, 77–82.

Kim, K. J., Duong, T., Poor, H., & Shu, L. (2012). Performance analysis of cyclic prefixed single-carrier spectrum sharing relay systems in primary user interference. *IEEE Transactions on Signal Processing* 60:12, 6729–6734.

Knopp, R. & Humblet, P. (1995). Information capacity and power control in single-cell multiuser communications. In *Proceedings of IEEE International Conference on Communications* 1, 331 –335.

Koufos, K., Ruttik, K., & Jäntti, R. (2011). Controlling the interference from multiple secondary systems at the TV cell border. In *Proceedings of 22nd IEEE International Symposium on Personal, Indoor and Mobile Radio Communications* 1, 645–649.

Lee, J., Wang, H., Andrews, J. G., & Hong, D. (2011). Outage probability of cognitive relay networks with interference constraints. *IEEE Transactions on Wireless Communications* 10:2, 390–395.

Liang, B. & Haas, Z. (2003). Predictive distance-based mobility management for multidimensional PCS networks. *IEEE/ACM Transactions on Networking* 11:5, 718–732.

Lim, S., Wang, H., Kim, H., & Hong, D. (2012). Mean value-based power allocation without instantaneous CSI feedback in spectrum sharing systems. *IEEE Transactions on Wireless Communications* 11:3, 874–879.

McKay, M., Grant, A., & Collings, I. (2007). Performance analysis of MIMO-MRC in double-correlated Rayleigh environments. *IEEE Transactions on Communications* 55:3, 497–507.

Miettinen, K. (1999). *Nonlinear Multiobjective Optimization*. Boston, USA: Kluwer Academic Publishers.

Mitola, J. (2000). *Cognitive radio: an integrated agent architecture for software defined radio*. Royal Institute of Technology. Department of Teleinformatics. Ph.D. thesis.

Mitola, J. & Maguire, G. Q. (1999). Cognitive radio: Making software radios more personal. *IEEE Personal Communications* 6, 13–18.

Musavian, L. & Aissa, S. (2009a). Capacity and power allocation for spectrum-sharing communications in fading channels. *IEEE Transactions on Wireless Communications* 8:1, 148–156.

Musavian, L. & Aissa, S. (2009b). Fundamental capacity limits of cognitive radio in fading environments with imperfect channel information. *IEEE Transactions on Communications* 57:11, 3472–3480.

Musavian, L. & Aissa, S. (2010). Effective capacity of delay-constrained cognitive radio in Nakagami fading channels. *IEEE Transactions on Wireless Communications* 9:3, 1054–1062.

Nakagami, M. (1960). The *m*-distribution, a general formula for intensity distribution of rapid fading. *Statistical Methods in Radio Wave Propagation,* 3–36. Oxford, England: Pergamon.

NTIA (2003). *United states frequency allocations: The radio spectrum.* National Telecommunications and Information Administration [Web document]. Available at: http://www.ntia.doc.gov/files/ntia/publications/2003-allochrt.pdf.

Ozarow, L., Shamai, S., & Wyner, A. (1994). Information theoretic considerations for cellular mobile radio. *IEEE Transactions on Vehicular Technology* 43:2, 359–378.

Papoulis, A. & Pillai, S. U. (2002). *Probability, Random Variables and Stochastic Processes*. 4th ed. New York: McGraw-Hill.

Peha, J. (2009). Sharing spectrum through spectrum policy reform and cognitive radio. *Proceedings of the IEEE* 97:4, 708–719.

Proakis, J. & Salehi, M. (2008). *Digital Communications*. 5th ed. New York: McGraw-Hill.

Qian, L., Li, X., Attia, J., & Gajic, Z. (2007). Power control for cognitive radio ad hoc networks. In *Proceedings of IEEE International Workshop on Local and Metropolitan Area Networks,* 7–12.

Ramanathan, R. & Partridge, C. (2005). Next generation (xg) architecture and protocol development (xap). AFRL-IF-RS-TR-2005-281, BBN Technologies [Web document]. Available at: http://www.dtic.mil/cgi-bin/GetTRDoc?Location=U2&doc=GetTRDoc.pdf&AD=ADA437096.

Rezki, Z. & Alouini, M. (2012). Ergodic capacity of cognitive radio under imperfect channel-state information. *IEEE Transactions on Vehicular Technology* 61:5, 2108–2119.

Simon, M. K. & Alouini, M.-S. (2005). *Digital Communication over Fading Channels*. 2nd ed. New York: John Wiley & Sons.

Srinivasa, S. & Jafar, S. A. (2010). Soft sensing and optimal power control for cognitive radio. *IEEE Transactions on Wireless Communications* 9:12, 3638–3649.

Stüber, G. L. (2001). *Principles of mobile communication*. 2nd ed. Norwell: Kluwer Academic Publishers.

Suraweera, H., Gao, J., Smith, P., Shafi, M., & Faulkner, M. (2008). Channel capacity limits of cognitive radio in asymmetric fading environments. In *Proceedings of IEEE International Conference on Communications,* 4048–4053.

Suraweera, H., Karagiannidis, G., & Smith, P. (2009). Performance analysis of the dual-hop asymmetric fading channel. *IEEE Transactions on Wireless Communications* 8:6, 2783–2788.

Suraweera, H., Smith, P., & Shafi, M. (2010). Capacity limits and performance analysis of cognitive radio with imperfect channel knowledge. *IEEE Transactions on Vehicular Technology* 59:4, 1811–1822.

Tang, J. & Zhang, X. (2007a). Quality-of-service driven power and rate adaptation for multichannel communications over wireless links. *IEEE Transactions on Wireless Communications* 6:12, 4349–4360.

Tang, J. & Zhang, X. (2007b). Quality-of-service driven power and rate adaptation over wireless links. *IEEE Transactions on Wireless Communications* 6:8, 3058–3068.

Telatar, I. E. (1999). Capacity of multi-antenna gaussian channels. *European Transactions on Telecommunications* 10:6, 585–595.

Thoen, S., Van der Perre, L., Gyselinckx, B., & Engels, M. (2001). Performance analysis of combined transmit-SC/receive-MRC. *IEEE Transactions on Communications* 49:1, 5–8.

Tse, D. & Hanly, S. (1998). Multiaccess fading channels. I. polymatroid structure, optimal resource allocation and throughput capacities. *IEEE Transactions on Information Theory* 44:7, 2796–2815.

Tse, D. & Viswanath, P. (2005). *Fundamentals of Wireless Communication*. Cambridge, United Kingdom: Cambridge University Press.

Wang, C.-X., Hong, X., Chen, H.-H., & Thompson, J. (2009). On capacity of cognitive radio networks with average interference power constraints. *IEEE Transactions on Wireless Communications* 8:4, 1620–1625.

Wang, P., Zhao, M., Xiao, L., Zhou, S., & Wang, J. (2007). Power allocation in OFDM-based cognitive radio systems. In *Proceeding of IEEE Global Communications Conference 2007,* 4061 –4065.

Win, M. & Winters, J. (2001). Virtual branch analysis of symbol error probability for hybrid selection/maximal-ratio combining in Rayleigh fading. *IEEE Transactions on Communications* 49:11, 1926–1934.

Wolfram (2014). From MathWorld – A Wolfram Web Resource [Web document] [Aug. 2012]. Available at http://functions.wolfram.com/.

Wu, D. & Negi, R. (2003). Effective capacity: a wireless link model for support of quality of service. *IEEE Transactions on Wireless Communications* 2:4, 630–643.

Wu, D. & Negi, R. (2004). Downlink scheduling in a cellular network for quality-of-service assurance. *IEEE Transactions on Vehicular Technology* 53:5, 1547–1557.

Wu, Q., Huang, Y., Wang, J., & Cheng, Y. (2012). Effective capacity of cognitive radio systems with GSC diversity under imperfect channel knowledge. *IEEE Communications Letters* 16:11, 1792–1795.

Yates, R. (1995). A framework for uplink power control in cellular radio systems. *IEEE Journal on Selected Areas in Communications* 13:7, 1341–1347.

Yilmaz, A., Yilmaz, F., Alouini, M., & Kucur, O. (2013). On the performance of transmit antenna selection based on shadowing side information. *IEEE Transactions on Vehicular Technology* 62:1, 454–460.

Yilmaz, F., Yilmaz, A., Alouini, M.-S., & Kucur, O. (2011). Transmit antenna selection based on shadowing side information. In *Proceedings of IEEE Vehicular Technology Conference 2011 Spring*, 1–5.

Zayen, B., Haddad, M., Hayar, A., & Øien, G. E. (2008). Binary power allocation for cognitive radio networks with centralized and distributed user selection strategies. *Elsevier Physical Communication Journal* 1:3, 183–193.

Zhang, R. (2008). Optimal power control over fading cognitive radio channel by exploiting primary user CSI. In *Proceeding of IEEE Global Communications Conference 2008,* 1–5

Zhang, R. (2009). On peak versus average interference power constraints for protecting primary users in cognitive radio networks. *IEEE Transactions on Wireless Communications* 8:4, 2112–2120.

Zhang, R., chang Liang, Y., & Cui, S. (2010). Dynamic resource allocation in cognitive radio networks. *IEEE Signal Processing Magazine* 27:3, 102–114.

Zhong, C., Ratnarajah, T., & Wong, K.-K. (2011). Outage analysis of decode-and-forward cognitive dual-hop systems with the interference constraint in Nakagami-fading channels. *IEEE Transactions on Vehicular Technology* 60:6, 2875 –2879.

Zou, Y., Zhu, J., Zheng, B., & Yao, Y.-D. (2010). An adaptive cooperation diversity scheme with best-relay selection in cognitive radio networks. *IEEE Transactions on Signal Processing* 58:10, 5438–5445.

APPENDICES

Appendix 1 Proofs for Chapter 3

Proof of the Ergodic Capacity Equation

We derive the ergodic capacity per Hz of the secondary user given in the section 3.3 for the case that the of the ST-PR link experience Nakagami-*m* fading and the ST-SR link amplitude follows Rayleigh distribution. The secondary receiver is equipped with a *L*-branch MRC receiver.

$$
\begin{aligned}
\frac{C}{B} &= \mathbb{E}_{g_{ss},g_{ps}}\left[\log\left(1+\left[\frac{1}{\lambda g_{ps}}-\frac{N_1B}{g_{ss}}\right]^{+}\frac{g_{ss}}{N_1B}\right)\right] \\
&= \int_0^{\infty}\int_{\frac{g_{ps}}{\gamma_0}}^{\infty}\log\left(\frac{\gamma_0 g_{ss}}{g_{ps}}\right)\frac{m^m g_{ps}^{m-1}e^{-mg_{ps}}}{\Gamma(m)}\frac{g_{ss}^{L-1}e^{-g_{ss}}}{(L-1)!}dg_{ss}dg_{ps} \\
&= \frac{m^m}{\Gamma(m)(L-1)!}\int_0^{\infty} g_{ps}^{m-1}e^{-mg_{ps}}\int_{\frac{g_{ps}}{\gamma_0}}^{\infty}\log\left(\frac{\gamma_0 g_{ss}}{g_{ps}}\right)g_{ss}^{M-1}e^{-g_{ss}}dg_{ss}dg_{ps} \\
&= \frac{m^m}{\Gamma(m)(L-1)!}\int_0^{\infty} g_{ps}^{m-1}e^{-mg_{ps}}\left(\frac{g_{ps}}{\gamma_0}\right)^{L}J_L\left(\frac{g_{ps}}{\gamma_0}\right)dg_{ps} \\
&= \frac{m^m}{\gamma_0^L\Gamma(m)(L-1)!}\int_0^{\infty} g_{ps}^{m-1+L}e^{-mg_{ps}}\frac{(L-1)!}{\left(\frac{g_{ps}}{\gamma_0}\right)^{L}}\times\sum_{k=0}^{L-1}\frac{\Gamma(k,\frac{g_{ps}}{\gamma_0})}{k!}dg_{ps} \\
&= \frac{m^m}{\Gamma(m)}\sum_{k=0}^{L-1}\frac{1}{k!}\int_0^{\infty} g_{ps}^{m-1}e^{-mg_{ps}}\Gamma(k,\frac{g_{ps}}{\gamma_0})dg_{ps} \\
&= \frac{m^{m-1}\gamma_0^m}{\Gamma(m)}\sum_{k=0}^{L-1}\frac{\Gamma(m+k)}{(1+m\gamma_0)^{m+k}k!}\times {}_2F_1\left(1,m+k;m+1;\frac{m\gamma_0}{1+m\gamma_0}\right)
\end{aligned}
$$

where the last step is with the help of (Gradshteyn & Ryzhik 2007: 6.455), and $\gamma_0 = 1/\lambda N_1 B$. $J_n(x)$ is defined in (Alouini & Goldsmith 1999) as

$$J_n(x) = \int_1^{\infty} t^{n-1}\log(t)e^{-xt}dt, \quad x>0,$$

and for n positive integers (Alouini & Goldsmith 1999),

$$J_n(x) = \frac{(n-1)!}{x^n}\sum_{k=0}^{n-1}\frac{\Gamma(k,x)}{k!}$$

where $\Gamma(\alpha,x)$ denotes the incomplete gamma function given by (Gradshteyn & Ryzhik 2007: 8.35-1)

$$\Gamma(\alpha,x)=\int_x^\infty t^{\alpha-1}e^{-t}dt$$

Proof of the Constraint Equation

We derive the constraint $Q_{av}/(N_1B)$ in terms of $\gamma_0=1/\lambda N_1B$ provided in the section 3.3.

$$\begin{aligned}
&\frac{Q_{av}}{N_1B}\\
&=\mathbb{E}_{g_{ss},g_{ps}}\left[\frac{p(g_{ss},g_{ps})g_{ps}}{N_1B}\right]\\
&=\int_0^\infty\int_0^{\gamma_0 g_{ss}}\left(\gamma_0-\frac{g_{ps}}{g_{ss}}\right)\frac{m^m g_{ps}^{m-1}e^{-mg_{ps}}}{\Gamma(m)}\times\frac{g_{ss}^{L-1}e^{-g_{ss}}}{(L-1)!}dg_{ps}dg_{ss}\\
&=\frac{m^m}{\Gamma(m)(L-1)!}\int_0^\infty g_{ss}^{L-1}e^{-g_{ss}}\int_0^{\gamma_0 g_{ss}}\left(\gamma_0-\frac{g_{ps}}{g_{ss}}\right)g_{ps}^{m-1}e^{-mg_{ps}}dg_{ps}dg_{ss}\\
&=\frac{1}{\Gamma(m)(L-1)!}\int_0^\infty g_{ss}^{L-1}e^{-g_{ss}}\left[\gamma_0\gamma(m,m\gamma_0 g_{ss})-\frac{1}{mg_{ss}}\gamma(m,m\gamma_0 g_{ss})\right]dg_{ss}\\
&=\frac{1}{\Gamma(m)(L-1)!}\left[\gamma_0\frac{(m\gamma_0)^m\Gamma(L+m)}{m(1+m\gamma_0)^{L+m}}{}_2F_1\left(1,L+m;m+1;\frac{m\gamma_0}{1+m\gamma_0}\right)\right.\\
&\left.-\frac{1}{m}\frac{(m\gamma_0)^{m+1}\Gamma(L+m)}{(m+1)(1+m\gamma_0)^{L+m}}{}_2F_1\left(1,L+m;m+2;\frac{m\gamma_0}{1+m\gamma_0}\right)\right]\\
&=\frac{m^{m-1}\gamma_0^{m+1}\Gamma(L+m)}{(1+m\gamma_0)^{L+m}\Gamma(m)(L-1)!}\\
&\times\left[{}_2F_1\left(1,L+m;m+1;\frac{m\gamma_0}{1+m\gamma_0}\right)-\frac{m}{1+m}{}_2F_1\left(1,L+m;m+2;\frac{m\gamma_0}{1+m\gamma_0}\right)\right]
\end{aligned}$$

where $\gamma(\alpha,x)=\int_0^x e^{-t}t^{\alpha-1}dt$ is the incomplete gamma function, and ${}_2F_1(a,b;c;z)$ denotes Gauss's hypergeometric function (Abramowitz & Stegun 1964).

Appendix 2 Proofs for Chapter 4

We derive the ergodic capacity per Hz of the secondary user given in the section 4.3 for the case with imperfect channel information of the ST-PR link in a Rayleigh fading environment. The secondary receiver is equipped with a L-branch MRC receiver.

Proof of the Constraint Equation

We derive the constraint $Q_{av}/(N_1B)$ in terms of $\gamma_0 = 1/\lambda N_1 B$ shown in section 4.3.

$$
\begin{aligned}
\frac{Q_{av}}{N_1B} &= \mathbb{E}_{g_{ss},\hat{g}_{ps}}\left[\frac{p_s(g_{ss},\hat{g}_{ps})\hat{g}_{ps}}{N_1B}\right] + \frac{\sigma_e^2\bar{P}}{N_1B} \\
&= \mathbb{E}_{g_{ss},\hat{g}_{ps}}\left[\left(\frac{\gamma_0\hat{g}_{ps}}{\hat{g}_{ps}+\sigma_e^2} - \frac{\hat{g}_{ps}}{g_{ss}}\right)^+\right] + \mathbb{E}_{g_{ss},\hat{g}_{ps}}\left[\left(\frac{\gamma_0\sigma_e^2}{\hat{g}_{ps}+\sigma_e^2} - \frac{\sigma_e^2}{g_{ss}}\right)^+\right] \\
&= \int_{\frac{\sigma_e^2}{\gamma_0}}^{\infty}\int_0^{\gamma_0 g_{ss}-\sigma_e^2}\left(\gamma_0 - \frac{\hat{g}_{ps}+\sigma_e^2}{g_{ss}}\right)\frac{1}{1-\sigma_e^2}e^{-\frac{\hat{g}_{ps}}{1-\sigma_e^2}}\frac{g_{ss}^{L-1}e^{-g_{ss}}}{(L-1)!}\,d\hat{g}_{ps}dg_{ss} \\
&= \frac{1}{(1-\sigma_e^2)(L-1)!}\int_{\frac{\sigma_e^2}{\gamma_0}}^{\infty} g_{ss}^{L-1}e^{-g_{ss}} \\
&\quad\times\int_0^{\gamma_0 g_{ss}-\sigma_e^2}\left(\gamma_0 - \frac{\hat{g}_{ps}+\sigma_e^2}{g_{ss}}\right)e^{-\frac{\hat{g}_{ps}}{1-\sigma_e^2}}\,d\hat{g}_{ps}dg_{ss} \\
&= \frac{1}{(L-1)!}\int_{\frac{\sigma_e^2}{\gamma_0}}^{\infty} g_{ss}^{L-1}e^{-g_{ps}}\left[\gamma_0 - \frac{1}{h} + \frac{1-\sigma_e^2}{g_{ss}}e^{\frac{\sigma_e^2}{1-\sigma_e^2}}e^{-\frac{\gamma_0 g_{ss}}{1-\sigma_e^2}}\right]dg_{ss} \\
&= \frac{1}{(L-1)!}\left[\gamma_0\Gamma\left(L,\frac{\sigma_e^2}{\gamma_0}\right) - \Gamma\left(L-1,\frac{\sigma_e^2}{\gamma_0}\right)\right. \\
&\left.+\frac{(1-\sigma_e^2)^L e^{\frac{\sigma_e^2}{1-\sigma_e^2}}}{(1+\gamma_0-\sigma_e^2)^{L-1}}\Gamma\left(L-1,\frac{\sigma_e^2}{1-\sigma_e^2}+\frac{\sigma_e^2}{\gamma_0}\right)\right]
\end{aligned}
$$

where $\Gamma(\alpha,x)$ denotes the incomplete gamma function defined in (Abramowitz & Stegun 1964) as

$$\Gamma(\alpha,x) = \int_x^{\infty} t^{\alpha-1}e^{-t}dt.$$

Proof of the Ergodic Capacity Equation

We derive the CR capacity per Hz shown in section 4.3.

$$
\begin{aligned}
\frac{C}{B} &= \mathbb{E}_{g_{ss},\hat{g}_{ps}}\left[\log\left(\frac{\gamma_0 g_{ss}}{\hat{g}_{ps}+\sigma_e^2}\right)\right] \\
&= \int_0^{\infty}\int_{\frac{\hat{g}_{ps}+\sigma_e^2}{\gamma_0}}^{\infty} \log\left(\frac{\gamma_0 g_{ss}}{\hat{g}_{ps}+\sigma_e^2}\right)\frac{e^{-\frac{\hat{g}_{ps}}{1-\sigma_e^2}}}{1-\sigma_e^2}\frac{g_{ss}^{L-1}e^{-g_{ss}}}{(L-1)!}\,dg_{ss}d\hat{g}_{ps} \\
&= \frac{1}{(1-\sigma_e^2)(L-1)!}\int_0^{\infty} e^{-\frac{\hat{g}+ps}{1-\sigma_e^2}}\int_{\frac{\hat{g}_{ps}+\sigma_e^2}{\gamma_0}}^{\infty}\log\left(\frac{\gamma_0 g_{ss}}{\hat{g}_{ps}+\sigma_e^2}\right)g_{ss}^{L-1}e^{-g_{ss}}dg_{ss}d\hat{g}_{ps} \\
&= \frac{1}{(1-\sigma_e^2)(L-1)!}\int_0^{\infty} e^{-\frac{\hat{g}_{ps}}{1-\sigma_e^2}}\left(\frac{\hat{g}_{ps}+\sigma_e^2}{\gamma_0}\right)^{L} J_L\left(\frac{\hat{g}_{ps}+\sigma_e^2}{\gamma_0}\right)dsd\hat{g} \\
&= \frac{1}{(1-\sigma^2)}\sum_{k=0}^{L-1}\frac{1}{k!}\int_0^{\infty} e^{-\frac{\hat{g}}{1-\sigma^2}}\Gamma\left(k,\frac{\hat{g}+\sigma^2}{\gamma_0}\right)d\hat{g} \\
&= \frac{1}{(1-\sigma^2)}\sum_{k=0}^{L-1}\frac{1}{k!}\int_0^{\infty} e^{-\frac{\hat{g}}{1-\sigma^2}}\int_{\frac{\hat{g}+\sigma^2}{\gamma_0}}^{\infty} e^{-t}t^{k-1}dtd\hat{g} \\
&= \sum_{k=0}^{L-1}\frac{1}{k!}\int_{\frac{\sigma^2}{\gamma_0}}^{\infty} e^{-t}t^{k-1}\left[1-e^{-\frac{\gamma_0}{1-\sigma^2}t}e^{\frac{\sigma^2}{1-\sigma^2}}\right]dt \\
&= \sum_{k=0}^{L-1}\frac{1}{k!}\left[\Gamma\left(k,\frac{\sigma_e^2}{\gamma_0}\right)-e^{\frac{\sigma_e^2}{1-\sigma_e^2}}\left(\frac{1-\sigma_e^2}{1-\sigma_e^2+\gamma_0}\right)^{k}\Gamma\left(k,\frac{\sigma_e^2}{\gamma_0}+\frac{\sigma_e^2}{1-\sigma_e^2}\right)\right]
\end{aligned}
$$

where $J_n(x)$ is defined as (Alouini & Goldsmith 1999)

$$J_n(x) = \int_1^{\infty} t^{n-1}\log(t)e^{-xt}dt, \qquad x>0,$$

and for n positive integers, $J_n(x)$ is given as (Alouini & Goldsmith 1999),

$$J_n(x) = \frac{(n-1)!}{x^n}\left(E_1(x)+\sum_{k=1}^{n-1}\frac{\Gamma(k,x)}{k!}\right)$$

Appendix 3 Proofs for Chapter 5

Proof of the Ergodic Capacity

$$
\begin{aligned}
C =& \mathbb{E}_{\gamma_{\mathrm{GSC,K}}}\left\{\log\left(1+\gamma_{\mathrm{GSC},K}\right)\right\} = \int_0^\infty \gamma\, {}_2F_1(1,1;2;-\gamma) f_{\gamma_{\mathrm{GSC},K}}(\gamma) d\gamma \\
=& \int_0^\infty \gamma\, {}_2F_1(1,1;2;-\gamma) \binom{M}{K} K^K \left\{ \frac{\gamma^{K-1}}{\overline{\gamma}^K (K-1)!} \exp\left(-\frac{K\gamma}{\overline{\gamma}}\right) \right. \\
&+ \frac{1}{\overline{\gamma}} \sum_{n=1}^{M-K} (-1)^{K+n-1} \binom{M-K}{n} \left(\frac{1}{n}\right)^{K-1} \\
&\left. \times \exp\left(-\frac{K\gamma}{\overline{\gamma}}\right) \left[\exp\left(-\frac{n\gamma}{\overline{\gamma}}\right) - \sum_{m=0}^{K-2} \frac{1}{m!} \left(-\frac{n\gamma}{\overline{\gamma}}\right)^m \right] \right\} d\gamma \\
=& \binom{M}{K} K^K \left\{ \frac{1}{\overline{\gamma}^K (K-1)!} \int_0^\infty {}_2F_1(1,1;2;-\gamma) \gamma^K e^{-\frac{K\gamma}{\overline{\gamma}}} d\gamma \right. \\
&+ \frac{1}{\overline{\gamma}} \sum_{n=1}^{M-K} (-1)^{K+n-1} \binom{M-K}{n} \left(\frac{1}{n}\right)^{K-1} \left[\int_0^\infty {}_2F_1(1,1;2;-\gamma) \gamma e^{-\frac{(K+n)\gamma}{\overline{\gamma}}} d\gamma \right. \\
&\left. \left. - \sum_{m=0}^{K-2} \frac{1}{m!} \left(-\frac{n}{\overline{\gamma}}\right)^m \int_0^\infty {}_2F_1(1,1;2;-\gamma) \gamma^{m+1} e^{-\frac{K\gamma}{\overline{\gamma}}} d\gamma \right] \right\} d\gamma \\
=& \binom{M}{K} K^K \left\{ \frac{1}{\overline{\gamma}^K (K-1)!} \frac{\Gamma(2) \left(\frac{K}{\overline{\gamma}}\right)^{-(K+1)}}{\Gamma(1)\Gamma(1)} E\left(\begin{matrix} 1,1,K+1 \\ 2 \end{matrix} \middle| \frac{K}{\overline{\gamma}} \right) \right. \\
&+ \frac{1}{\overline{\gamma}} \sum_{n=1}^{M-K} (-1)^{K+n-1} \binom{M-K}{n} \left(\frac{1}{n}\right)^{K-1} \left[\frac{\Gamma(2) \left(\frac{K+n}{\overline{\gamma}}\right)^{-2}}{\Gamma(1)\Gamma(1)} E\left(\begin{matrix} 1,1,2 \\ 2 \end{matrix} \middle| \frac{K+n}{\overline{\gamma}} \right) \right. \\
&\left. \left. - \sum_{m=0}^{K-2} \frac{1}{m!} \left(-\frac{n}{\overline{\gamma}}\right)^m \frac{\Gamma(2) \left(\frac{K}{\overline{\gamma}}\right)^{-(m+2)}}{\Gamma(1)\Gamma(1)} E\left(\begin{matrix} 1,1,m+2 \\ 2 \end{matrix} \middle| \frac{K}{\overline{\gamma}} \right) \right] \right\} \\
=& \binom{M}{K} \left\{ \frac{\overline{\gamma}}{K!} G_{2,3}^{3,1}\left(\begin{matrix} 1,2 \\ 1,1,K+1 \end{matrix} \middle| \frac{K}{\overline{\gamma}} \right) + K^K \overline{\gamma} \sum_{n=1}^{M-K} (-1)^{K+n-1} \binom{M-K}{n} \left(\frac{1}{n}\right)^{K-1} \right. \\
&\left. \times \left[\frac{G_{2,3}^{3,1}\left(\begin{matrix} 1,2 \\ 1,1,2 \end{matrix} \middle| \frac{K+n}{\overline{\gamma}} \right)}{(K+n)^2} - \sum_{m=0}^{K-2} \frac{1}{m!} (-n)^m \frac{G_{2,3}^{3,1}\left(\begin{matrix} 1,2 \\ 1,1,m+2 \end{matrix} \middle| \frac{K}{\overline{\gamma}} \right)}{K^{m+2}} \right] \right\}.
\end{aligned}
$$

where the second last step is with the help of (Gradshteyn & Ryzhik 2007: eqn. (7.522-1)), and the last step is with the help of eqn. (5.12).

Proof of the SEP

The symbol error probability expression is proved as follows.

$$
\begin{aligned}
P_e =& \frac{a}{2\sqrt{\pi}} E_{\gamma_{\mathrm{GSC,K}}}\left[G_{1,2}^{2,0}\left(\begin{smallmatrix}1\\0,1/2\end{smallmatrix}\middle| b\gamma_{\mathrm{GSC,K}}\right)\right] \\
=& \frac{a}{2\sqrt{\pi}} \int_0^{\infty} G_{1,2}^{2,0}\left(\begin{smallmatrix}1\\0,1/2\end{smallmatrix}\middle| b\gamma\right) f_{\gamma_{\mathrm{GSC},K}}(\gamma)d\gamma \\
=& \frac{a}{2\sqrt{\pi}} \int_0^{\infty} G_{1,2}^{2,0}\left(\begin{smallmatrix}1\\0,1/2\end{smallmatrix}\middle| b\gamma\right) \binom{M}{K} K^K \left\{ \frac{\gamma^{K-1}}{\overline{\gamma}^K (K-1)!} \exp\left(-\frac{K\gamma}{\overline{\gamma}}\right) \right. \\
& + \frac{1}{\overline{\gamma}} \sum_{n=1}^{M-K} (-1)^{K+n-1} \binom{M-K}{n} \left(\frac{1}{n}\right)^{K-1} \\
& \left. \times \exp\left(-\frac{K\gamma}{\overline{\gamma}}\right) \left[\exp\left(-\frac{n\gamma}{\overline{\gamma}}\right) - \sum_{m=0}^{K-2} \frac{1}{m!} \left(-\frac{n\gamma}{\overline{\gamma}}\right)^m\right] \right\} d\gamma \\
=& \frac{a}{2\sqrt{\pi}} \binom{M}{K} K^K \left\{ \int_0^{\infty} \frac{\gamma^{K-1}}{\overline{\gamma}^K (K-1)!} e^{-\frac{K\gamma}{\overline{\gamma}}} G_{1,2}^{2,0}\left(\begin{smallmatrix}1\\0,1/2\end{smallmatrix}\middle| b\gamma\right) d\gamma \right. \\
& + \frac{1}{\overline{\gamma}} \sum_{n=1}^{M-K} (-1)^{K+n-1} \binom{M-K}{n} \left(\frac{1}{n}\right)^{K-1} \left[\int_0^{\infty} e^{-\frac{(K+n)\gamma}{\overline{\gamma}}} G_{1,2}^{2,0}\left(\begin{smallmatrix}1\\0,1/2\end{smallmatrix}\middle| b\gamma\right) d\gamma \right. \\
& \left. \left. - \sum_{m=0}^{K-2} \frac{1}{m!} \left(-\frac{n}{\overline{\gamma}}\right)^m \int_0^{\infty} \gamma^m e^{-\frac{K\gamma}{\overline{\gamma}}} G_{1,2}^{2,0}\left(\begin{smallmatrix}1\\0,1/2\end{smallmatrix}\middle| b\gamma\right) d\gamma \right] \right\} \\
=& \frac{a}{2\sqrt{\pi}} \binom{M}{K} K^K \left\{ \frac{1}{K!\,(b\overline{\gamma})^{K-1}} G_{2,2}^{2,1}\left(\begin{smallmatrix}0,K\\K-1,K-1/2\end{smallmatrix}\middle| \frac{b\overline{\gamma}}{K}\right) \right. \\
& + \sum_{n=1}^{M-K} (-1)^{K+n-1} \binom{M-K}{n} \left(\frac{1}{n}\right)^{K-1} \left[\frac{1}{K+n} G_{2,2}^{2,1}\left(\begin{smallmatrix}0,1\\0,1/2\end{smallmatrix}\middle| \frac{b\overline{\gamma}}{K}\right) \right. \\
& \left. \left. - \sum_{m=0}^{K-2} \frac{1}{m!Kb^m} \left(-\frac{n}{\overline{\gamma}}\right)^m G_{2,2}^{2,1}\left(\begin{smallmatrix}0,m+1\\m,m+1/2\end{smallmatrix}\middle| \frac{b\overline{\gamma}}{K}\right) \right] \right\}
\end{aligned}
$$

where the last step is with the help of (Gradshteyn & Ryzhik 2007: eqn. (7.813-1)), and (Gradshteyn & Ryzhik 2007: eqn. (9.31-5))

$$
z^k G_{p,q}^{m,n}\left(\begin{smallmatrix}\mathbf{a}_p\\\mathbf{b}_q\end{smallmatrix}\middle| z\right) = G_{p,q}^{m,n}\left(\begin{smallmatrix}\mathbf{a}_p+k\\\mathbf{b}_q+k\end{smallmatrix}\middle| z\right).
$$

Appendix 4 Proofs for Chapter 7

The error function Eqn.(7.5) can be modified as

$$e_i(t) = \lambda_{i,1}\left(P_i(t) - P_{min}\right) + \hat{\lambda}_{i,2}\left(\Gamma_i(t) - \Gamma_i^T\right) + \hat{\lambda}_{i,3}\left(P_i(t)g_{0i} - \frac{Q}{M}\right)$$

where $\hat{\lambda}_{i,2} = \lambda_{i,2} \cdot \text{sign}\left(\Gamma_i(t) - \Gamma_i^T\right), \quad \hat{\lambda}_{i,3} = \lambda_{i,3} \cdot \text{sign}\left(P_i(t)g_{0i} - \frac{Q}{M}\right),$

and $\text{sign}(x) = \begin{cases} +1, & x \geq 0 \\ -1, & x < 0 \end{cases}$ is the sign function.

We assume that the power $P_i(t)$ is described by an autoregressive model shown in Figure 51, and here we consider the one-tap case (see (Elmusrati *et al.* 2008; 2007) for multi-tap case derivation), then the transmission power can be represented as,

$$P_i(t) = w_i P_i(t-1)$$

Then we obtain the following error function

$$\begin{aligned} e_i(t) =& \lambda_{i,1}\left(w_i P_i(t-1) - P_{\min}\right) + \hat{\lambda}_{i,2}\left(\frac{w_i P_i(t-1)}{\hat{I}_i(t)} - \Gamma_i^T\right) \\ &+ \hat{\lambda}_{i,3}\left(w_i P_i(t-1)g_{0i} - \frac{Q}{M}\right) \\ =& \lambda_{i,1} w_i P_i(t-1) - \lambda_{i,1} P_{\min} + \hat{\lambda}_{i,2}\frac{w_i P_i(t-1)}{\hat{I}_i(t)} - \hat{\lambda}_{i,2}\Gamma_i^T + \hat{\lambda}_{i,3} w_i P_i(t-1) g_{0i} \\ &- \hat{\lambda}_{i,3}\frac{Q}{M} \\ =& \alpha_t w_i P_i(t-1) - \lambda_{i,1} P_{\min} - \hat{\lambda}_{i,2}\Gamma_i^T - \hat{\lambda}_{i,3}\frac{Q}{M} \end{aligned}$$

where $\alpha_t = \lambda_{i,1} + \frac{\hat{\lambda}_{i,2}}{\hat{I}_i(t)} + \hat{\lambda}_{i,3} g_{0i}$. Let $L = e_i^2(t)$.

Minimizing the cost function with respect to P_i is transformed into another minimization problem with respect to the weight parameter w_i. The necessary condition should satisfy (Boyd & Vandenberghe 2004):

$$\frac{\partial L}{\partial w} = 2e_i(t)\frac{\partial e_i(t)}{\partial w}\left[\alpha_t w_i P_i(t-1) - \lambda_{i,1} P_{min} - \hat{\lambda}_{i,2}\Gamma_i^T - \hat{\lambda}_{i,3}\frac{Q}{M}\right] = 0$$

Then we have

$$\alpha_t w_i P_i(t-1) = \lambda_{i,1} P_{min} + \hat{\lambda}_{i,2} \Gamma_i^T + \hat{\lambda}_{i,3} \frac{Q}{M}$$

Further, we obtain the equation for weight w_i,

$$w_i(t) = \frac{\lambda_{i,1} P_{min} + \hat{\lambda}_{i,2} \Gamma_i^T + \hat{\lambda}_{i,3} \frac{Q}{M}}{\alpha_t P_i(t-1)}$$

Finally, the transmit power of secondary user i at time slot t becomes

$$\begin{aligned} P_i(t) =& \frac{\lambda_{i,1} P_{min} + \hat{\lambda}_{i,2} \Gamma_i^T + \hat{\lambda}_{i,3} \frac{Q}{M}}{\alpha_t P_i(t-1)} P_i(t-1) \\ =& \frac{\left(\lambda_{i,1} P_{min} + \hat{\lambda}_{i,2} \Gamma_i^T + \hat{\lambda}_{i,3} \frac{Q}{M}\right) P_i(t-1)}{\lambda_{i,1} P_i(t-1) + \frac{\hat{\lambda}_{i,2}}{\hat{I}_i(t)} P_i(t-1) + \hat{\lambda}_{i,3} g_{0i} P_i(t-1)} \\ =& \frac{\left(\lambda_{i,1} P_{min} + \hat{\lambda}_{i,2} \Gamma_i^T + \hat{\lambda}_{i,3} \frac{Q}{M}\right) P_i(t-1)}{\lambda_{i,1} P_i(t-1) + \hat{\lambda}_{i,2} \Gamma_i(t-1) + \hat{\lambda}_{i,3} g_{0i} P_i(t-1)} \end{aligned}$$

Here only positive values of $\hat{\lambda}_{i,2}$ and $\hat{\lambda}_{i,3}$ are considered (Elmusrati *et al.* 2007), i.e. $\hat{\lambda}_{i,2} = \lambda_{i,2}$ and $\hat{\lambda}_{i,3} = \lambda_{i,3}$. As pointed out in (Elmusrati *et al.* 2007) that though this simplification only slightly degrades the convergence speed, it considerably reduces the complexity of the algorithm. Finally, the algorithm becomes

$$P_i(t) = \frac{\left(\lambda_{i,1} P_{min} + \lambda_{i,2} \Gamma_i^T + \lambda_{i,3} \frac{Q}{M}\right) P_i(t-1)}{\lambda_{i,1} P_i(t-1) + \lambda_{i,2} \Gamma_i(t-1) + \lambda_{i,3} g_{0i} P_i(t-1)}$$